α-Helical Coiled Coil Mimicry by Alternating Sequences of β- and γ-Amino Acids

Dissertation zur Erlangung des akademischen Grades des Doktors der Naturwissenschaften (Dr. rer. nat.)

eingereicht im Fachbereich Biologie, Chemie, Pharmazie
der Freien Universität Berlin

vorgelegt von

Raheleh Rezaei Araghi

aus Teheran, Iran

Juli, 2011

1. Gutachterin: Prof. Dr. Beate Koksch (Freie Universität Berlin)

2. Gutachter: Prof. Dr. Rainer Haag (Freie Universität Berlin)

Disputation am: 01.09.2011

Declaration

The work presented here was carried out in the research group of Prof. Dr. Beate Koksch at the Institute of Chemistry and Biochemistry in the Department of Biology, Chemistry, and Pharmacy of Freie Universität Berlin.

The work presented in this thesis was performed solely and this thesis has been written independently except where otherwise stated.

Berlin, July 2011

Raheleh Rezaei Araghi

The work on this dissertation resulted so far in the following publications:

- Raheleh Rezaei Araghi, Christian Jäckel, Helmut Cölfen, Mario Salwiczek, Antje Völkel, Sara C. Wagner, Sebastian Wieczorek, Carsten Baldauf , and Beate Koksch, *ChemBioChem*, 2010, 11, 335 – 339.

- Raheleh Rezaei Araghi**,** Beate Koksch, *ChemCommun*, 2011, 47, 3544– 3546.

- Raheleh Rezaei Araghi, Carsten Baldauf, Ulla I. M. Gerling, Cosimo Damiano Cadicamo, Beate Koksch, *Amino Acids,* Special Issue Foldamers, **2011**, 41, 733-742.

Further Publications:

- Sara C. Wagner, Meike Roskamp, Manjula Pallerla, Raheleh Rezaei Araghi, S. Schlecht, B. Koksch *Small,* 2010*, 6,* 1321-1328.

- Kevin Pagel*, Sara C. Wagner*, Raheleh Rezaei Araghi , Hans von Berlepsch, Christian Böttcher, Beate Koksch, *Chem. Eur. J.* 2008, *14*, 11442 – 11451.

For data security reasons the curriculum vitae has been omitted from the published version.

For data security reasons the curriculum vitae has been omitted from the published version.

Acknowledgment

It is a pleasure to convey my appreciation to all the people whose contribution in assorted ways to this thesis deserved special mention.

Foremost, I would like to record my gratitude to my supervisor Prof. Dr. Beate Koksch for her guidance, optimism, trust and the large degree of freedom she gave me during my research. Above all and the most needed, she provided me encouragement and support which exceptionally inspired and enriched my scientific growth.

I gratefully acknowledge Prof. Dr. Rainer Haag for reviewing this work in the midst of all his activity.

Many thanks go in particular to Dr. Carsten Baldauf for very supportive molecular dynamics simulations and computational modeling. All his cooperative contributions in shared publications are gratefully acknowledged. I would like to thank M.Sc. Elisabeth Nyakatura and M.Sc. Sebastian Wieczorek for performing the phage display experiments, and for helpful conversations on the outcoms.I wish to express my gratitude to Dr. Rudolf Volkmer and Dr. Carsten Mahrenholz for facility of spot synthesis and analysis. It is a pleasure to thank Dr. Allison Berger and Dr. Pamela Winchester for their constructive comments on my manuscripts as well as this dissertation. Thanks go to current and former students in the Prof. Dr. Koksch's research group. They all have provided support and assistance that allowed me to achieve my goals. I am indebted especially to Dr. Mario Salwiczek for all productive scientific discussions we had. My special thanks to my good friend Cosimo for being helpful when I really needed it.

I feel a deep sense of gratitude for whole my family and friends and above all my parents, who will always be there for and believing in me no matter what. Their constant love, care, support and encouragement have made it possible for me to pursue my dreams.

Last but not least, my special thanks to my husband, Ali, his ongoing support and love has kept me going during difficult times and has guided me when I have thought to be lost.

Table of Contents

Referat

Die vorliegende Arbeit beschäftigt sich mit synthetischen β,γ-Foldameren, die dazu designed worden, die α-helikale Konformation zu imitieren. Im Rahmen der Wirkstoffentwicklung könnte es mit Hilfe derartiger Strukturen ermöglicht werden, Einfluss auf unerwünschte z.B. im Rahmen bestimmter Krankheiten auftretenden Protein-Protein-Interaktionen zu nehmen. Basierend auf dem Prinzip, die Anzahl der Atome im Peptidrückgrat konstant zu halten, sollten alternierende Sequenzen aus β- und γ-Aminosäuren eine der α-helikalen Konformation nahe kommende Struktur einnehmen. Als Modell, um diese Hypothese zu überprüfen, wird im Rahmen dieser Studie das α-helikale *Coiled-Coil*-Faltungsmotiv verwendet.

Hierzu wurde ein Segment einer *Coiled-Coil* bildenden α-Sequenz durch β- und γ-Aminosäuren ersetzt, um somit ein α,β,γ-Chimär zu generieren. Das Design der α,β,γ-Sequenz wurde dabei so gewählt, dass die natürlichen Seitenketten beibehalten wurden, um dadurch das native Packungsmuster zu gewährleisten. Die Helixbildung in diesem System wird durch Oligomerisierung induziert, während die isolierte β,γ-Sequenz größtenteils unstrukturiert vorliegt. Im Folgenden wurden verschiedene α,β,γ-Chimäre hinsichtlich ihrer Oligomerisierung sowohl an dem Modell als auch im Rahmen einer natürlich vorkommenden *Coiled-Coil*-Sequenz, GCN4pLI, untersucht. Dabei kam eine von Vielzahl von theoretischen und experimentellen Methoden und Assays wie Molekulardynamic-Simulationen, CD-Spektroskopie, Größenausschluss-Chromatografie, analytische Ultrazentrifugation, Transmissionselektronen-Spektroskopie sowie auch Fluoreszenz-Resonanz-Energietransfer, Disulfid-Austauschexperimente und „Native Chemische Ligation“ zur Anwendung.

Im Anschluss an diese Untersuchungen wurden mit Hilfe zweier *Medium-Throughput*-Methoden (*Spot*-Synthese und *Phage-Display*) optimale Interaktionspartner für die artifizielle α,β,γ-Sequenz identifiziert. Während der rationale Ansatz bei der *Spot*-Synthese von vorn herein bestimmte Sequenzen ausschloss, schöpfte die *Phage-Display*-Technik aus dem gesamten *Pool* codierter Aminosäuren, sodass hiermit dem Wildtyp zwar strukturell wenig ähnelnde jedoch strukturell stabilere Bindungspartner gefunden werden konnten.

Die Funktion des künstlichen Faltungsmotivs wurde im Kontext der templat-gesteuerten

„Nativen Chemischen Ligation“ untersucht. Um die reaktiven funktionellen Gruppen in räumliche Nähe zu bringen, muss die α,β,γ-Sequenz die natürliche α-helikale Struktur imitieren können. Diese Eigenschaft konnte im Rahmen dieser Untersuchungen bestätigt werden.

Weitere Auswirkungen der strukturellen Veränderungen durch den isosteren α,α,α→β,γ-Austausch, wie z.B. Verlust lokaler Packung und Gewinn an konformationeller Flexibilität durch die Eliminierung von Wasserstoffbrücken im Rückgrat wurden ebenfalls untersucht. In Disulfid-Austausch-Experimenten konnte gezeigt werden, dass die Paarung der chimären Sequenz mit der natürlichen GCN4pLI-Sequenz thermodynamisch nur erlaubt ist, wenn die β- und γ-Reste einer bestimmten Sequenz (βγβγ) folgen. Dies weist darauf hin, dass nur in diesem Fall die lokale Packung der Reste dem natürlichen Packungsmuster hinreichend ähnlich ist. Diese Beobachtungen stimmen mit den theoretischen Studien überein und zeigen, dass die Stabilität der Interaktionen mit α,β,γ-chimären Sequenzen durch das Ausmaß an Wechselwirkungen zwischen den Seitenketten in der helikalen Interaktionsdomäne kontrolliert werden kann.

Abstract

The goal of this work was to develop helical conformations by using synthetic foldamers that could be functionally modulated to selectively disrupt unfavourable helix-helix interactions. Adhering to the principle of “equal backbone atoms”, the alternating βγ sequence appears to be well-suited to mimic an α-helical conformation. As a case study, the backbone modification is applied to a natural helical protein folding motif, the α-helical coiled coil.

First an extended sequence of and amino acids was substituted in a coiled coil forming sequence. The helical structure is induced through oligomerization while the individual βγ segment is mostly unstructured. The natural side chains were preserved to more accurately imitating natural packing of αβγ chimera. The self- and hetero-assembly of a series of αβγ-chimeric sequences is investigated in model peptide systems as well as the biologically-derived GCN4pLI sequence by means of a variety of theoretical and experimental methods and assays, such as MD simulations, CD, SEC, AU, TEM, as well as FRET, disulfide exchange and template-directed native chemical ligation assays.

The next task was to optimize the interactions between the artificial sequence and the native partner by means of two medium-throughput methods. Spot synthesis/analysis and phage display techniques revealed the key side chain properties that are required for coiled coil assembly. The phage display technique selected α-sequences with primary structures that would not have been considered in a rational design approach, but were observed to be better binding partners for the αβγ-chimera.

Further, the function of the artificial folding motif was studied in the context of its catalytic activity in the native chemical ligation. In order to bring the essential functional groups together and present a well-formed catalytic site, αβγ-chimera had to be and were shown to mimic the natural α-helical coiled coil structure.

The structural consequences of the ααα→βγ isosteric backbone substitution, such as disruption in local packing or conformational degrees of freedom due to further loss of H-bond are other interesting aspects which were studied in detail. As determined by disulfide exchange assays, the pairing of αβγ-chimeric sequences with the native GCN4pLI sequence is thermodynamically allowed only in the case of an ideal arrangement of β-

and γ-residues. This indicates a similarity in the local side chain packing of β- and γ-amino acids at the helical interface of αβγ-chimeras and the native α-peptide.

Altogether, the observations are consistent with the theoretical studies and show that the stability of a αβγ-peptide bundle can be tuned by controlling the extent of the side chain interactions at the interhelical recognition domains.

Abbreviation

Abu	amino butyric acid
ACHC	*trans*-2-aminocyclohexane carboxylic acid
ACPC	*trans*-2-aminocyclopentane carboxylic acid
Aib	α-aminoisobutyric acid
AMPA	4-(aminomethyl)phenylacetic acid
APC	*trans*-3-amino-pyrrolidine-4-carboxylic acid
AUC	analytical ultracentrifuge
BLUs	boehringer light units
Boc	t-butylcarbonate
bZIPs	basic zippers
CD	circular dichroism
CPPs	Cell penetrating peptides
Dap	(S)-1,3-diaminopropionic acid
DCHC	*trans*-2,5-diaminocyclohexanecarboxylic acid
DIC	N,N'-diisopropylcarbodiimide
DMF	dimethylformamide
DMSO	dimethylsulfoxide
DNA	deoxyribonucleic acid
DTT	dithiothreitol
Fmoc	fluorenylmethyloxycarbonyl
FRET	förster resonance energy transfer
gem	geminal
HBS	hydrogen bond surrogate
HIV	human immunodeficiency virus
HOAt	1-hydroxy-7-azabenzotriazole
HOBt	1-hydroxy-benzotriazole
HP	Hewlett-Packard
HPLC	High performance liquid chromatography
Lcp	left-handed circularly polarized light
MALDI	matrix-assisted laser desorption/ionization
MD	molecular dynamics

MO	molecular orbital
Nle	norleucine
Nip	Nipecotic acid
NMP	N-methyl-2-pyrrolidon
NMR	nuclear magnetic resonance
NRPSs	non-ribosomal peptide synthases
Nva	norvaline
PDB	protein data bank
Rcp	right-handed circularly polarized light
SARS	severe acute respiratory syndrome
SEC	size-exclusion chromatography
SI	signal intensities
SPPS	solid-phase peptide synthesis
TAMRA	5-(and 6)-carboxy-tetramethylrhodamine
TBS	tris-buffered saline
tBu	tert-butyl
TEM	transmission electron microscopy
TFA	trifluoroacetic acid
TFE	trifluoretanol
UV	ultraviolette

Abbreviations of the 20 canonical amino acids are consistent with the biochemical nomenclature proposed by the IUPAC-IUB commission (*European Journal of Biochemistry* **1984**, *138*, 9).

1. Introduction

In nature, biopolymers are the main origin of superimposed information, which are responsible for the most important biologically relevant functions such as molecular recognition, catalysis, and electron transfer. Chemists attempt to understand and apply this information in the design of synthetic polymers. The achievement of such compact structures with specific functions in proteins is a hierarchically pathway, according to which specific arrangement of the functional groups provides tertiary structures with sophisticated functionalities. However, the generation of a specific tertiary structures without identification of unnatural backbones, which are prone to adopt secondary structure, is not possible.[1] The helix is by far the most frequently occurring structural motif in proteins and their synthetic analogous allow many key important biological functions in living systems such as molecular recognition, replication, and catalytic activities. The helical structures in proteins direct the triple helical collagen cable,[2] which provide mechanical strength and stability in bones and tissues; Lac repressor,[3] the regulatory protein required for galactose; the Bak peptide-Bcl-x_L complex[4] that regulates cell processes via protein interactions related to cell apoptosis and gramacidine A,[5, 6] which allows for selective transport of chemicals through the cell membrane.

In all aforementioned cases, only a properly folded protein guarantees the expected function. Remarkably, in spite of the relatively simple organic monomers, the helical peptides are able to be involved in the most important cellular functions. While the covalent interactions between subunits in flexible peptidic chains provide random coil structures, the helical orders are largely stabilized by the presence of weak and reversible non covalent contacts such as hydrogen bonds, solvophobic and electrostatic interactions between the remote parts of the biomolecule. Therefore, the structure formation of biopolymers is a dynamic equilibrium process which depends on the number of these interactions. Accordingly, a minimum number of non-covalent interactions restricting the conformational space are required to compensate for the unfavorable entropy change associated with the folding of the flexible molecules.

Moreover, a huge number of protein-protein interactions use helical interfaces to direct important biological processes including both desirable ones like transcriptional control, cellular differentiation, and replication, as well as non-desirable ones like infections and tumor growth. For example HIV, influenza, and severe acute respiratory syndrome (SARS)

viruses rely on interactions both among their own proteins and with host cell proteins to infect cells. Since such helical interactions determine the specificity for these processes, the selective disruption via peptide-based molecules should be an excellent strategy for drug discovery.

Despite the appreciable advantages of the well-ordered and stable structure of helical peptides, there are two major concerns about the intrinsic properties of native molecules. The intrinsic protease susceptibility of natural peptides as well as the low number of conformations limit the accessible functionalities in α-peptides in general and their clinical use in particular. This fact has motivated the design of oligomers, which have unnatural residues with comparable contact elements to α-amino acids in order to trigger the adoption of natural helical assemblies.

The attempt to generate foldamers[1, 7] (bioinspired oligomers with well-defined conformational properties) that mimic the ability of biopolymers to self-organize and present functional motifs has resulted in successful examples such as a group of foldameric cell penetrating peptides (CPPs), including those based on peptoids,[8] polyproline-based helices,[9] antibacterial β-peptides[10, 11] and cationic β-peptide 14-helices[12]. In the last decade, many research groups have studied the development of various secondary structures in foldamers, which resemble the natural biopolymers. The systematic backbone modifications (isosteric or isoelectronic) and systematic alterations of the repeat units are the most relevant strategies in the design of foldamers. There has been also a growing interest in the foldamer field regarding the backbones of which they are composed. Recent developments include elucidating the sequence specificity of various secondary structures, stabilizing secondary structures in aqueous solution, and creating tertiary structures such as helical bundles. Such efforts have also included the study of peptides based on homologous amino acids such as β- or γ-amino acids.[13]

Peptides composed of homologous amino acids, that are synthetically accessible from the proteinogenic amino acids are at present among the most widely studied foldamers that adopt well-defined helical conformations. The homologous amino acids that have an additional number of methylene groups compared to natural amino acids have much higher torsional freedom compared to α-residue, and therefore result in an expansion of energetically accessible conformational space. The resistance of unnatural oligomers made of homologous amino acids against proteases and their biological activities suggest these unnatural scaffolds as useful tools in peptide and protein mimicry in order to

optimize natural peptide properties. However, still the differences between the packing observed in the resulting artificial quaternary assemblies and that of the corresponding natural assemblies have thus far impeded the combination of both classes into compact protein-like unnatural structures. This fact has encouraged the recent efforts in discovering new design strategies such as application of heterogeneous backbones to expand the structural and functional repertoire of foldamers.

Among different type of foldameric patterns, of particular interest are the βγ-foldamers that based on the theoretical studies have the same hydrogen bonding pattern and helix dipole direction of the native α-helical peptides. Based on this hypothesis and inspired by the principle of "equal backbone atoms",[14, 15] a modular backbone substitution of a trimeric unit of ααα with a dimeric βγ sequence can be applied to the α-helical coiled coil structure. Structural stability and well-defined conformational properties are the important factors in the successful design of any engineered coiled coil with artificial oligomers. Therefore, this project particularly studied the biophysical behavior of foldameric patterns of β- and γ-amino acids and their selectivity in the assembling with natural α-helical partners. As a result, αβγ-chimera will have great potential as a new class of helix-forming unnatural oligomers for application in many biological processes utilizing helix-helix interactions.

2 α-Helical structure

2.1 Characteristics of α-helices

There are usually two substantially populated conformers available for a natural peptide, α and β, which correspond to the allowed conformational space designated by Ramachandran plot for the backbone torsion angles (Figure 2.1). The repetitive β-values in the region of ϕ= -110 to -140 and ψ= +110 to +135 result in extended chains with conformations that allow interactions between closely folded parallel segments. Similarly, the repetition of α-values (ϕ= -57, ψ= -47) for successive α-amino acids results in a helical structure. Moreover, there are some regions in the ϕ, ψ plot not typically occupied. The repetition of certain values in peptidic chains, however, results in an interesting survey of a 3_{10} helix, a π-helix, and a single turn which exists only occasionally in proteins.[16, 17]

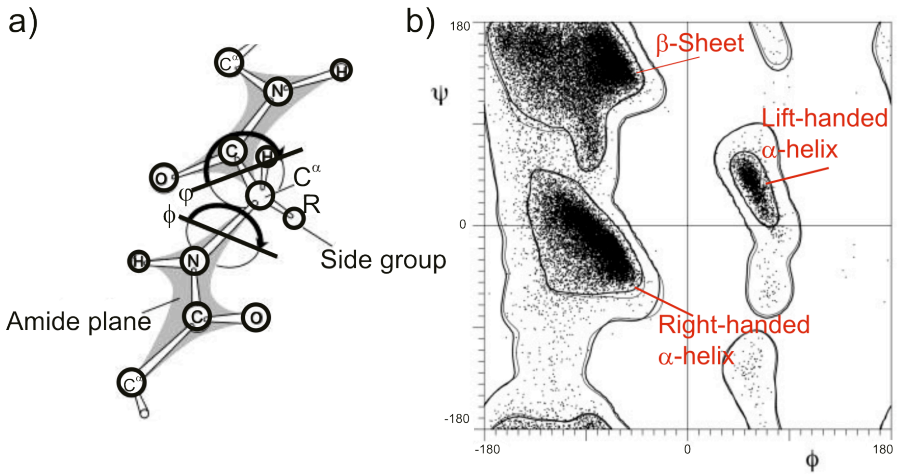

Figure 2.1 *a) The repeating torsion angles along the peptide backbone chain called φ and ψ.*[7] *b) Ramachandran plot (φ,ψ plot), with data points around the global energy minimum for right- and left-handed α-helical backbone conformation as well as the favorable region for β-sheet residues.*

The α-helix is the most abundant secondary structure element in both fibrous and globular proteins, with overall about 30% of the α-residue in protein being present in such structures. It is formed by winding the polypeptide backbone into a right-handed helix with a regular repeat of 3.6 residues per complete turn. The α-helix is stabilized by internal backbone hydrogen bonding which connects the carbonyl group of the *i* residues with the NH of the *i+4* residues.

The stability of the α-helix is mainly controlled by achieving a balance between a favorable enthalpic contribution of the stabilizing interactions and the unfavorable entropic costs from freezing the backbone and side chain atoms in a specific conformational space. The backbone hydrogen bonding and a tight main chain packing are the most important features for the helical stability of the main chain.[18, 19] The helix formation in peptides containing only Ala indicates that the helical conformation is the preferred state of the backbone unless helix-disfavoring factors arise in the side chains and consequently deform the helix or induce a β–strand structure. The side chains pay a significant entropic price for helix formation and predispose segments of the chain toward either α or β regions of the ϕ,ψ map. Depending on the structural characteristics of the side chains, the unfavorable loss in conformational entropy due to the helical folding differs from one residue type to the next. Another factor is the decrease in solvent accessibility of the hydrophobic side chain because of the coil-helix transition. Therefore, some amino acids occur more frequently in α-helices than others (e.g., Ala, Leu, and Glu), and this tendency is known as helix propensity. The side chain-side chain and side chain-main chain intrahelical interactions such as aromatic, electrostatic, disulfide bonding, hydrogen bonding, and hydrophobicity, determine the helical-forming tendency of the sequence. For example: i) Lys residues proximity to the C-terminus and Glu proximity to the N-terminus can stabilize the helical structure mainly due to side chain backbone H-bonding. ii) Ala and Leu experience less entropic penalty from the coil-helix transition compared to Val and Ile.[20] This is expected, as the loss of conformational freedom on restriction of the side chain conformation will not be so acute for the non-branched amino acids, and there will be fewer destabilizing steric interactions with adjacent side chains of the helix. The effects of hydrophobic side-chains upon helix stability can be observed by incorporating helix-inducing unnatural hydrophobic amino acids such as (amino butyric acid (Abu), norvaline (Nva) and norleucine (Nle). Peptides containing α,α-disubstituted amino acids such as α-aminoisobutyric acid (Aib) or 1-amino-1-cyclohexylcarboxylic acid (Ch) tend to be helical. iii) Asn is a helix breaker, whereas the nearly isosteric Leu is a helix former, presumably because Asn is able to stabilize a number of nonhelical conformations through H-bonded interactions.[21]

In the absence of sufficient helix-inducing factors, monomeric α-helices often tend to not be well-defined or long-lived secondary structures and pack together in order to gain additional stabilizations through hydrophobic and electrostatic contacts with other complementary α-helices. In order to maximize the hydrophobic interactions the α-helices

tend to be amphiphilic, that is, they possess an apolar face comprising the hydrophobic residues and a polar face with hydrophilic residues. It is this amphipathic nature that drives two or more helices to associate at their hydrophobic face in order to provide helix-helix packing in the context of the helix bundles.

2.2 Helix-helix interactions

α-Helices constitute the largest class of protein secondary structures and play a major role in mediating protein-protein interactions. Such helix-helix interactions can be found in different architectures from a simple dimeric α-helical coiled coil structure to more complex folding motifs in four α-helix bundles (common among globular proteins), 8α/8β TIM-barrel (common among conserved proteins) and the Rossmann fold (frequently occurring folding motif in nucleotide binding proteins).[22] Protein interactions utilizing α-helical interfaces in particular are involved in the regulation of a wide variety of biological processes. A selection of complexes in which a short α-helical domain targets the biomolecule is shown in Figure 2.2.[23]

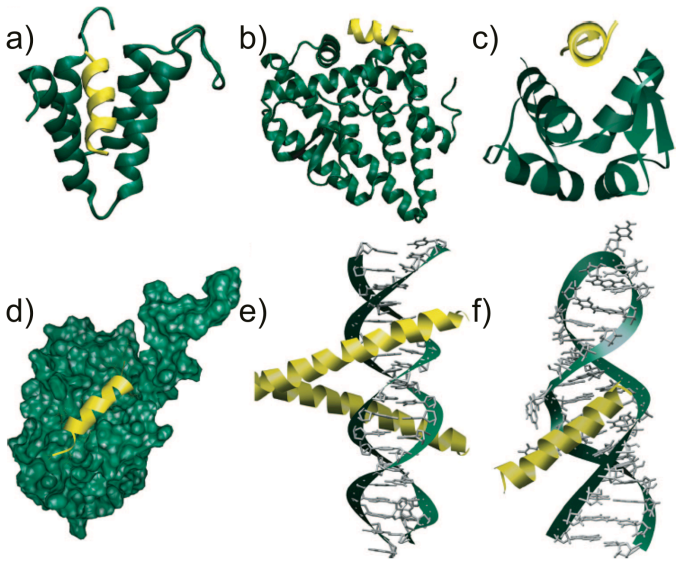

Figure 2.2 *Biomolecular recognition with short α-helices: (a) corepressor Sin3B bound with transcription factor Mad (PDB code 1E91); (b) recognition between Bcl-xL-Bak regulators of apoptosis (PDB code 1BXL); (c) subunit of human estrogen receptor α ligand-binding domain in complex with glucocorticoid receptor interacting protein (PDB code 3ERD); (d) GCN4 region of leucine zipper bound to DNA (PDB code 1YSA); (e) MDM2 oncoprotein complexed with the p53 tumor suppressor-transactivation domain (PDB code 1YCR); (f) α-helix-RNA major groove recognition in an HIV-1 rev peptide-RRE RNA complex (PDB code 1ETF). According to Patgiri et al. with permission, Copyright© American Chemical Society.*[23]

Considering the ubiquitous nature of these relationships and the information that inappropriate helix-helix interactions can lead to disease, it should not be surprising that helix-helix interactions have become an important target for developing therapeutic agents.

2.3 α-Helix mimetics

The application of both peptidic (natural and unnatural) and non-peptidic segments with close similarities to the α-helical fold, in order to display the relevant functionality of such secondary structures is part of the "peptidomimetics".[24-27] While the small molecules often face difficulties targeting the shallow surface of protein interfaces with high affinity and selectivity, short peptidic or nonpeptidic segments with folded subdomains (foldamers) tend to more selectively interact with proteins. Peptidomimetics are valuable tools for identifying natural, biologically active α-helices and form a scaffold to precisely project binding motifs of natural α-helix structure in space (Figure 2.3). The side chain cross-linked, salt bridges, and metal chelates have been reported as approaches to stabilize this conformation in peptides, and they may well impart proteolytic stability to such peptide analogs.[16]

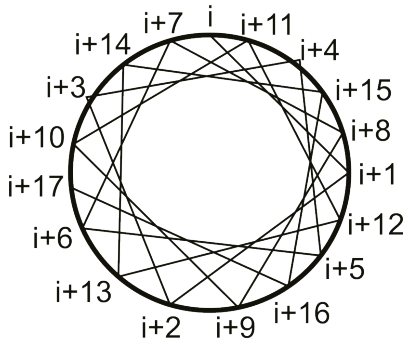

α-Helix, 13-Helix

Figure 2.3 *Helical wheel representation of α-helix illustrating the spatial orientation of side chains.*

Due to the periodicity of the α-helical turns, the side chains of the *i* and *i*+4 residues in each α-helical heptad appear at the same face of the helix, and hence pairs of these residues are amenable to synthetic modification. The induced stability is limited to the modified section so that multiple modifications are required to control the high flexibility of the polypeptide chains.

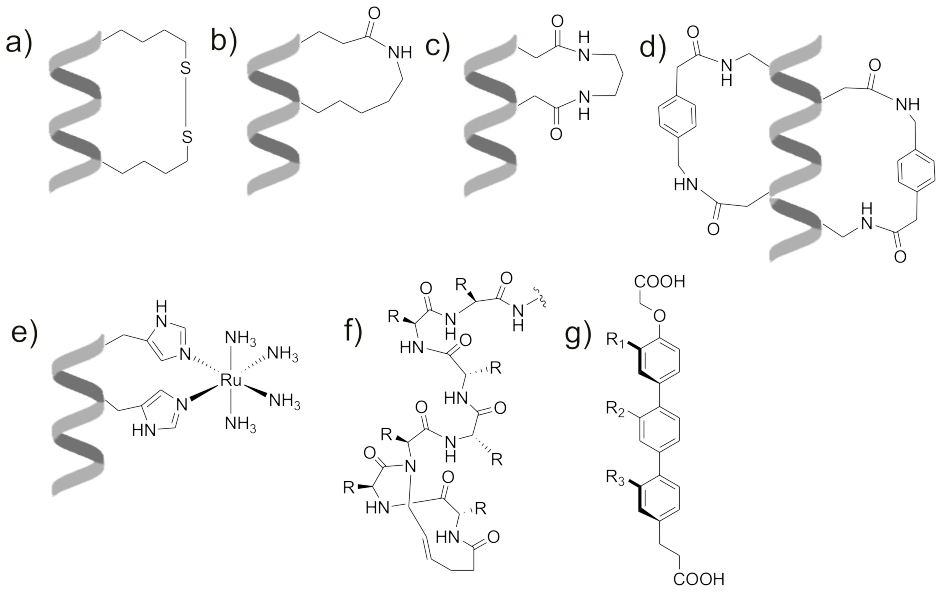

Figure 2.4 *a) and b) Stabilized helical structure by means of disulfide and amide bonds as covalent side-chain cross-linkers. c) and d) Stabilized helices with covalent linkers.[28, 29] e) α-Helix stabilization through binding of Ru(III) by His.[30](a-e are reproduced based on Andrews et al.) f) The hydrogen bond surrogate (HBS) derived α helix.[23] g) Terphenyl helix mimetics.[31]*

The incorporation of disulfide bridge[28,29] via oxidation of Cys residues between *i* and *i*+7 and lactam bridges[30] via amide bond formation between Lys and Asp/Glu residues at *i* and *i*+4, have been the most common methods constraining the conformational flexibility of peptides and locking segments of these peptides into a helical conformation (Figure 2.4a, b).

To date, there are several covalent cross-linkers such as α, ω-diaminoalkanes (1,4-diaminopropane or 1,5-diaminopentane linkers) (Figure 2.4c).[31] Stabilization of helical conformation using two rigid, overlapping *i, i+7* bridges has also been developed a novel and rigid side-chain bridge in which (S)-1,3-diaminopropionic acid (Dap) and Asp side chains in *i* and *i+7* positions in the peptide chain, respectively, are linked by condensation with 4-(aminomethyl)phenylacetic acid (AMPA) (Figure 2.4d).[32] Additionally, the binding of transition metals by appropriate residues can be used in the stabilization of helical peptides. For example, the interaction between ruthenium salts and His residues imparts remarkable stability to the helix via the formation of an exchange-inert complex (Figure 2.4e).[33] Main chain hydrogen bond surrogate (HBS) is another advanced strategy which features a carbon-carbon bond derived from a ring-closing metathesis reaction in place of an N-terminal intramolecular hydrogen bond between the peptide *i* and *i+4* residues (Figure 2.4f).[23] The HBS approach was devised to afford internally constrained helices so

that the molecular recognition surface of the helix and its protein binding properties are not compromised by the constraining moiety. In a different approach the secondary subdomain is replaced by unnatural synthetic or peptidic oligomers as helix mimetics that potentially participate in selective interactions with biomolecules.

Non-peptidic scaffold were also reported with the ability to project side chain functionality with similar distances and angular relationships to those found in α-helices [34] (e.g. terphenyls, terpyridines, enaminones, terephthalamides, trisbenzamides, trispyridylamides). Figure 2.4g depicts the side chain arrangements in terphenyl/terpyridine family which superimpose the *i*, *i*+4 and *i*+7 side chain positions of highly α-helical poly-Ala.[35] Synthetic peptides comprising β- and γ-amino acids are known to favor helical conformations which are structurally similar to the α-helix, and hence their incorporation in the design of α-helical mimetics has been investigated.[36] Finally, the helical structure can also be induced through oligomerization even if the individual artificial molecules are fully or partially unstructured and a classical example of that is the coiled coil formation.

3. Foldamers

3.1 Concepts

The term foldamer is defined as unnatural oligomer that folds into a conformationally ordered state in solution, and is stabilized by a collection of noncovalent interactions between nonadjacent monomer units.[1, 7] Foldamer research is motivated by the fact that folding into a specific compact structure is the key to many biological functions such as molecular recognition and binding.[1] Considering the masterful control over non-covalent forces that nature exhibits in biological macromolecules, it should be possible to design artificial backbones capable of similar functions. Since the non-covalent forces such as hydrophobic, hydrogen-bonding, electrostatic and van der Waals are common interactions in both natural and unnatural oligomers, certain non-natural polymers/oligomers are also able to adopt well-defined structures.[37] In the past decade, many research groups focused on a rich diversity of novel unnatural backbone structures capable of conformational properties as well as on the synthesis and analysis of such unnatural oligomers. Another motivation beyond the evaluation of artificial backbones that cannot be degraded by nature, was to overcome the intrinsic in vivo susceptibility of biopolymers.

An early short list of such oligomers includes poly(pyrol/imidazole) DNA-binding oligomers[38,39], aromatic polyamides,[40-42] N-alkylglycines (peptoids),[43, 44] aedamers (aromatic oligomers) [45], oligo(phenylene-ethylenes)[46] and nucleic acids with alternative sugar[47, 48] and peptidic[49, 50] backbones. The structural simplicity and relatively easy synthesis of many foldamers allow them to be used as three-dimensional scaffolds for various biological applications. The functional foldamers target a number of molecular and biological molecules such as RNA, proteins, membranes, and carbohydrates, often binding with affinities approaching or equaling those of natural biopolymers.

The design of a foldameric sequence can be categorized as “top-down” [51] or “bottom-up”[52]. The “top-down” approach starts with a native peptides and attempts to reengineer its structure with unnatural oligomers to perform new functions. The “bottom-up” design starts with the already designed building blocks and assembles them in order to endow the native-like structures and functions. To date, a considerable progress has been made to modify biological systems whose design is primarily based on a top-down approach. This method more in particular refers to the process of making one or a relatively small number of mutations in a natural sequence to enhance, elucidate, or mimic their structure and properties. The mutations can be applied either rationally or combinatorially, and are guided by computational methods and searches. At the other extreme, bottom-up design refers to attempts to mimic biological structure and properties by backbones that bear little resemblance to natural chains (mainly abiotic foldamers).

Two important concepts in the top-down approach are positive and negative design. In positive design, sequence to structure rules are used to direct the formation and stabilization of the foldameric structure, whereas negative design refers to an idea of designing against alternative and often competing natural structures. Both design methods aim to develop unique structures that exhibit similarity in the components and mechanisms of biochemical systems. The designed foldameric sequences are classified, with regard to the structure of the backbone repeat unit, into two categories: first, abiotic foldamers that utilize aromatic, charge-transfer, and other type of interactions, and are not common in nature; and second, bio-inspired foldamers that can be divided into nucleotidomimetic and peptidomimetic. These two latter mentioned classes are inspired by the structure of proteins and nucleic acids, being mainly based on modification of the chemical structure of the monomer (amino acids and nucleotides).[53] Peptidomimetic foldamers are among the most intriguing models of unnatural oligomers and are the particular interest of this work.

3.2 Peptidomimetic foldamers

There is a growing interest in peptides as drugs. Peptides have evolved in nature to take on highly specific functions, work with great potency, and are far smaller than recombinant proteins. But they are inherently unstable and suffer from storage and stability problems *in vitro* and degradation *in vivo*. Since peptidomimetic compounds are unlikely to be substrates for the enzymes that degrade the polymers, it is expected that such non-natural structures will be more stable than their natural counterparts.[54] Peptidomimetic strategies include the modification of amino acid side chains, the introduction of constraints to fix the location of different parts of the molecule, the development of templates that induce or stabilize secondary structures of short chains, the creation of scaffolds that direct side-chain elements to specific location, and the modifications of peptide backbone. Of these strategies, systematic backbone modifications are most relevant for the field of foldamers. Efficient monomer preparations have recently been developed for many biologically inspired, unnatural chain molecules.[55] Backbone modifications may involve an isosteric or isoelectronic exchange of units or introduction of additional fragments. Among these particular modified systems the non-natural oligoamides built from backbone-modified α-amino acid residues (e.g. peptoids)[44] and higher homologues (e.g. β-, γ-, and δ-peptides)[37] are the epitomes of peptidomimetic foldamers. These foldamers, and in particular those containing β- and γ-amino acid more closely resemble conventional α-peptides, mainly because their building blocks represent the smallest step away from α-amino acids in backbone space. A substantial increase in the number of backbones with known folding propensities came from the exploration of various β-[13,56,57] and γ-peptide[58] families. [1, 54, 59]

3.3 Peptidomimetics through homologation strategy

A variety of peptidomimetic strategies is centered on the development of templates that mimic or stabilize several common architectural elements of peptide and protein structure, e.g. β-turns, α-helices, and β-sheets due to the replacement of individual peptide bonds by nonpeptidic ones. This has been done by defining structural scaffolds that favor certain conformations, and then by incorporating these into a sequence, or replacing a sequence by a constrained structure. These peptide surrogates are complemented by the synthesis of peptides incorporating unnatural amino acids and will probably require isosteric

replacements, and conformational constraints as logical steps in the process.[60] These compounds bridge the gap between simple peptide analogs and completely nonpeptidic structures.

A large range of noncoded amino acids have been applied to generate analogs of biologically and structurally interesting compounds. A new and promising dimension to the field of biomimetic structures has arisen through the creation of structures that incorporate backbone expanded β- and γ- residues, that are synthetically accessible from the proteinogenic amino acids.[58, 61-64] On the other hand, certain β- or γ-amino acids are naturally synthesized in cells, and are incorporated into many biologically active compounds frequently isolated from plants or marine organisms (Figure 3.1),[54] however, there are no ribosomally synthesized proteins that contain β- or γ-residues. Instead, their biosynthesis takes place in non-ribosomal peptide synthases (NRPSs) which is capable of processing not only the proteinogenic amino acids, but also a great range of non-proteinogenic β- and γ-amino acid derivatives.[65]

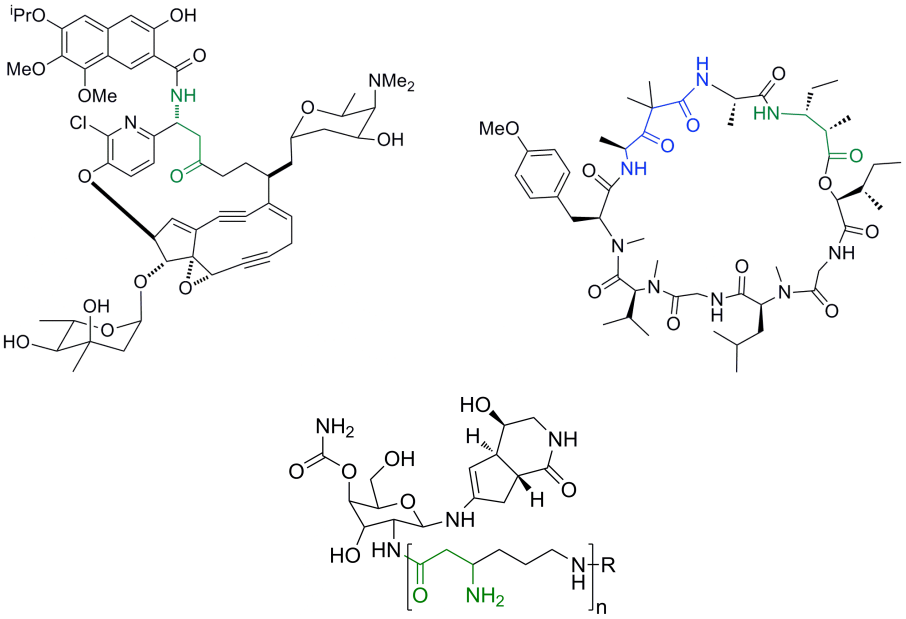

Figure 3.1 *Some natural products containing β- and γ-amino acid building blocks. Left-top) Kedarcidin belongs to antitumor antibiotic family and contains a β-amino-β-arylpropanoic acid residue.[66] Right-top) The natural cyclic depsipeptide dolastatin 11 contains β^3 and one γ-amino acid residues.[24,67] Bottom) Nourseothricins possess a broad activity spectrum (against viruses, bacteria, fungi, insects, fish), but are toxic for mammal. These nucleoside peptides contain a poly β-lysine chain of variable lengths attached in amide linkage to the amino sugar moiety gulosamine of the nucleoside.[68] The side chain made up of ε-peptide-linked βhLys units is typical. β– and γ-esidues are highlighted green and blue, respectively (reproduced based on Seebach et al.).[54]*

Homologated amino acids are defined as residues in which a variable number of backbone atoms are introduced between the terminal amino and carboxylic acid groups involved in amide bond formation. The insertion of additional atoms between the flanking peptide units enhances the number of degrees of torsional freedom, resulting in an expansion of energetically accessible conformational space.

For example, in the β- and γ-amino acid residue, local backbone conformations are determined by values of three (φ, θ, ψ) and four (φ, θ_1, θ_2, ψ) torsional variables, respectively, while for the α–residue, the number of torsional variables is two (φ, ψ) (Figure 3.2a). On the basis of the known high flexibility of glycine-rich peptides, one might expect such extended backbones to possess too much flexibility and, therefore, to be entropically unable to acquire ordered conformations.

In contrast to this view, certain substitution patterns in homologated amino acid families impart a strong bias against most of the possible torsional energy surfaces, enabling the formation of certain regular conformations. Substitution at the backbone carbon atom in amino acids can result in the creation of new chiral centers, which can then highly restrict the torsional freedom and, in turn, the stability and handedness of folded backbone conformations (Figure 3.2b).[69]

Large numbers of mono-substituted β- and γ-residues, especially those with bulky substituents adopt gauche conformations, which are required for helical or turn like conformations. On the other hand, a trans rotamer leads to a fully extended conformation and is readily accommodated into β–strand structures. The conformational space can be further restricted by different strategies:

- Di-substitution: C^2-C^3 substituted residues are more conformationally constrained compared to the mono substituted residues and favor antiperiplanar torsion angles for the threo isomer and consequently extended chains in this case, while the erythro isomer is more prone to adopt the synclinal torsion angles[70] necessary for helical folding in the backbone.

- Geminial substitution: Going from the C^α unsubstituted Gly gradually to the monosubstituted residue Ala and disubstituted residue α-aminoisobutyric acid, Aib dramatically decreases the sterically allowed regions of φ, ψ (Ramachandran) space. Likewise, geminally (gem) disubstituted β- and γ-amino acids have shown extremely valuable features of novel folding patterns in hybrid sequences. The

presence of geminal substituents efficiently restricts the torsional freedom and primarily directs to gauche conformations (Figure 3.3a).[69, 71]

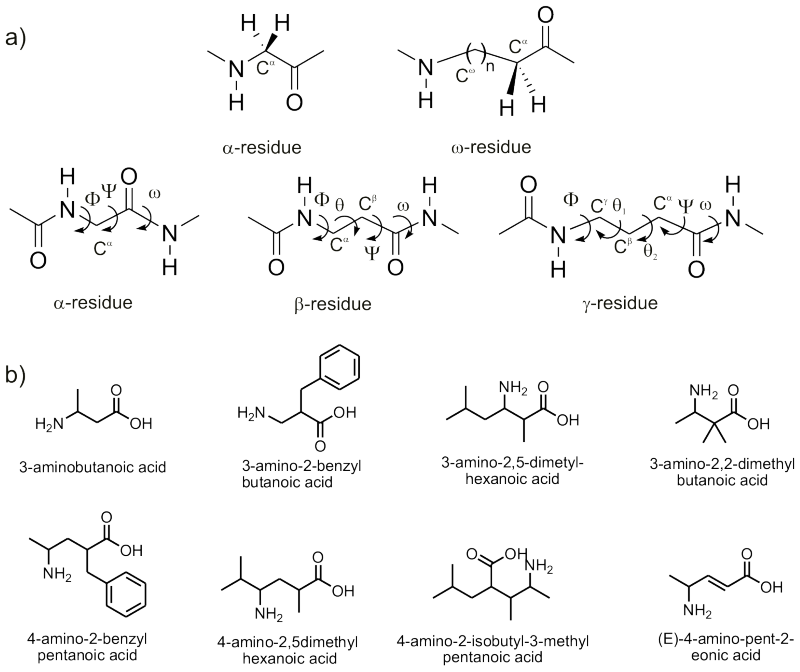

Figure 3.2 *a) Chemical structure of α- and ω-amino acid residues (top) and definition of the backbone torsion angles of residues (bottom).The number of torsional variables is also indicated. b) Synclinal and antiperiplanar conformations about the C_α-C_β bond of β-amino acid residues.*[7,69]

- Cyclization: Accessible conformational space can also be restricted by side chain backbone cyclization. Gauche-type torsion angles are even more promote to contain three, four, five, or six atoms which were applied first by Gellman.[72-74] Crystallographic characterization of Gellman's β-oligomers containing residues such as *trans*-2-aminocyclohexanecarboxylic acid (ACHC), *trans*-2,5-diaminocyclohexanecarboxylic acid (DCHC), *trans*-2-aminocyclopentane-carboxylic acid (ACPC), or *trans*-3-amino-pyrrolidine-4-carboxylic acid (APC), revealed that the dihedral angle is constrained to conformation close to the gauche form (Figure 3.3b,c).[7,69] The ring size determines the precise C^2-C^3 torsional preference, which in turn influences the helix type.

As described above, the effective conformational constraints on backbone torsional freedom can be introduced by both strategies of substitution and backbone-side chain cyclization, in order to achieve distinct conformations. However, only specific

conformational constraints result in helical structures.

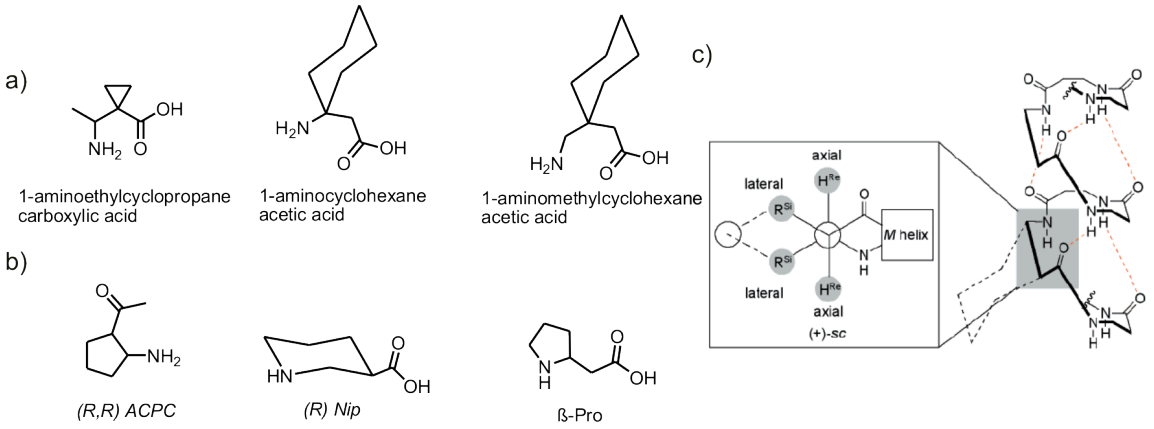

Figure 3.3 *Examples of β and γ-amino acid residues in which torsional freedom has been restricted using a) geminal dialkyl substitution and b) side chain backbone cyclization. c) Synclinal conformation about the C_α-C_β bond of trans-ACHC residue.*[7,69] *According to Hill et al and reproduced with permission, Copyright© American Chemical Society.*

As Vasudev et al. have described, the geminally substituted Ac_6c and its β- and γ-amino acids derivatives behave differently in comparison to the cyclic β-amino acids. The cyclic residues largely support helical conformations and can also be readily accommodated into hybrid helical structures.[69] In contrast, the gem dialkyle substituents are almost entirely restricted to nonhelical conformations.

It seems likely that the use of cyclic β- and γ-amino acid residues described above, instead of α-residues, offer enhanced helix stability, because the covalent ring promotes the appropriate backbone torsion angles. The rigorously unnatural β- and γ-peptides built of cyclic homologous amino acids have been shown to some extent to fulfill the structurally and sterically less sharply defined interactions that result in the antiproliferative[75] and antimicrobial[10,76,77] effects. Although, for such an unnatural backbone to be able to perform the peptidomimetic activity (e.g. bind to well-defined α-peptidic receptors), it is particularly important to use compounds possessing the natural proteinogenic side chains, as these often make a decisive contribution to the docking, and hence to the affinity for the receptor.[54] Namely, there are many reported helical mediating epitopes, and their highly selective recognition depends on the specific side chain alignment against the residues on the surface of the binding site.[78] Therefore, only foldamers bearing the same overall distribution of physicochemical properties as exist in natural folding motifs have been shown to mimic the biological activity.

Inspired by the advantages and disadvantages of constrained residues, the design of chimeric foldamers composed of different monomer types has received considerable attention and complementary benefits: the constrained unnatural residues provide conformational preorganization, while the non-constrained natural or unnatural residues allow facile introduction of side chains at specific positions.[79]

The β- and γ-foldamers can mimic the regularly repeating structures analogous to naturally occurring secondary structures such as turns, helices, and sheets while enhancing resistance to enzymatic degradation relative to a conventional α-peptide. The investigation of β-, γ-peptidic foldamers consisting of acyclic β- and γ-amino acids,[80,81] of F-substituted[82] β-amino acids, and cyclic β-amino acids (cyclopentane/pyrrolidine derivatives)[77,83] revealed their relative resistance towards proteolytic enzymes of all kinds (endo- and exopeptidases, serine-, threonine-, cysteine-, aspartyl-, or metalloproteases, -peptidases, or amidases). This is namely due to their different side chain spacing, as compared to natural α-peptides.[54] Furthermore, none of the investigated peptides has the side chains next to amide bonds in the same spatial arrangement, as do natural α-peptides. The inherent advantage of enzymatic stability suggests the foldameric sequences made of β- and γ-residues are very promising candidates for active-substance research.

3.4 Structural diversity of β- and γ-peptides

Extensive studies on poly β- and γ-amino acids revealed evidence for ordered conformations in both solution and solid states.[54] Similar to the secondary structures formed by polypeptide chains, the conformations adopted by poly β- and γ-amino acids are principally based on the intramolecular hydrogen bonding as a dominant force in determining folded conformations.

On the other hand, it has to be considered that hydrogen bonded attractive interactions are not always favored. The nearest neighbor interactions between amides in hybrid peptides could dominate the potential energy surface by providing torsional strain in the segment linking the two amide groups and consequently be against the formation of long-range conformational order. Hence, γ–peptides appeared to be less suitable than β–peptides for foldameric patterns since they are conductive to nearest neighbor hydrogen bonding.[7, 84]

However, there are useful design elements in the case of γ-peptides, such as amide-stacking, which energetically compete with nearest neighbor H-bonding and facilitate conformational control.[85] Furthermore, the dihedral preference of the homologated β- and γ-amino acid can influence the conformations in short chains. The importance of torsional bias can be inferred from the crystal structure of the β^3-tripeptide *t*-Boc-β^3-HVal-β^3-HAla-β^3-HLeu-OMe reported by Seebach.[80] It is apparent that the bulky substituent imposes a tight turn. Unlike short α-peptides segments, the β- and γ-oligomers with hexameric or tetrameric sequences are able to adopt different stable conformational choices, which are likely to be influenced by the nature of cooperative hydrogen bond interactions formed in the folded conformation of the hybrid peptides.[7, 59]

The accommodation of homologous amino acids in extended strand structures is favored when the backbone torsion angles adopt values close to 180° (trans conformation).[69] There are in principle two types of polar and apolar sheet secondary structure available for peptides containing backbone expanded amino acids in contrast to the corresponding structures derived from α-amino acids, which have a regular alternation of orientation of amide groups.[86] In polar sheet structures, one face presents acceptor CO groups (Figure 3.4a, b) while the other presents donor NH groups and each residue has an anti C_2-C_3 torsion angle. In apolar sheets CO and NH groups are alternating and each residue has a gauche C_2-C_3 torsion angle (Figure 3.4c).[86,87] The polar sheet formation is property of those with an even number of backbone atoms between CO and NH groups. Examples of both parallel and anti-parallel sheet formation have been demonstrated in the crystal structures of several short amino acids containing peptides.[88,89]

Homologated amino acids can also be inserted into a turn-like conformation, either to generate helical structures by continuously repeating or to promote chain reversal for generating β-hairpin structures. Helices represent one of the most common structural motifs in nature.

One third of all protein residues adopt an α-helical conformation, leading to many foldameric designs that mimic the helical structure and function. Inspired by the biological helices and functions, the helical architectures in synthetic oligomers and particularly in β- and γ-peptides are promising to emerging opportunities for applications to specific functionalities. Considering the importance of intramolecular hydrogen bonding in determining the local conformation, a broad range of hydrogen bonded ring sizes with

opposing directionalities of hydrogen bonds for β- and γ-oligomers results in greater conformational versatility compared to α-amino acid peptides.

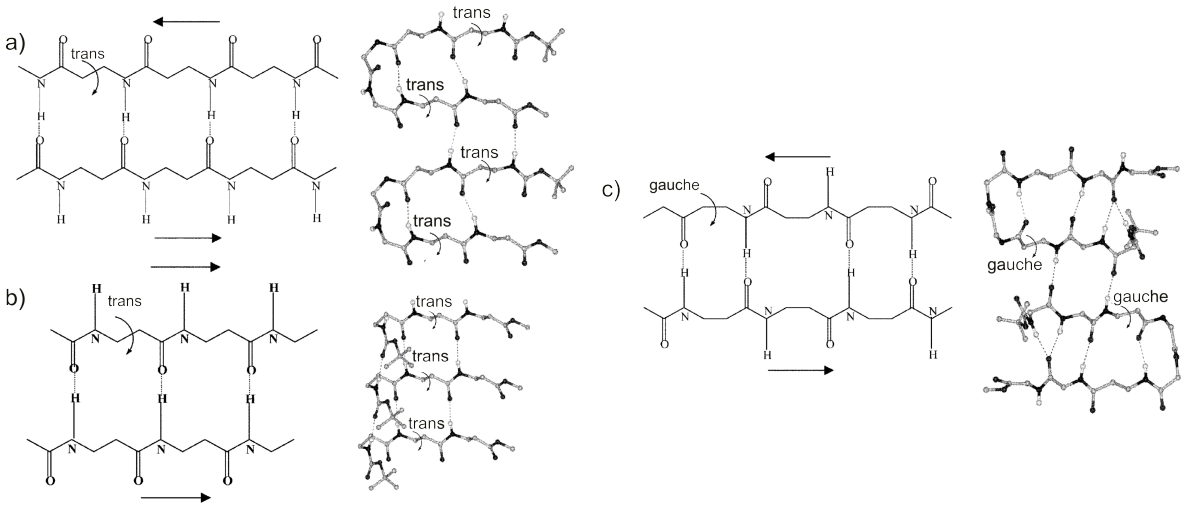

Figure 3.4 *Schematic representations of two proximal strands of β-peptides: a) The arrangements of antiparallel β-sheet when the β-residue adopts the trans conformation. b) The parallel association of β-strands formed by β-residues when the β-residue adopts the trans conformation. c) The antiparallel β-sheet, when the β-residue adopts the gauche form. According to Sengupta et al. reproduced by permission of The Royal Society of Chemistry.*[86]

3.5 Helical conformation in β- and γ-family

Hydrogen bonds in helical structures of peptides containing α-amino acids have the directionality *i*, *i*+3 for a 3_{10} helix, *i*, *i*+4, for an α-helix, and *i*, *i*+5, for a π-helix. This results in hydrogen bonded ring sizes of 10 atoms (C_{10}), 13 atoms (C_{13}), and 16 atoms (C_{16}). The extension of the backbone in β- and γ-residues increases the possible H-bond patterns (Table 3.1).

Among the β-peptide helical conformations the 14-helix is a particularly stable and frequently observed conformation in synthetic β-peptides, which is reasonably similar to the α-helix in its overall dimensions. The 14-helix is stabilized by hydrogen bonding between NH(*i*), OC(*i*-2) and has approximately three residue repeat (βββ) per turn. Similar to natural α-helices, the 14-helix can be stabilized by disulfide bridges[90] or electrostatic interactions between oppositely charged residues one turn apart (positions *i*, *i*+3 in 14-helix versus *i*, *i*+4 in α-helix)[76]. The stability of the 14-helix conformation was shown to be

pH dependent.[91]

Table 3.1 *Conformational characteristics of typical helices composed of α-, β-, and γ-amino acids.*

Helix type	*Residue repeat*	*Atoms in hydrogen bond ring*	*Residues / turn*	*H-bond directionality* [a]
3_{10}-helix	αα	10	3.0	(4 → 1)n
α-helix	ααα	13	3.6	(5 → 1)n
12-helix	ββ	12	2.6	(4 → 1)n
14-helix	βββ	14	3.1	(1 → 3)r
14-helix	γγ	14	2.4	(4 → 1)n
11-helix	αβ	11	3.1	(4 → 1)n
12-helix	αγ	12	4.3	(4 → 1)n
13-helix	βγ	13	2.1	(4 → 1)n
14-helix	ααβ	14	8.2	(5 → 1)n
15-helix	ββα	15	9.7	(5 → 1)n
11/9-helix	αβ	11 and 9	2.8	Mixed
12/10 helix	αγ	12 and 10	3.9	Mixed

[a] Helices with normal and reversed directionality are designated with n and r, respectively.

Indeed, the CD intensity was shown to reach a maximum at a pH value in which the salt bridge existed. Similar aspect to natural constructs is the 14-helix promoting effect of specific side chains (e.g. the γ-branched β^3-amino acids such as β^3hVal and β^3hIle).[92] Despite the similarities found between a 14–helix and an α-helical construct, the overall structure of the 14-helix differs from that of the α-helix in many respects. The 14-helix has an opposite direction of the helix macrodipole (Figure 3.5a)[93] and slightly wider radius as well as a shorter rise for a given chain length than the α-helix.[94]

The 12-helix is interesting from the perspective of mimicking α-helices among conventional peptides and proteins. The internal hydrogen bond orientation and macrodipole of the β-peptide 12-helix (*i*, *i*+3 COHN hydrogen bonds) are analogous to α-helix (*i*, *i*+4 COHN hydrogen bonds) (Figure 3.5b, c).[93] In contrast, the hydrogen bond orientations of other β-peptide helices (e.g., *i*, *i*-2 COHN hydrogen bonds for the 14-helix and alternating *i*, *i*-1 COHN and *i*, *i*+3 COHN hydrogen bonds for the 10/12-helix) are not observed in α-peptide

helices. The β-peptide 12-helix has been found mainly with constrained cyclic residues containing five membered rings such as *trans*-2-amino-cyclopentanecarboxylic acid (ACPC).[38] The cyclohexyl ring of *trans*-cyclohexyl amino acid (ACHC) stabilizes the θ torsional angle to a value near ±60 which specifically stabilizes the 14-helical conformation. The smaller ring size of ACPC biases θ toward larger values, providing the 12-helix, as the most favorable helical conformer. Peptides with alternating β^2- and β^3-monosubstituted amino acids can adopt the 10/12 helix conformation. The 10/12 helix consists of an intertwined network of 10- and 12- membered hydrogen-bonded rings. The 10-atom ring amides are approximately perpendicular to the helical axis, while the 12-atom ring amides are nearly aligned with the helical axis. This fact results in a smaller helix dipole compared to the other helical conformations. β-Peptides containing three and four membered ring constituents have shown inherent preferences for different helical conformation, 8- and 10-helices respectively.[13]

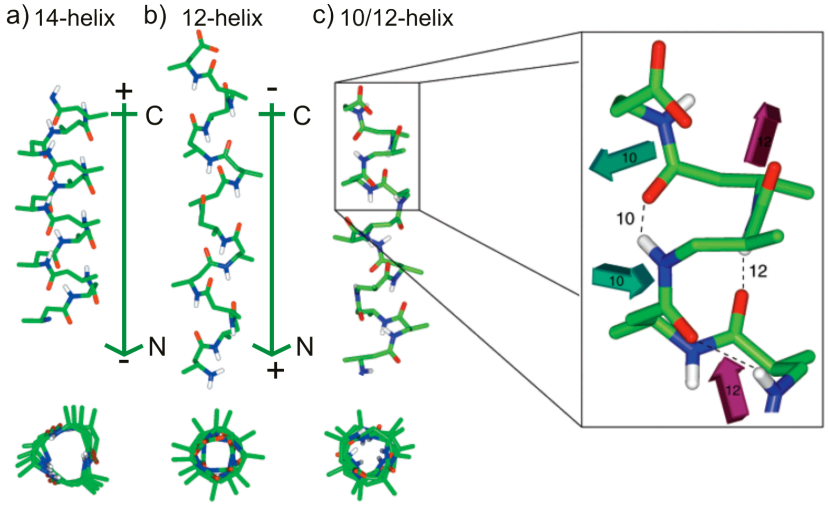

Figure 3.5 *a-c) Comparison of 14-helix, 12-helix, and 10-12 helix. Carbon atoms are shown in green, nitrogen in blue, and oxygen in red.[13,91,93] According to Cheng et al. with permission, Copyright© American Chemical Society.*

The added torsional degrees of freedom in γ–amino acids would be expected to promote conformationally disordered chains. However, as is the case for β–peptides, γ-peptide sequences form remarkably stable helical conformations in solution. As noted by both Seebach and Hannessian, the conformational analysis of short γ–peptides revealed a right-handed (similar to α-peptides) 14-helix structure with 2.6 residues per turn in solution (Figure 3.6).[63, 95] There are obvious differences, however, in these two constitutions. In the

case of β–peptides, the 14-helix results from the N-H of residue *i*-2 being donated to the carbonyl of residue *i*, while in the case of γ-peptides the H-bond results from *i*, *i*+3, so that the direction of dipole moment is reversed.

The application of γ-amino acids expands the foldamer library due to many substituent patterns and stereoisomers, which are possible for γ-peptides. The possible well-formed conformations in γ-peptides acids are considerably limited, however, because of nearby H-bonding interactions. This fact can be avoided entirely or partially with the insertion of other natural or unnatural subunits in continuous sequences of γ-amino acids resulting in chimeric helices, e.g. $(\alpha\gamma)_n$, $(\beta\gamma)_n$ (please see next section).

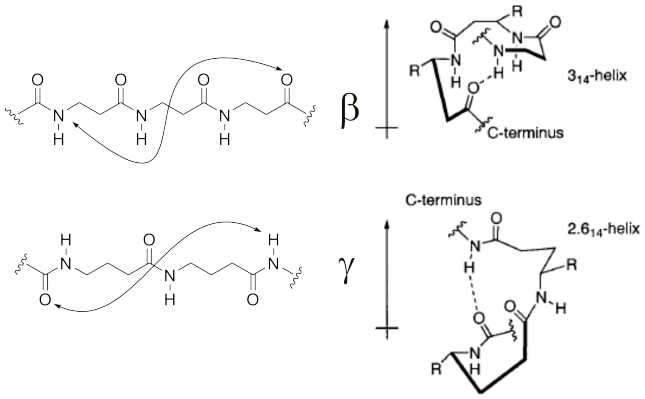

Figure 3.6 *Comparison of 14-helix conformation in β- and γ-peptides.*[91] *Reproduced with permission, Copyright© American Chemical Society.*[7]

3.6 Mixed and chimeric helices: heterogeneous backbones

The backbone heterogeneity offer several advantages over homogeneous backbone counterparts, including access to many new conformational structures based on variations in the stoichiometries and patterns of the subunit combinations as well as side chain diversification.[27] A general approach for heterogeneity in oligoamides is to mix two or more types of ω-amino acid residues in an alternating fashion. Such chimeric patterns can be divided into two conceptually distinct classes. The first includes entities prepared using a "block" strategy, in which segments of unnatural subunits are combined with natural segments comprising α-amino acids to form a hybrid oligomer or, in other words, the replacement of a specific element of protein secondary structure with an unnatural subunit.[28] For example, this approach has been used to replace the C-terminal α-helical

segment of interleukin-8 with a helical segment composed entirely of β-amino acid residues; the resulting chimeric molecule retained weak signaling activity.[96] Gellman and coworkers applied chimeric oligomers in which either the N-terminal portion or the C-terminal portion of αβ peptides are replaced by an α-amino acid segment resulting in (α+αβ) patterns. The new chimeric peptides have shown to inhibit efficiently the Bcl-x_L/Bak interactions.[97]

In the second approach the unnatural subunits are scattered in a regular pattern throughout an oligomer sequence. Multiple approaches, either experimental or theoretical, have been considered to define the ensemble of helical conformations formed by new chimeric hybrid backbones composed of multiple ω-amino acid residue types. Oligomers with periodicity at the level of dimer (e.g. αβ[98, 99], αγ[100], βγ[101] peptides), trimer (e.g. ααβ- and ββα-peptides)[99], tetramer (αααβ repeats) or heptamer (ααβααaβ, ααβαβαβ)[59] have been studied (Figure 3.7).[102] As already confirmed by several studies on chimeric foldamers composed of extended backbone residues, there are numerous representatives for helices with exclusively forward or backward directions of the hydrogen bonds and mixed helices. Although only the most stable backbone-folding patterns have a chance to be formed in solution, the knowledge about all possible conformers may be a good basis for a selective structure design by the introduction of structure-promoting substituents or backbone cyclization. Thus, the unstable backbone conformers may be preferable to others, which were originally rather stable.[103]

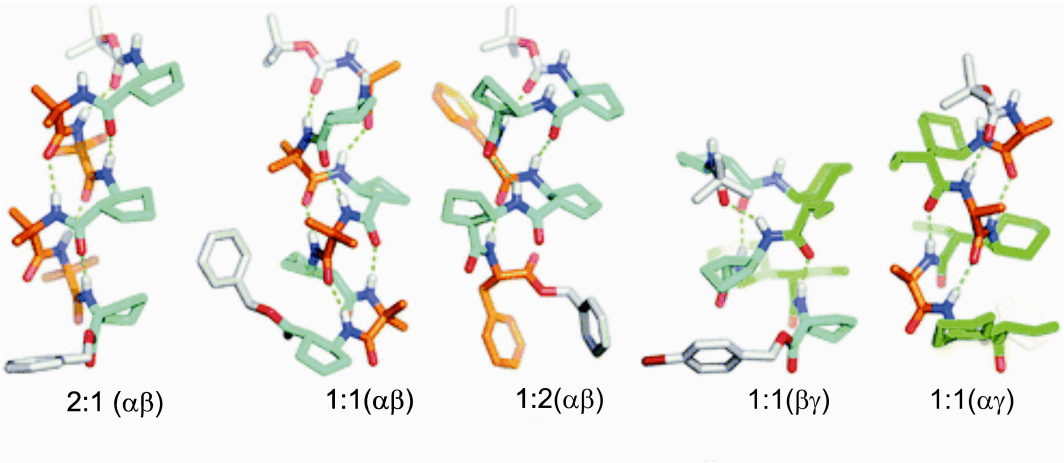

Figure 3.7 *Representative crystal structures of helical heterogeneous peptide backbones composed of various ratios of α-, β- and/or γ-amino acid residues. Carbon atoms of α-, β- and γ-amino acid residues are shown in orange, cyan and green, respectively. According to Guichard and Huc[102], reproduced by permission of The Royal Society of Chemistry.*

The heterogeneous backbones may adopt a mixed helical conformation. In contrast to

common periodic peptide helices in which all backbone CO bond vectors point in the same direction, a unique feature of most mixed helices is the alternating direction of the CO bonds along the sequence.[103] Such mixed helices have thus only a small resulting macrodipole which implies that they are energetically disfavored in a polar environment compared with common periodic helices that have their H bonds oriented in the same direction. However, some mixed helices occasionally (10/12-, 14/15-, 12/10- and 11/13-mixed helices in $\beta^2\beta^3$-, $\alpha\beta$-, $\alpha\gamma$- and $\beta\gamma$-hybrid peptides, respectively)[79, 104-106] have a considerable stability in a polar environment and represent competitive folding patterns.

The heterogeneous sequences comprising α- and β-amino acids are the most studied class of this type. The initial designs of $\alpha\beta$-peptides were composed of conformationally constrained β-amino acid residues such as ACHC and ACPC.[79, 106] Detailed NMR analysis of such chimeric peptides revealed a complex pattern that could be explained by assuming rapid interconversion between two helical conformations, namely a 11-helix and a 14/15-helix. Increase in chain length seems to favor the 14/15 helical shape relative to the 11-helix. The analogy to α-peptides which also show chain length-dependent conformational transition between 3_{10} helix and α-helix is striking. Foldameric behavior is not limited to a 1:1 $\alpha\beta$ residue alternation but 2:1 and 1:2 $\alpha\beta$ backbone patterns have also been shown to support helix formation in short oligomers.[99]

The mixing of the extended backbone units may result in the equivalence of the nature of the hydrogen bonded rings observed by homogenous peptides such as α-, β-, γ-peptides. Thereby these chimeric peptides have been shown to exhibit close relationships to typical secondary structure elements of these homogenous peptides. Such relationships are expected when comparing the basic dipeptide units of the $\alpha\gamma$-hybrid peptides with those of β-peptide sequences and when comparing $\beta\gamma$-dimers with α-peptide trimers. In the $\alpha\gamma$-hybrid peptides, the 12-, 10/12- and 18/20-helices are the most stable helices in an aqueous medium, for both β-peptides and $\alpha\gamma$-hybrid peptides. Of particular interest are the $\beta\gamma$-hybrid peptides, which, similar to native α-peptides, belong to helices of the 13-helix group, and their secondary structures correspond formally to the well-known α-helix.

3.7 Natural α-helical coiled coil versus artificial helix bundles

A peptide molecule may assemble with other appropriate molecules to form a complex with a defined structure and function that is sometimes far different from one with unfolded

or otherwise folded individual peptides. Therefore, assembly and aggregation are among the strategies to induce a distinct structure especially to unstructured artificial systems.[107] A classical example for peptide assembly is the leucine zipper, which is a common motif found in fibrous proteins, most membrane proteins, as well as in a wide range of globular proteins. In nature, the coiled-coil motif is employed to perform a diverse array of functions, including structural roles, for example, in cytoskeletal proteins and DNA transcription factors, and dynamic roles such as pH sensitive hinges that control the release of viral constituents into cells.

In order to assemble into a coiled coil folding motif, two or more α-helical peptides interdigitate in a rope-like manner, which result in a slight winding of each individual helix that there are 3.5 residues per turn of helix. Thus, seven residue positions define two turns of a helix and the positions are labeled by convention with the letters, *a, b, c, d, e, f,* and *g*.[108, 109] The first *a* and fourth *d* positions are predominantly occupied by hydrophobic residues and form the inner-face called the hydrophobic core, while the *e* and *g* positions frequently consist of polar or charged residues, packing the electrostatic interface (Figure 3.8a).[110-112]

The specificity of the binding is due to the arrangement of the hydrophobic residues at *a*, and *d* positions (e.g. leucine, isoleucine, or valine), which interact with the hydrophobic residues of another coiled coil forming peptide (*a'* and *d'*), thereby gluing the helices together via hydrophobic contacts. The packing of the helices is guided by the "knobs-into-holes" principle, according to which knobs of each peptide strands fit into holes formed by other hydrophobic side chains on the same and adjacent strands.[113] Two stranded coiled coil structures with chains parallel and in register are the general characteristic, although the hydrophobic volume and rigidity of the side chains mediate the switch between the dimer, trimer, and even higher order conformations in order to achieve an optimum side chain burial at the hydrophobic core. In the trimeric and tetrameric helix bundles the interlocking knob-into-holes packing interactions are extended to *e*, *g* position in each heptad. Interestingly, the side-chain packing between pairs of helices in a tetramer shows a considerably similar geometry to the packing commonly found in the two-stranded coiled coil. In a parallel tetrameric coiled coil structure the interaction between *g'* and *a* is similar to the interactions formed by two adjacent *d*, *d'* residues in a two-stranded coiled coil and the interaction of *e'* and *d* is equivalent to interactions between *a* and *a'* positions (Figure 3.8).[45,114,116]

The steric and volumic parameters of the side chains may result in parallel, perpendicular, or acute packing at the hydrophobic core (Figure 3.8c, d, e). While the packing of the hydrophobic *a* and *d* positions produces most of the binding energy, the size and polarity of these side chains specify the binding characteristics such as oligomerization state and orientation. The alanine side chain is too small to completely fill the empty space between the higher order oligomers. Therefore upon the insertion of a single alanine residue the dimeric state dominates over the trimeric, as the dimer interface state is more closely packed.[114]

Kennan and coworkers have shown that replacing alanine by an unnatural cyclohexylalanine increases the stability of a coiled-coil protein trimer derived from GCN4 due to more extensive hydrophobic contacts.[117] Similarly the existence of a H-bond forming asparagine residue at the hydrophobic core can induce the dimerization as well as the parallel orientation.[118] However, the increased structural specificity is achieved at the cost of global stability.

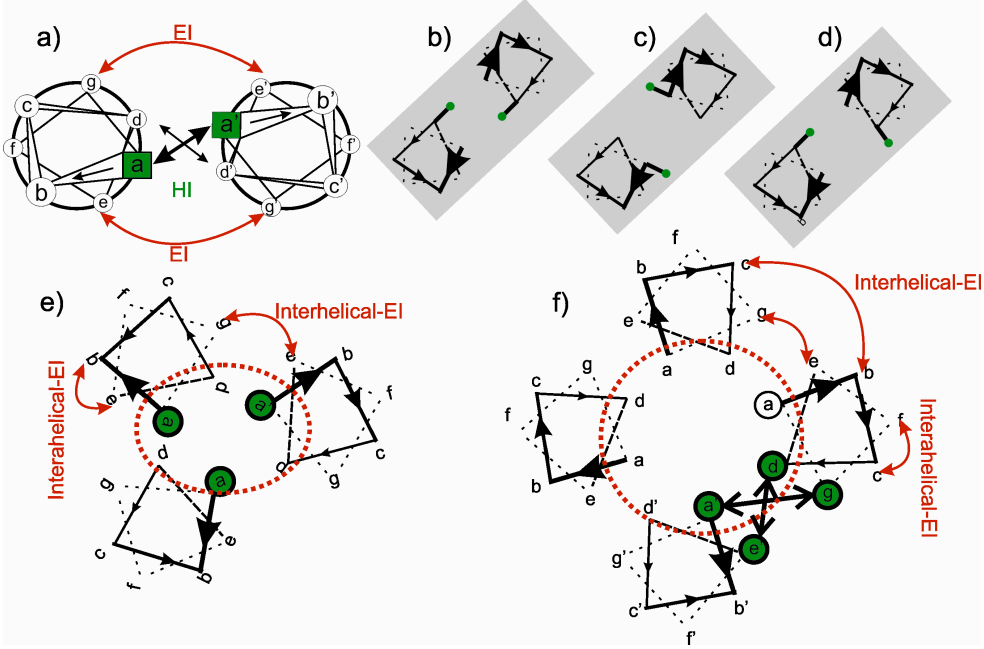

Figure 3.8 *a) Helical wheel representation illustrating the interactions between residues at the dimer interface of the dimeric coiled-coil structure. b) Perpendicular, c) parallel, and d) acute types of knobs-into-holes packing interactions in dimeric coiled coils. e-f) Representations illustrating the interactions between residues at the trimeric and tetrameric interfaces of the corresponding coiled-coil structures. The geometric similarity in side-chain packing between pairs of helices in a tetramer to the parallel, two-stranded coiled coil, is highlighted in the frames. HI and EI designate the hydrophobic and electrostatic interactions, respectively.*

The side chains of the *e* and *g* positions are mostly occupied by charged residues and are therefore orientation-determining due to the charge-matching between the adjacent peptide strands in coiled coil assembly. It is thus tempting to speculate that inter- and intra-helical electrostatic interactions should play a major role in the homo- and hetero-assembly of peptide molecules. As described above, these residues flank the hydrophobic interface, packing against the residues of the hydrophobic core, and may also participate in interhelical hydrophobic core specifically in higher order oligomers. Furthermore, in the coiled coil assembly with four helices the electrostatic interaction domain has been shown to extend to further solvent exposed side chains of *b* and *c* positions at the outer face of the helix.[119] The noncovalent association of these peptides is sensitive to environmental changes such as pH, temperature, ionic strength, and metal ions, which affect the electrostatic or hydrophobic interactions. The hydrophobic ligands such as cyclohexane or benzene present in solution can increase the apparent thermal stability of the peptide assembly.[120]

Coiled coil domains perform a variety of functions. The assembly of ion channel signaling complexes and transcription factors (proteins that bind to specific sequences of DNA to either activate or repress gene transcription) are common examples of binding function. Another example is the connection of three types of SNARE proteins (involved in the exocytosis of neurotransmitters from neurons) due to a very stable heterotetrameric coiled-coil complex formed between these three proteins.[112,121] The wide spectrum of functionalities in addition to the structural properties of the coiled coils make them an attractive object in the field of de novo designed proteins. The de novo design of α-helical coiled coils explores the features that specify the stoichiometry and stability of the tertiary structure and define the requirements for folding into structures that resemble native, functional proteins. The design process often occurs in a series of discrete hierarchical steps required for stabilizing tertiary structures, beginning with hydrophobic forces and adding more specific interactions as required to achieve a unique, functional protein. The initial efforts in this area aim the successful design of synthetic coiled coil motifs with similar or greater binding stability compared to the natural ones while retaining the other properties of coiled coils. Additionally, several modifications within artificial peptides have been introduced to modify the structure while stabilizing the coiled coil assembly. The insertion of the bulky unnatural hydrophobic side chains (e.g. cyclohexylalanine)[117] or burial of unnatural polar side chains (e.g. argenine analogs) have been shown to control the stability and selectivity of the whole structural motif.[122] Introducing fluorinated amino

acids resulted in a general thermal stability of the corresponding supramolecular system based on the lower flexibility of a fluorinated chain and the larger van der Waals volume of fluorinated amino acid compared to natural one.[123, 124]

A complementary approach is to modify the polypeptide backbone while retaining the original side chain sequence, which reveals the contribution of the backbones to coiled coil folding behavior. The application of unnatural backbone for the construction of helix binders may resolve the intrinsic protease-susceptibility of natural peptides as well as provide potentially larger accessible conformations and functionalities. This approach has been used to prepare peptide analogs in which α-amino acid residues are replaced by unnatural backbones bearing the same side chain, for instance, replacement of backbone amide with triazole rings (Figure 3.9a).[125]

Efforts to generate artificial tertiary structures possessing an extended sequence of unnatural amino acids have revealed the great potential of oligomers containing homologous amino acids and has led to the discovery of both homomeric and heteromeric peptide helix bundles.[126-129] The studied helix bundles are stabilized either by the constrained interactions using disulfide bonds, nucleobase pairing, metal chelation or the long-range tertiary contacts between the unnatural peptides. Namely, short β-peptides assemble noncovalently into a well-defined homomeric helix bundle characterized by an integral stoichiometry, highly stabilized secondary structure, and a cooperative melting transition. The amphilphilic arrangement of the side chains provide three distinct faces controlling the self and hetero assembly of the β-peptide. The electrostatic side chains along one helical face promote the 3_{14} helix through salt-bridge formation, while the hydrophobic interactions and the cross-complementary charges of the apolar and polar side chains located on the second and third faces, respectively, drive hetero- or homo-oligomerization, akin to leucine zipper proteins (Figure 3.9b).[130] However, there are significant differences in the packing between the artificial helices and that of the corresponding natural coiled coil assemblies. Another type of homologous-based design is the mixed or “heterogeneous” backbones in which the unnatural subunits are introduced to an α-peptide.[27] These chimeric structures have highlighted the potential of mixed or “heterogeneous” backbones to expand the structural and functional repertoire of unnaturally designed folding motifs. The $\alpha \rightarrow \beta^3$ substitution outside the recognition domains of the dimeric GCN4p1 (a helix forming sequence embedded in the yeast protein GCN4) showed a very close relation to the α-helix conformation but, the assembly

behaviors of the α- and αβ-peptides significantly diverge in both oligomerization state and stability.[131] Similar mutations in GCN4pLI (parallel tetrameric analogs of GCN4p1) reveals an altered self association behavior: an anitparallel four-helix bundle in the crystalline state (Figure 3.9c). The lower stability of the helix bundles composed of homologous amino acids is attributed to the greater flexibility of the backbone due to each $\alpha \rightarrow \beta^3$ substitution.[131] The helix formation requires that each flexible backbone bond be torsionally constrained. Therefore application of the conformationaly constrained residues may offer enhanced helix stability if the covalent ring promotes the torsion angles that are consistent with the helix.

Extensive work by Gellman and coworkers suggested that the five- and six-membered ring constraint of an apolar residue (e.g. *trans*-2-aminocyclopentanecarboxylic acid, ACPC) and a pyrrolidine-based polar residue (e.g. *trans*-3-amino-pyrrolidine-4-carboxylic acid, APC) provide the local folding propensity necessary for an α-helix-like conformation. Although this approach benefits from the structural preorganization imparted by the cyclic residues, it involves unavoidable deviation from the side chain sequence and positioning of the α-peptide prototype. Therefore the replacement of conformationally constrained residues may not provide the desired helical and association property for the foldameric helix-bundle formation in every case.[131]

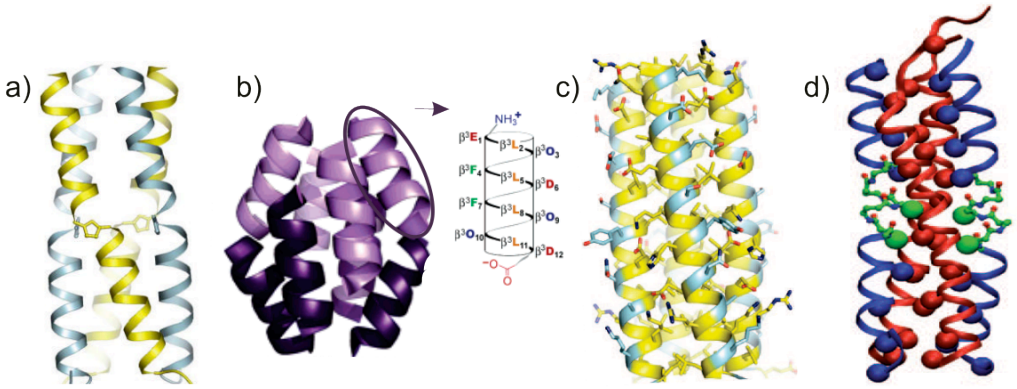

Figure 3.9 *Artificial coiled coil assemblies. Modification of helical assemblies through: a) octameric 3^{14} helix bundle, according to Goodman et al. with permission, Copyright© American Chemical Society, b) triazole modified tetrameric coiled coil, according to Horne et al. with permission, Copyright© American Chemical Society, c) αβ tetrameric helix bundle, according to Horne et al. with permission, Copyright© American Chemical Society, d) αβγ tetrameric helix bundle, according to Rezaei Araghi et al.*

In a substantially different design approach, one can take advantage of the flexibility of the backbone: Such flexibility provides a wider range of conformations for the backbone which

opens up the possibility to favor the one or the other helix type due to specific substitution pattern and tertiary interactions in the resulting helix bundle. In addition, the natural proteinogenic side chains of homologous amino acids make a decisive contribution to the interhelical interaction domains of the corresponding helix bundles. Among the different substitution patterns being studied, a particulary interesting one is the alternative sequence of amino acids which resemble the α-backbone pattern and is well-suited to mimic an α-helical conformation.

Our investigation on the $\alpha\beta\gamma$-chimeric backbones resulted in the first example of the substitution of an entire heptad repeat in an α-helical coiled coil motif by a non-natural fragment consisting of an extended sequence of alternating β- and γ-amino acids (Figure 3.9d) with retention of global conformation and the stability of the fold.[132-134]

4 Applied analytical methods and assays

4.1 Circular dichroism spectroscopy

Circular dichroism (CD) is a phenomenon that results when chromophores interact with polarized light in an asymmetrical environment. CD spectroscopy measures differences in the absorption of circularly left-handed polarized light (Lcp) versus right-handed circularly polarized (Rcp) light. The absence of regular structure results in zero CD intensity, while an ordered structure results in a spectrum which can contain both positive and negative signals. Therefore, this method is frequently used for efficient monitoring of global conformational changes at the level of secondary structure.[135]

A circularly polarized beam consists of two orthogonal plane-polarized beams 90° out of phase. The original method of CD spectroscopy is based on the differential absorption of the circular components which convert the plane polarized light into elliptically polarized light:

$$\Delta A = A_L - A_R = \varepsilon_L C l - \varepsilon_R C l = \Delta \varepsilon C l$$

A_L and A_R are absorptions of Lcp and Rcp respectively and l is the distance through the medium containing the chiral solute. C is the molar concentration and εl and εr are the decadic molar extinction coefficient of the solute for Lcp and Rcp respectively. This fact results in an average electric vector which traces out an ellipse rather than oscillating in a plane or forming a circle (Figure 4.1a). When the electric vectors of the two circular components are the same direction, the major axis of such an ellipse corresponds to the sum of magnitude of these vectors, and when the electric vectors are in opposite directions, the difference of their magnitude gives the minor axis of the ellipse. Then the ellipticity is referred to the ratio of the minor and major axes, which is the tangent of the θ angle. Since this angle is very small, tan θ is approximated well by θ in radians.

CD spectra consist of a series of bands which corresponds to different electronic transition from ground state to an electronically excited state. In peptides, the most abundant chromophore which interacts with light is the amide bond, which dominates the CD spectra of proteins below 250 nm (Figure 4.1b). Three centers, nitrogen, carbon and oxygen atoms of the amide linkage are combined to form three orthogonal linear combinations, the π+, π_o, and π- bonds. four π electrons fill the first two molecular orbitals ππ*.

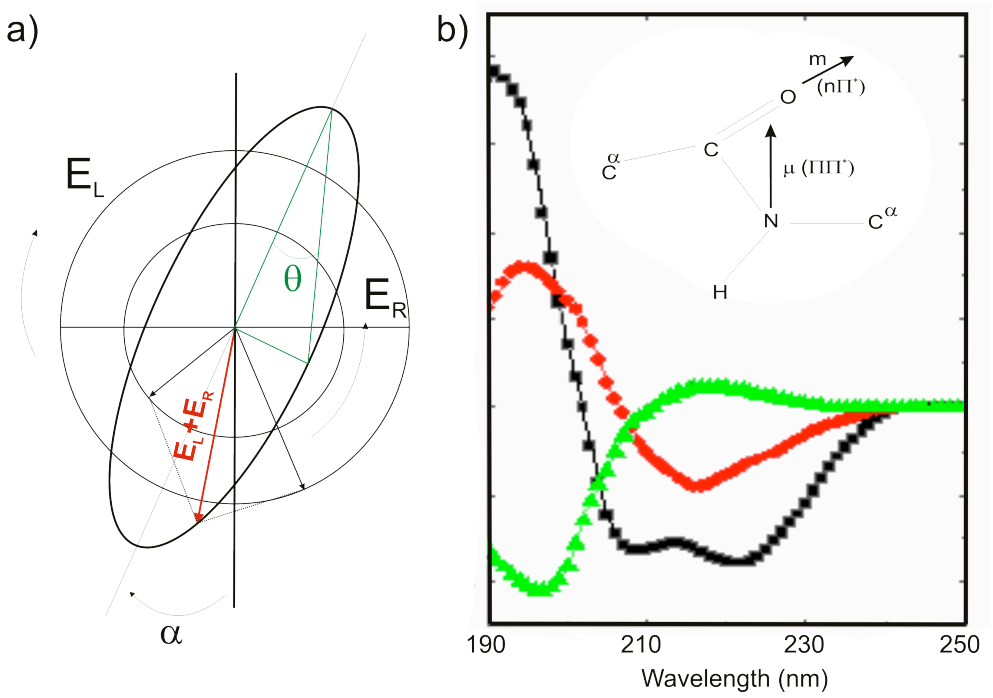

Figure 4.1 *a) different absorption of the left- and right hand polarized component leads to ellipticity which is designated by θ. The tan is the ratio of the minor to the major axis of the ellipse. The angle is the optical rotation, and is the angle between the major axis of the ellipse and the plane of polarization of the initially plane-polarized light. b) The circular dichroism spectra of the α-helical (black), β-sheet (green), and random coil (red) conformations. Inlet: The electric dipole transition μ (ππ*) and magnetic dipole transition moment of the amide μ (nπ*) transition.*

Additionally there are two remaining electrons which are non-bonding electrons on the oxygen atoms of the amide bond which are conventionally labeled the $2P_y$ electrons. There is another lone pair at substantially lower energies and mixes strongly with the orbitals. The n-π* transition (215 - 230 nm) involves the promotion of an electron from the n to the π- orbital. The transition is the lowest energy transition in the amide group. The n-π* transition is energetically forbidden because the ground and excited states have nodal planes which are perpendicular to one another. However, the transition is permitted magnetically. In contrast, π -π* transition (185 – 200 nm) is electrically allowed and involves the promotion of an electron from the π_o to the π-orbital. Transitions and intensities recorded for three different secondary structures are tabulated in Table 3.1. The theoretical studies as well as the experimental measurements have proven the high sensitivity of CD spectra toward protein secondary structures. Figure 3.1b gives CD spectra of polypeptides that present a pure type of different secondary structures. Each of these structures at most has two CD bands between 240 and 200 nm. A strong double

minimum at 222 and 208-210 nm and a stronger maximum at 191-193 nm are characteristic of an α-helix. The intensity of the band at 222 nm is indicative of the α-helical content, since it is related to the strong hydrogen-bonding environment of α-helices and is relatively independent of the peptide length. All β-proteins usually have a single, negative and a single positive CD band, whose intensities are much lower than those of an α-helix. Almost all regular β-proteins have a single minimum between 210 and 225 nm and a stronger positive maximum between 190 and 200 nm. The class of unordered proteins includes many oligopeptides, short polypeptides, and denatured proteins. This class usually shows a CD spectrum with a strong negative band near 200 nm and some weak bands between 220 and 230 nm, which can have either positive or negative signs. The spectrum for an all α-helical protein has two negative bands of similar magnitude at 222 and 208 nm, and a positive band at ~ 190 nm (Figure 4.1b). One of the main applications of CD for the study of proteins is the estimation of secondary structure of proteins. There has been much progress in the design of artificial amino acids that has resulted in the production of a large number of new secondary structures. However, analysis of those based on high resolution information from X-ray diffraction or nuclear magnetic resonance is sometimes difficult or even impossible. CD compared with these techniques can not solely lead to details about the structure of a protein, but can give a very good estimation of the fraction of the residues in the structure which are involved in well-known secondary structure and thereby confirm the orderly or disorderly structure formation. There are bounties of information in CD signals which are specially useful when information about the structure at high resolution does not exist. One can predict the secondary structure of a protein. For example, the fractional helicity within the peptide or protein is usually calculated as proportional to the experimental molar residue elipticity at 222 nm, $[\theta]_{222}$. One of the simplest methods, and yet fairly reliable, for estimating the quantity of α-helix is the evaluation of the signal at 222 nm using one or both of the following equation:

$$f_H = 100 \times ([\theta_{222}]/^{max}[\theta_{222}]) \text{ where } ^{max}[\theta_{222}] = -40{,}000\,[1 - (2.5/n)]$$

n is number of amino acid residues. For almost 100% α-helix such as $(Lys)_n$ the intensities are about -40,000 deg cm^2 $dmol^{-1}$. For other peptides which are only partially α-helix with a negative band centered at 222 nm, the helical content is taken directly proportional to the mean residue ellipticity at 222 nm.[136]

Table 4.1 *Transitions and intensities recorded for three different secondary structures*

Secondary structure	***CD band***	***Electronic transition***	***Wavelengths (nm)***	$[\theta]$ ***(deg cm^2 dmol^{-1})***
α-helix	positive	ππ*	190-195	60,000 to 80,000
	negative	ππ*	208 -36	000 ± 3,000
	negative	nπ*	222	-36,000 ± 3,000
β-sheet	positive	ππ*	195 - 200	30,000 to 50,000
	negative	nπ*	215 - 220	-10,000 to -20,000
random	negative	ππ*	ca. 200	-20,000

Furthermore, some additives are also used to increase the propensity of certain polypeptides to form secondary structure, sometimes at very high level of concentration up to 100%. They are trifluoretanol (TFE), hexafluoroisopropanol, ethylene glycol, glycerol and others. The most widely used is TFE.[137] Differences in the solvent acidity and basicity between TFE and water are proposed to change the relative stability of hydrogen bonds. This was probed by NMR; the results indicate that the dominant effect of TFE is caused by its significantly weaker basicity. Hydrogen bonding of amide protons to the solvent is decreased, which strengthens intramolecular hydrogen bonds and therefore stabilizes secondary structures. In addition, TFE is a less polar or more hydrophobic solvent. It interrupts hydrophobic interactions and can act as a denaturant of tertiary and quaternary structure.

4.2 Size exclusion chromatography

Size-exclusion chromatography (SEC) is a chromatographic method in which molecules in solution are separated by their size and it is usually applied in the characterization of polymers with different sizes (Figure 4.2a). The separation of solutes in SEC separation is based on the distribution of solute molecules between the interstitial and the pore size, and is processed using an isocratic elution. Molecules that are smaller than the pore size can

enter the particles and therefore have a longer path and longer transist time than larger molecules which cannot enter the particles. The separation efficiency of SEC comes only from the stationary phase, while the mobile phase should have no effect. Therefore, the right choice of the column for a given polymer is crucial point. Resins are usually classified by manufacturers by their capacity to separate into different sizes of a hypothetical, globular protein. The lower range is the range below which all molecules will see the entire internal volume of the beads allowing for no selection below this size. The upper range is the range at which molecules are completely excluded from seeing the inside of a bead also allowing for no separation. There is a linear range between these two extremes at which decent separation of molecules occurs. This range is usually reported for each matrix and the pore size is dependent on the desired range of separation. Aside from the application of the SEC to remove small molecule contaminants from protein molecules, this method is used to determine the solution subunit composition of a multimeric protein, and to isolate different multimers from each other. In the latter case, in order to calculate the apparent aggregation state, the retention time of the solute should be compared with a series of samples applied for calibration. Samples for calibration are usually chosen from a wide range of size and molecular weight.

4.3 Analytical ultracentrifugation

Analytical ultracentrifugation (AU) is a unique technique that enables an accurate determination of the native molecular weight as well as the stoichiometry of a protein complex from the determined molecular mass.[138,139] For instance, it can be easily established with high quality data whether the native conformation of a peptide/protein is a dimer- or a tetramer. Monitoring the sedimentation of macromolecules in the centrifugal field allows their hydrodynamic and thermodynamic characterization in solution, without any interaction from a matrix or surface. The instrumental detail is presented in Figure 4.2b. The instrument itself spins a rotor at a controlled speed and temperature under vacuum while recording the concentration distribution at set times. This is achieved using either refractometric methods or photoelectric absorption measurements.

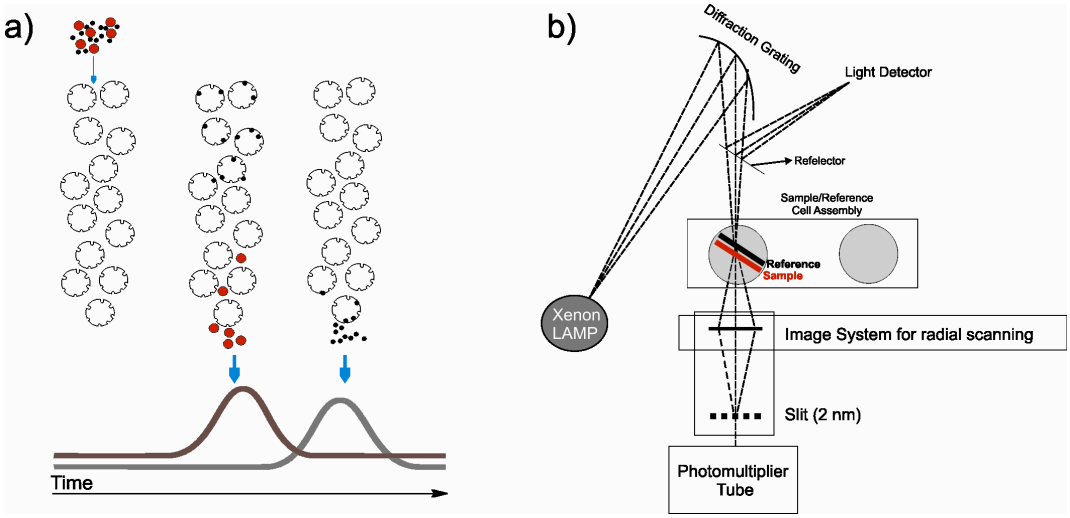

Figure 4.2 *Schematic presentation of a) a size-exclusion chromatography column and b) analytical ultracentrifugation instrument.*

In addition to determination of concentration distribution, several other quantities may be required. The density of the solvent and the partial specific volume of the solute are required for molecular weight determination. The viscosity of the solvent and its temperature dependence is required in order to account for the effects of solvent and temperature on sedimentation behavior. The two basic types of experiments are sedimentation velocity and sedimentation equilibrium.

Sedimentation equilibrium

At low enough centrifugal fields, the solute particles redistribute over time with increasing concentration as the distance from the center of rotation increases (Figure 4.3). After an appropriate period of time, the process of diffusion equals the process of sedimentation, which is called the sedimentation equilibrium. Measurement of the solute concentration at different time points leads to the determination of the molar weight of the sedimenting solute. The concentration gradient develops as the flux of sedimenting molecules is exactly balanced by the flux of diffusing molecules at each point in the cell, where the sedimentation reflux is:

$$J_S = \frac{c.V}{A}$$

where c is concentration of macromolecules, and V is their velocity, which can be defined in terms of the sedimentation coefficient:

$s = \frac{V}{\omega^2 r}$, (ω is the angular velocity in cgs units)

and according to Svedberg equation is related to M_b value:

$$\frac{s}{D} = \frac{M_b}{RT}$$

The M_b value (buoyant mass) is achievable due to

$$M_b = M(1 - \bar{\nu}\rho)$$

If M is the solute molar mass (expressed in g/mole), the displaced solvent mass is $M\bar{\nu}\rho$,

where $\bar{\nu}$ is the solute's partial specific volume in ml/g and ρ is the solvent density in g/ml.

The flux through P due to diffusion is described by Fick's first law:

$$J_D = -D(\frac{\partial c}{\partial r})_t$$

At equilibrium, these two fluxes are equal:

$$c.s\omega^2 r = D\frac{dc}{dr} \Rightarrow \frac{s\omega^2}{D} = \frac{1}{rc}\frac{dc}{dr} = \frac{d\ln c}{d\frac{r^2}{2}} = \sigma$$

and finally result in σ value which is a variable of r (distance from the center of rotation, in cm) and c (concentration) and can be defined in terms of the molecular weight:

$$\sigma = \frac{M_b\omega^2}{RT}$$

Sedimentation equilibrium measurement allows determination of:

- Molecular weight
- Homogeneity with respect to molecular weight
- Aggregation states
- Stoichiometry and equilibrium constants for association processes

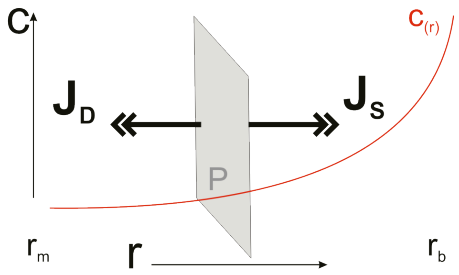

Figure 4.3 *A schematic of the process for sedimentation equilibrium. A solution containing macromolecules is confined to the region between the air-liquid meniscus (r_m) and the base of the cell (r_b). The gravitational field points from left to right and is directed along the radial axis (r). According to Laue et al.*[139]

Sedimentation velocity

Sedimentation velocity is applicable for systems that are not sufficiently stable for the extended time required in sedimentation equilibrium measurement and often provides complementary information. The study of self-associating systems by sedimentation velocity allows the determination of the sedimentation coefficients and hydrodynamic shape of the reversibly formed oligomers in solution, which can be used to build simple geometric models for assembly of the oligomers. The simplest method for analysis of sedimentation velocity experiments is to plot the natural logarithm of the radial position of the boundary midpoint or the second moment boundary position versus time. The slope of this plot is proportional to $\omega^2 s$, in which *s* represents an apparent *average* sedimentation coefficient.

4.4 Spot synthesis and analysis

With appropriate linker/spacer chemistry, cellulose membranes are applied for the screening of immobilized peptides with area-specific functionalities which are from 0.1 to 1 μmol/cm^2.[140] Arrays of spot reactors provide suitable anchor functions for peptide assembly such as amino- or hydroxyl-functionalized cellulose membranes. The amine-functionalization can be applied by esterification of a protected amino acid such as Fmoc-hAla-OH to accessible hydroxyl functions on a cellulose membrane. Next, the array of spot reactors is generated by spotwise coupling of a suitable linker compound (e.g. βhomoAla-OH), and all residual amino functions in between spots are blocked by acetylation. The array formation step requires very accurate pipetting especially if high density arrays are to be prepared. A conventional Fmoc/tBu chemistry protocol is utilized for solid phase synthesis which can be applied to both coded and noncoded amino acids. Activation of 0.2–0.3 M solutions of protected amino acid derivatives, generally dissolved in NMP, can be carried.

In order to control the quality of synthesis, the cleavage of few control spots is carried out with trifluoroacetic acid in dichloromethane with triisobutylsilane and water as scavengers. The characterization of the synthesized spot was carried out applying analytical HPLC and MALDI mass spectrometry. Having a complete library immobilized on the membrane allows screening methods such as binding assays. The binding assays are often performed directly on the peptide array followed by visualization of peptides binding the

interaction partner in an additional step. In order to perform the binding assay the probed peptide array is subsequently immersed in a solution containing a label conjugate with high binding affinity to the analyte. The labeling of the analyte with fluorescent dyes provides detectable moieties which are incorporated synthetically to the analyte. Thereafter, the signal intensities can be used to distinguish between different affinities (Figure 4.4).

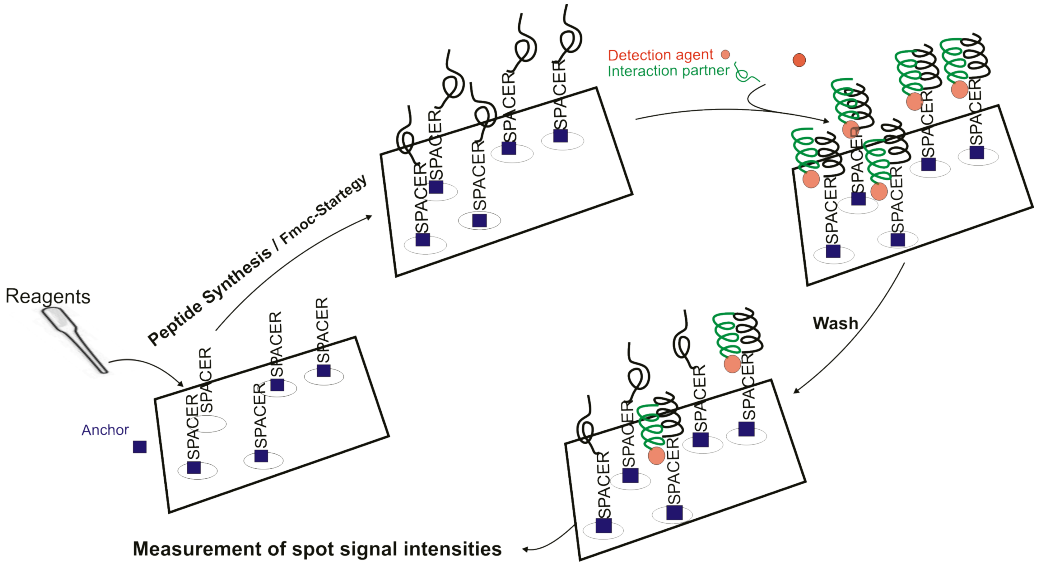

Figure 4.4 *A schematic presentation of the spot synthesis and binding analysis on the cellulose membrane.*

The great advantages of spot method, such as no need for any physical separation of reactor zone, a variety of support materials with a broad range of capacities as well as straight-forward incorporation of non-coded residue to the library, provide the right SPOT-synthesis for many different bioassay and screening formats.[142] This method allows determination of:

- a large variety of search strategies to identify peptides that represent natural protein binding sites (epitopes)
- mimics of such sites (mimotopes)
- selectively bound target molecules besides proteins.

Applied assay:

Cellulose-bound peptide arrays were prepared according to standard SPOT synthesis protocols using a SPOT synthesizer (Intavis, Köln, Germany) on amino-functionalized

cellulose membranes (Whatman, Maidstone, Great Britain) of the ester type prepared by modifying cellulose paper with Fmoc-b-alanine as the first spacer residue. In the second coupling step, the anchor position Fmoc-b-alanine- OPfp in dimethylsulfoxide (DMSO) was used. The Fmoc group was removed using 20% piperidine in dimethylformamide (DMF). The cellulose-bound peptide arrays were assembled on these membranes by using 0.3 M solutions of Fmoc-amino acid-OPfp in 1-Methyl-2- pyrrolidone (NMP). Side-chain protection of the Fmoc-amino acids used was as follows: Glu, Asp (OtBu); Tyr (tBu); Lys, (Boc). After the last coupling step, the acid-labile protection groups of the amino acid side chains were cleaved using 90% trifluoro-acetic acid (TFA) for 30 min and 60% TFA for 3 h. The peptide library was generated by a SPOT synthesizer (Intavis, Köln, Germany). The quality of the synthesis was assessed by analytical HPLC and MALDI-TOF spectrometry for control spots. The chimeric peptides was synthesized by standard Fmoc-protocol and manually labeled with 5-(and 6)-carboxy-tetramethylrhodamine (TAMRA); fluorescent dye provides a detectable moiety. Thereafter, the membrane was washed with ethanol and TBS (TBS: 50 mM Tris-(hydroxymethyl)-aminomethane, 137 mM NaCl, 2.7 mM KCl, pH 7.4) each three times for 10 min. Then membrane-bound peptide arrays were blocked (3 h) with blocking buffer (casein-based blocking buffer concentrate (Sigma-Genosys, Cambridge, UK), 1:10 in TBS containing 5% (w/v) sucrose), and then washed with TBS (1x10 min). The binding study was performed by incubation of the immobilized peptides in a solution containing the labeled chimera (c = 10 μM) which has high binding affinity to the specific peptides on the cellulose membrane for 10 min in TBS blocking buffer. The incubation and washing steps were carried out under gentle shaking at room temperature. After washing for 120 min with TBS, analysis and quantification of peptide-bound TAMRA were carried out using a Lumi-Imager. Analysis and quantification of spot signal intensities were executed by scanning in the visible light range using a HP Scanjet G3010 (Hewlett-Packard, Böblingen, Germany), resulting in a digital image file (referred to as densiometric analysis). The spot signal is calculated from a circular region around the spot center detected on the image. The background signal for each spot is determined with a safety margin in relation to this circular region, and then the global background mean was subtracted from each individual spot signal. Results are shown as the interspot global background-corrected mean value over three replica spots for each sequence. Intensity of the TAMRA-labelled sequences was measured at 645 nm.

The binding affinity of B3β2γ sequence was evaluated after incubation of the membrane in a solution of 10 μM chimera. Then, the arrays were washed intensively and the affinity of

the mutants for binding to TAMRA-labelled chimeric sequences was evaluated from the intensity of the emitted light out of each spot.

4.5 Phage display

Phage display technology is a peptide-based screening system that can be used for the high-throughput screening of protein interactions out of a pool of all coded amino acids.[143,144] This means the screening set includes 20^n when n is the number of randomized amino acid positions. In this approach the peptide that contains the library is displayed on the surface of bacteriophage. The randomized positions in the gene coding for the peptide mutated via the $(NNK)_n$ strategy where N corresponds to a mixture of all four deoxynucleotides and K to a mixture of guanidine and thymidine. Different types of bacteriophage can be used for library selection. In this work the randomized positions are displayed as fusions of the p-III coat protein at one end of the filamentous bacteriophage M13.

The M13 genome composes a circular single stranded DNA molecule of about 6400 nucleotides, which encodes proteins that are required for i) the replication of genome; genes II, V and X; ii) the membrane associated assembly of the bacteriophages I, IV and XI iii) the minor and major capsid proteins pIII, pVI, pVII, pIX and pVIII. Among all these proteins, pIII plays a major role in phage-host interaction during infection. Infection starts by recognition of the bacterial F-pilus by the phage pIII protein, followed by disassembly and fusion with the bacterial membrane, whereby the virus genome enters the cytoplasm.

In order to construct the pIII peptide, the insert was ligated with T4 DNA ligase in pComb3HSS phagemid vector after digestion with endonuclease Sfi1 which results in two non-complementary sticky-ends. This fact reduces a self ligation of an empty vector. The phagemide library was transformed into E. coli ER2738 cells by electroporation and the phage library was generated upon infection with helper phages. Screening of the phage library is based on the immobilizing a relevant DNA or protein target(s) to the surface, and incubation of the phages on the surface. A phage containing a sequence that binds to one of those targets on surface will remain while others are removed by washing. Those that remain can be eluted, used for amplification of phage by means of bacterial infection so produce a phage mixture that is enriched with preferred phage. Therefore, phage display is a well-established method for studying protein-protein interactions as well as screening

for specific antibodies in therapeutic, diagnostic or research applications.

Phages carrying a peptide, whose amino acid sequence has an affinity to the screening peptide, are bound through non-covalent interactions. This process of selecting binding partners is called (bio)panning (Figure 4.5). Afterwards, the particles are collected on the reaction vessel wall with an external magnet and phages with no or low affinity fusion peptides are washed out. By increasing the concentration of detergent or denaturation agent in the washing solutions in every new panning round, the selection pressure can be increased and only very strong binders are accumulated. These remaining phages are eluted from the immobilized particles by proteolytic hydrolysis of the fusion peptide, short enough to only degrade the fusion peptide. The obtained phage suspension is used to reinfect *E. coli* bacteria. The infected bacteria can be streaked out to prepare single colonies for DNA sequencing, and thus for revealing the peptide sequence of the best interaction partners. On the other hand, the reinfected bacteria host the phagemid genome of the selected phages and upon infection with helper phages, phages for further panning rounds can be produced.

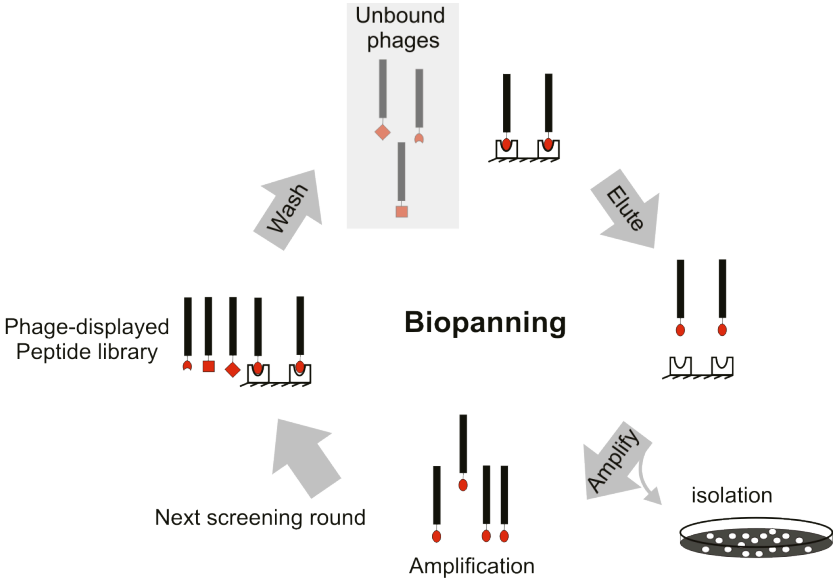

Figure 4.5 *Schematic overview: Selection of binding partners for a synthetic peptide out of a phage library via biopanning.*

5. Aim of the work

Many biological processes depend on the interaction of two (or more) α-helical domains. An external control of some of these processes, e.g. virus-cell interactions, bear therapeutic potential, since the disruption of such helical interactions may be employed as a tool to interfer with these processes. Considering the importance and abundance of the α-helical structure in nature, this project is focused on the mimicry of α-helix by alternating sequences of β- and γ-amino acids.

The structural differences observed between the packing in most of the previously reported unnatural oligomers and that of natural α-helical assemblies motivated the design and characterization of new class of helix-forming foldamers. Therefore, this thesis aims to experimentally evaluate the compatibility of the βγ-pattern with a very common helical quaternary structure in nature - the α-helical coiled coil motif.

Towards the long-term goal of future practical applications by selectively pairing the newly designed unnatural oligomer (αβγ-chimera) with natural helical targets, this work also aims at the optimization of interaction profile of the αβγ-chimera with natural counterparts by means of both rational and combinatorial approaches.

6. Results and Discussions

The results presented in this chapter have partly been published in the following peer reviewed reports:

- **Raheleh Rezaei Araghi**, Christian Jäckel, Helmut Cölfen, Mario Salwiczek, Antje Völkel, Sara C. Wagner, Sebastian Wieczorek, Carsten Baldauf, and Beate Koksch, *ChemBioChem*, **2010**, 11, 335–339.

- **Raheleh Rezaei Araghi,** Beate Koksch, *ChemCommun*, **2011**, 47, 3544–3546.

- **Raheleh Rezaei Araghi**, Carsten Baldauf, Ulla I. M. Gerling, Cosimo Damiano Cadicamo, Beate Koksch, *Amino Acids,* **2011**, 41, 733-742.

Results that are not part of these publications as well as further considerations and interpretations are presented in additional sections. The unpublished results are discussed in section 6.2.

6.1 Publication I: A β/γ Motif to Mimic α-Helical Turns in Proteins

Raheleh Rezaei Araghi, Christian Jäckel, Helmut Cölfen, Mario Salwiczek, Antje Völkel, Sara C. Wagner, Sebastian Wieczorek, Carsten Baldauf, and Beate Koksch, *ChemBioChem*, **2010**, 11, 335 – 339.

The original paper with supporting information is available at:

http://dx.doi.org/10.1002/cbic.200900700

6.1.1 Concept

The α-amino acid as lead backbone of the natural peptides often lacks the general properties such as protease stability and bioavailability for making it a variable clinical candidate. Therefore, the α-amino acid backbones can be modified to reduce or eliminate these undesirable features, namely due to isosteric substitution with unnatural backbones. One main strategy is the insertion of ω-amino acids into peptide sequences which results in replacement of scissile peptide bonds by proteolytically stable C-C bonds.[54] Accordingly, a close relationship is expected between a dimeric sequence of β- and γ-amino acid and three units of α-amino acids. This isosteric similarity suggests that the shape and the stability of the corresponding helix types may correlate in the two peptide classes of α- and βγ-peptides. Similar agreements between βγ-hybrid peptides and secondary structures of the native α-peptides were predicted as well by theoretical studies of Hoffman *et al*., according to which in extended βγ-peptides the two-residue hydrogen-bonded rings (*i*, *i*+3) resemble three-residue rings (*i*, *i*+4) of the known α-helices (Figure 6.1).[103]

The insertion of three CH_2 units per substitution greatly enhances the repertoire of the possible stable internally hydrogen bonded folded structures. Among different possible H-bonding patterns for an alternating βγ sequence, of particular interest is the H_{13} helix, since it corresponds formally to the well-known α-helix of native peptides and proteins. Despite the different number and positions of the peptide bonds in the basic units of the two peptide classes, the same hydrogen bonding orientations and helix dipole direction of the native α-helical peptides can be found in the alternating βγ-sequence. Therefore the βγ-peptide units are appropriate candidates to well adopt the α-helix conformation in native peptide sequences. The successful but limited incorporation of an unsubstituted dimeric segment composed of βAla and γ-aminobutyric acid (Abu) into the center of helical

structures in octa- and undecapeptides has been reported.[14]

In other examples the incorporation of a streochemically constrained residue has been shown to bias the C_{13} helix formation in a tripeptide of Boc-βLeu-Gpn-Val-OMe and Boc-βPhe-Gpn-Val-OMe sequences.[15] In a more recent study Gellman *et al.* show that appropriately preorganized residues promote the formation of the 13-helical conformation in short βγ-peptides.[101] All these studies having some aspects in common: i) they were inspired by the principle of "equal backbone atoms", ii) they are based on either unsubstituted or conformationally constrained βγ-amino acids, iii) these conformational analysis are at the level of secondary order structures.

Still inspired by the isosterism strategy, however, in a significantly different approach extended sequences of β- and γ-amino acids that can be incorporated into an α-helical coiled coil were identified to produce otherwise-natural folding motifs. Previous efforts to build unnatural quaternary structures with additional properties and functions applying homologous amino acids have led to the discovery of stable homomeric and heteromeric peptide helix bundles. However, the differences between the packing observed in these artificial quaternary assemblies and that of the corresponding natural assemblies have thus far impeded the combination of both classes into compact protein-like chimeric structures. The approach of the current thesis, however, differs substantially. While the stability of the reported foldameric quaternary structures is mainly provided by pre-organized backbone conformation of the foldameric sequence, the applied underlying β- and γ- amino acids are non-constrained and therefore closely resemble the natural non-rigid backbone of the natural α-peptides. In this approach, the focus will be on the formation of aggregates with a defined composition such as duplexes or triple in order to induce a distinct and well-formed helical structure through intermolecular interactions.

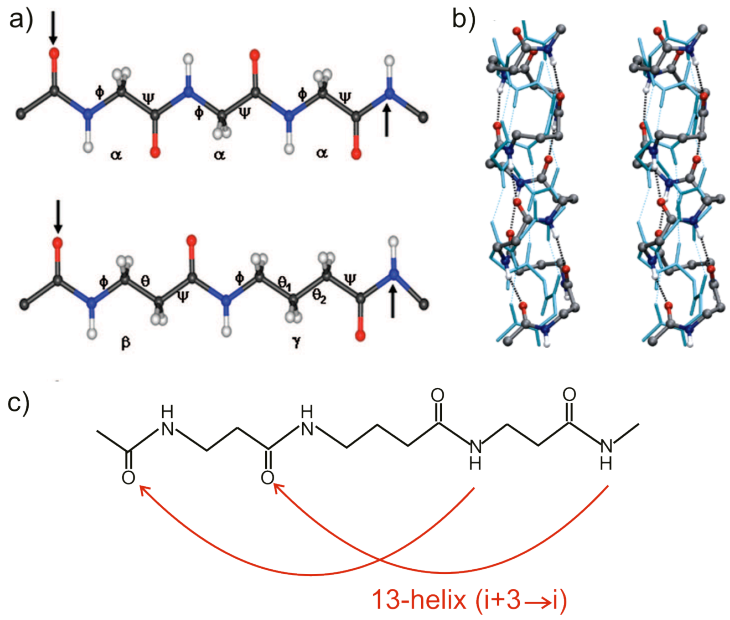

Figure 6.1 *Formal equivalence of a three residue ααα H_{13} hydrogen bonded turn to two residue H_{13} turns formed by βγ backbone atoms in polypeptides, according to Vasudev et al. with permission, Copyright© American Chemical Society b) Stereoview of the superimposition of the helix H13 of the βγ-peptide and an α-helix dodecamer, according to Baldauf et al. with permission, Copyright© American Chemical Society c) H-bonding in 13 helix of βγ-peptides.*

6.1.2 Summary

The aim of the current study was to identify extended sequences of β- and γ-amino acids that can be incorporated into an α-helical coiled coil as a highly populated class of protein folding motifs. Theoretical studies (*ab initio* MO theory) have shown that β/γ-hybrid peptides composed of alternating β- and γ-amino acid building blocks is well suited to mimic α-helical conformations. The present study establishes the first example of the substitution of an entire heptad repeat in a natural α-helical coiled coil motif by a non-proteinogenic fragment consisting of an extended sequence of alternating β- and γ-amino acids. We showed that a heptad of α-amino acids in a protein motif, comprising three 13-atom H-bonded turns of the helix, could be substituted by a pentad repeat of alternating β- and γ-amino acids with retention of the helix dipole, global conformation and the stability of the fold quaternary structure. The formation and stability of the new chimeric assembly is confirmed and exhaustively characterized. The model system described here comprises one basic and one acidic α-poly peptide (35 amino acids) which have a high propensity for

heterooligomerization to an α-helical coiled coil in the presence of one another (Figure 6.2). Heterooligomerization is driven by the burial of hydrophobic surface area and is directed by electrostatic interactions between charged residues that flank the hydrophobic core. In the chimera B3β2γ, the two central turns of α-helix in the basic peptide were replaced by a pentad of alternating β- and γ-amino acid residues. We thought that making substitutions at the center of a helix forming sequence would likely have a pronounced effect on the peptide's association energy intact which drives folding of the desired tetrameric state. This report in particular provides strong evidences for heterotetrameric artificial coiled coil assembling between chimeric peptide and natural α-peptide by the most reliable theoretical and experimental methods to date; such as molecular dynamics, circular dichroism, chemical and thermal denaturation, AUC.

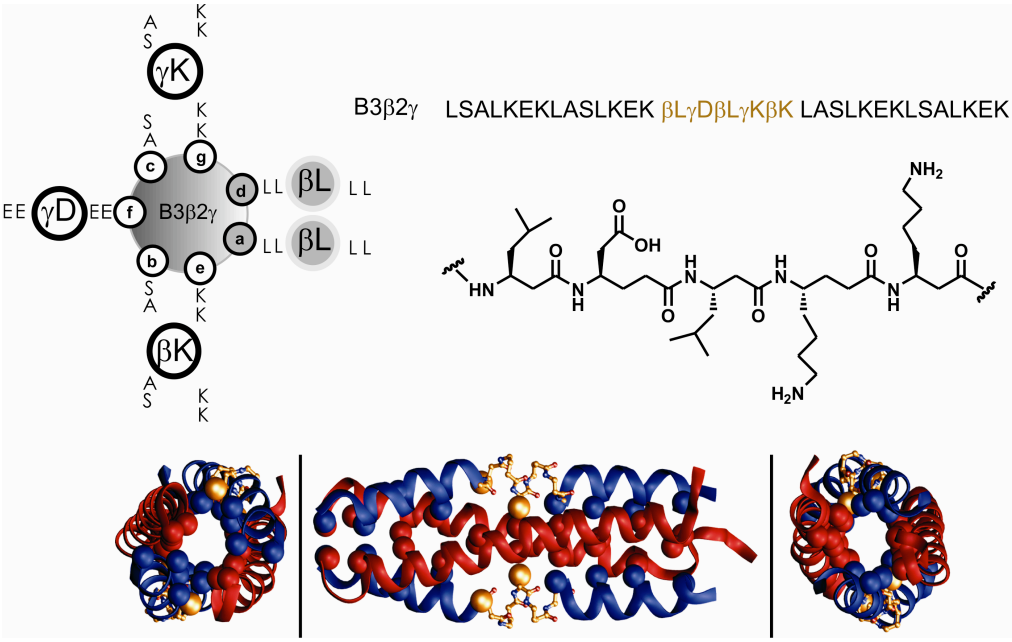

Figure 6.2 *(top) Helical representation and primary sequence of B3β2γ and the structure of the substituted βγ-segment. (bottom) Molecular model of chimera B3β2γ (blue ribbon) engaged in parallel (left) and antiparallel (right) coiled coil interaction with Acid-pp (red ribbon). The β/γ segment is shown in gold.*

The side chains of the βγ fragment participate in the formation of the characteristic interaction domains of the α-helical coiled-coil folding motif similar to those of the natural system. Although an anticipated partial decline in stability of the entire quaternary structure is observed due to the loss of one peptide bond and therewith one H-bond donor and one H-bond acceptor per α→βγ isosteric substitution; the Acid-pp/B3β2γ heterooligomer is still extremely thermostable and not fully denatured at 100 °C. The specific contributions of the β- and γ-amino acid side chains to the artificial coiled coil folding motif is studied further

thermodynamically by alanine scanning, as a standard mutation method. In addition, the comparison of the thermodynamic stability of the several side-chain mutants of B3b2g indicate the prodigious complementarities in side chain packing between the βγ segment and its α interaction partner, unless α→βγ substitution is accompanied by structural consequences such as a defected interhelical packing. The gradual degradation of the side chain length at two positions in the hydrophobic core (isopropyle→ methylene→ no side chain) results in gradual destabilization of the heteromeric assembly as judged by T_m and $D_{50\%}$ values of the variants.

Author contributions

All experiments including SPPS, CD, thermodynamic studies, which were applied in order to characterize the αβγ-chimeric coiled coil assembly as well as the design of the αβγ-chimera are parts of this thesis and carried out by the author. The αβγ-chimeric molecule was designed based on an alternating pattern of β- and γ-amino acids, initially suggested by Dr. C. Jäckel, in the group of Prof. Dr. Koksch. MD simulations and molecular modeling were conducted by Dr. C. Baldauf (Fritz-Haber-Institut der Max-Planck-Gesellschaft). The hetero-assembly of αβγ-chimera and its variants with native peptide was studied by regular CD spectroscopy, the stoichiometry of the assemblies were determined by SEC. The stability of the hetero-assemblies was assessed by thermal and chemical denaturations. Additionally, AUC measurements were applied in order to study the oligomerization states of the hetero-species in cooperation with Dr. Helmut Cölfen, Antje Völkel and Dr. M. Salwiczek. M. Sc. S. Wieczorek participated in alanine scanning experiments during his bachelor internship in the group of Prof. Dr. Koksch that was supervised by the author. S. C. Wagner carried out the TEM measurements at concentrations above 200 μM.

6.2 Unpublished section: Complementary studies toward design of heteromeric artificial coiled coil folding motif

6.2.1 βγ-Hybrid peptides versus αβγ-chimeric sequences

This thesis focused initially on characterization of isolated βγ alternating sequences, which were hypothesized to complementarily bind to α-helical coiled coil forming natural peptides. The investigation of this hypothesis is the subject of current section.
In order to induce the α-helix structure into hybrid βγ-peptide in the framework of a coiled coil tertiary structure, a heterooligomerizing natural α-peptide with complementary hydrophobic and electrostatic elements was designed. The primary sequence of the 25-mer natural peptide contains a heptad repeat (*abcdefg*) with hydrophobic Leu side chains in *a* and *d* positions whose burial in a tightly packed core is the primary basis for association with the βγ-peptide (Figure 6.3a and b). The heterooligomerization of the α-peptide is further directed by positioning of exclusive positively charged Lys residues at *e* and *g* positions. The remaining *b*, *c*, and *f* positions are at the solvent exposed regions of the helix and therefore occupied by polar residues. The structure of the hybrid peptide is different due to the extended backbone amino acids. The additional CH_2 groups at the backbone of the peptide reduce the number of backbone residues per helix turn (~2.5 instead of 3.6 of the coiled coil forming α-helix). Therefore, this type of hybrid peptide experiences a five residue repeat (pentad, *a'b'c'd'e'*) instead of a heptad.

Our structural investigation was conducted first by molecular dynamic simulation, which defined the structural preference of the alternating βγ sequence. However, the deviation from the helical conformation occurs over time and is more significant at the N terminus (Figure 6.3b). Circular dichroism spectroscopy and size exclusion chromatography were applied to study experimentally the possible interaction between the α-peptide and βγ-peptide. While, the spectrum of the α-peptide demonstrates a random coil structure with typical minimum about 200 nm, in the absence of any known reference the positive ellepticity of the peptide at 218 nm was not structure-indicative (Figure 6.3d).

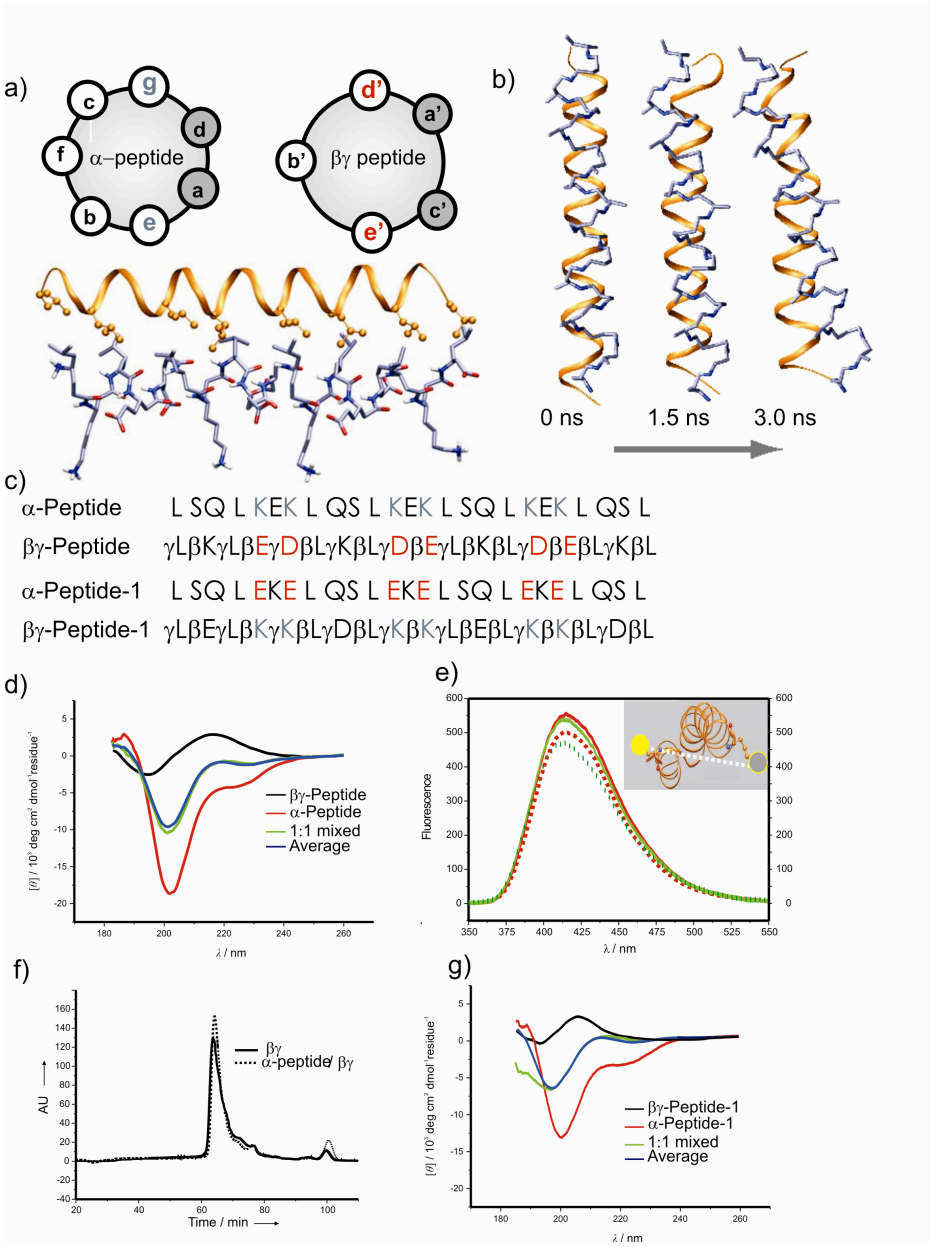

Figure 6.3 *a) Helical wheel representation of α-peptide and βγ-peptide (top). Molecular models of βγ (blue ribbon) engaged in parallel coiled coil interaction with α-peptide (gold ribbon) (bottom). b) Snapshots from the MD simulation of βγ-peptide. c) Sequences of α- and βγ-peptides. d) CD spectra of βγ at 50 μM, α-peptide 50 μM, and an equimolar mixture (50 μM in each peptide) in Tris/HCl buffer solution at pH 7.4. e) The 50μM N-terminally attached Anthranilic acide isolated (red, solid-line) and mixed with 100μM N-terminally attached nitrotyrosine (red, dash-line), 50μM C-terminally attached anthranilic acide (green, solide-line) and mixed with 100μM N-terminally attached Nitrotyrosine (green, dash-line). f) SEC of the βγ-peptide, and equimolar mixture of α-peptide/βγ-peptide at 50 μM. The peak at 100 min is the internal reference. g) CD spectra of βγ at 50 μM, Acid-pp 50 μM, and an equimolar mixture (50 μM in each peptide) in Tris/HCl buffer solution at pH 7.4.*

To determine the interaction between two α and βγ sequences in solution, the spectrum of the 1:1 ratio mixture was required, which clearly overlaps the mathematical average of ellepticities observed by isolated sequences. Although the unknown CD signal for hybrid peptide needs more structural investigation in order to define the related conformation, the result of the mixed spectrum clearly suggests the absence of any significant interactions between the unnatural sequences.

Additionally, to study possible hetero-assembly, we carried out FRET experiments, such studies have been shown to be of use in investigating the formation of the leucine zipper motif.[145,146] Here, the acceptor 3-nitrotyrosine (Y(NO_2); λ_{abs} = 420 nm) was introduced at the N-terminus of βγ-peptide and donor 4-aminobenzoic acid (Abz; λ_{ex} = 320 nm; λ_{em} = 420 nm) was incorporated into α-peptide at either the primary amine of an additional Lys residue (Lys19) or as an additional amino acid at the N-terminus. This strategy enables investigation of the heterooligomerization of the component peptides in both parallel and anti-parallel orientations.[145-147] The Förster radius R_0 of this particular donor-acceptor pair is 29-31 Å. In a hybrid α/βγ coiled coil this distance is between 20-25 Å (corresponding to the diameter of the helix bundle) which is less than the Förster radius. Therefore, intermolecular quenching is expected to occur upon heteromeric coiled coil formation. The resulting fluorescence spectra of N-terminally labelled α-peptide-Abz in the presence of different concentrations of N-terminally labelled βγ-Y(NO_2) is shown in figure 6.3e. An increase in the concentration of βγ-Y(NO2) does not result in a change in Abz fluorescence intensity, meaning that no association can be demonstrated. The experiments were also carried out with C-terminally labelled α-peptide-Abz which similarly resulted in no quenching effect (Figure 6.3e).

Furthermore the oligomerization states of the mixture solution were examined by size exclusion chromatography. These results indicate a single peak at 64 min and reveal the monomeric state of the components overlapping the obtained peak by the isolated hybrid βγ-peptide at the same concentration (Figure 6.3f).

According to the applied modelling, the side chains of the residues at *e* and *g* positions of α-peptide are not in close contact with the side chains at equivalent positions of *e'* and *d'* in hybrid βγ-peptide, mainly because the side chains at electrostatic interface of the hybrid peptide are more tilted toward the outer face of the helix. This fact precludes interactions of the complementary charged residues facing at the electrostatic domain, and therefore destabilizes the entire coiled coil structure.

In order to test whether the design could be improved by the electrostatic interactions, the complementary charged side chains on βγ-peptide and α-peptide were exchanged, resulting in another model system: βγ-peptide-1/α-peptide-1 (Figure 6.3b). The positively charged Lys residues possess longer and more flexible side chains; therefore, they are expected to approach better the complementary carboxylate groups on the α-peptide-1. The interaction of the peptides was examined in a 1:1 mixture by CD spectroscopy. However, similar to βγ-peptide/α-peptide, the CD spectrum of the mixture solution did not support the interaction between the two peptides (Figure 6.3g).

In the absence of any high resolution analysis, the structural conformation of the βγ-hybrid peptides can not be identified but the obtained results illustrate the unflavoured heterooligomerization between βγ-peptide and the native one. It is likely that either the excess of the entropic penalty of the highly flexible βγ strand to adopt a helix conformation or the difference in packing of βγ-hybrid peptide and α-sequence are the prohibitive factors for the hetero-association.

Next to improve the design, following strategies were concerned, which control but not exclude the flexibility of the backbone as well as reduce the non-buried hydrophobic surface which is achievable in general by solvent. i) Shortening the chain length. ii) Integrating the βγ alternating segments into a helix forming natural peptidic sequence. iii) Providing maximum contacts of the side chain (e.g. interlocking the side chains) at the interhelical recognition domains. The latter case sometimes demands the pre-organization of the side chains (mostly constrained residues) or the challenging synthesis of backbone extended residues with specifically positioned or otherwise natural side chains. The shortest α-peptide chain enable to adopt an α-helical structure has a limit of three heptad repeats, while the unnatural peptide containing β-amino acids are reported with helical structures having only six residues. However, to achieve the optimum contacts through a coiled coil assembly, the interacting peptides should be similar in length. Therefore, the shortening of the sequence is not a relevant strategy in design of an artificial assembly between an α-peptide and a complementary βγ-chain.

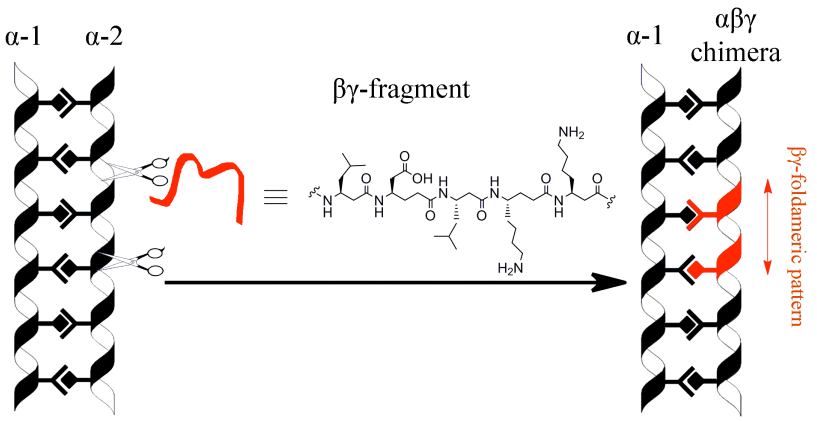

Figure 6.4 *Schematic presentation of the chimeric peptide design based on a dimeric coiled coil system (α-1/α-2). A heptad in a coiled coil forming peptide (α-2) is substituted with an alternating βγ-foldameric pattern (in red). The flanking α-segments induce the helicity to the βγ-sequence. Naturewise, the heterooligomerization of the αβγ-chimera and the natural α-peptide is driven by interhelical interactions.*

We combined this strategy with the second suggested, by introducing systematically an extended sequence of β- and γ-amino acids with proteinogenic side chains in an α-helix forming natural polypeptide (Figure 6.4). The systematic substitution of a specific pattern in a functional α-peptide, reduces the disturbing alteration of sequence encoded information which in turn avoids the apparent changes in association behavior as has been observed in many cases of backbone modification. Additional side chain contacts, by means of precise positioning, elongation or bulkiness of the side chains providing for more interhelical contacts, are the suggestions in order to optimize this design strategy.

6.2.2 Heteromeric α-helical coiled coil forming parent system

The sequence-based backbone modification has to be applied to a natural α-sequence which can tolerate a variety of backbone replacement patterns without losing the ability to associate as a helix bundle with biophysical behavior similar to that of the parent α-peptide. This suggests that the self- or hetero-assembling capability encoded in the side chain sequence tolerates significant variations in backbone structure. This tolerance is particularly noteworthy of the backbone modification, which is applied to the interhelical recognition domain of the resulting chimeric coiled coil. Among the most abundant helix bundles of dimeric, trimeric, and tetrameric coiled coil, the tetrameric quaternary structures are more amenable to subtle and systematic backbone and amino acid substitution without significant perturbation of the overall structure. This is attributed to more buried surface

area in the tetrameric structure compared to the dimeric one (Figure 6.5).[118] According to investigation by Harbury *et al.* the *e* and *g* residues in the tetramer are almost as buried as *a* and *d* residues of the dimer.[118] Similarly, the *b* and *c* residues of the tetramer are almost as buried as the equivalent residues of *e* and *g* in the dimeric structure. Other significance of the tetrameric structure compared to other naturally-derived dimeric or trimeric coiled-coils is the greater interhelical distance between the interwined helices. The diagonally related helices of the tetramer have the same relative orientation but are further apart allowing for the burial of the groups that, in the dimeric state, would be solvent exposed. Apparently, the specific properties of tetrameric coiled coils provide a well-conserved packing geometry for bulky side chains and extended backbones at the hydrophobic core.

Geometric Parameters of the Refined Structures*

Parameter	Dimer	Tetramer
Supercoil radius, R_0 (Å)	4.9	7.6
Amino acids per supercoil turn, ω_0	100	139
Supercoil pitch (Å)	147.6	205.4
buried surface area (Å^2)	900	1640
Helix separation (Å)	8.46	9.84

*Parameters are based on the crystal structures of the dimeric GCN4p1 and tetrameric GCN4pLI

Figure 6.5 *Schematic presentation and geometric parameters of the refined dimeric and tetrameric structures.*[114]

Noteworthy to mention, in spite of the high stability of the described well-arranged packing, the tetrameric coiled coils are *per se* very sensitive to the sequence-encoded data, and therefore perfectly reflect the energetic impact of any backbone or side chain mutations as low as a single residue. Therefore, tetrameric helix bundles were subject of many backbone modifications.[125,131,146]

To this end, we hypothesized that the tetrameric helix bundle is a more attractive and appropriate scaffold for the $\alpha\alpha\alpha\rightarrow\beta\gamma$ backbone engineering due to the above mentioned advantages of tetrameric systems to dimeric ones. Therefore, initially the sequence-based approach was applied to a tetrameric coiled coil system composed of two peptides, Base-pp and Acid-pp (figure 6.6a and b). The designs of both acidic and basic peptides are

characterized by hydrophobic Leu at *a* and *d* positions and the *e* and *g* positions are predominantly occupied by charged residues. The two peptides differ only at the *e* and *g*. Glutamic acid residues were located at these positions in one peptide, designated Acid-pp, whereas lysine was chosen in Base-pp.

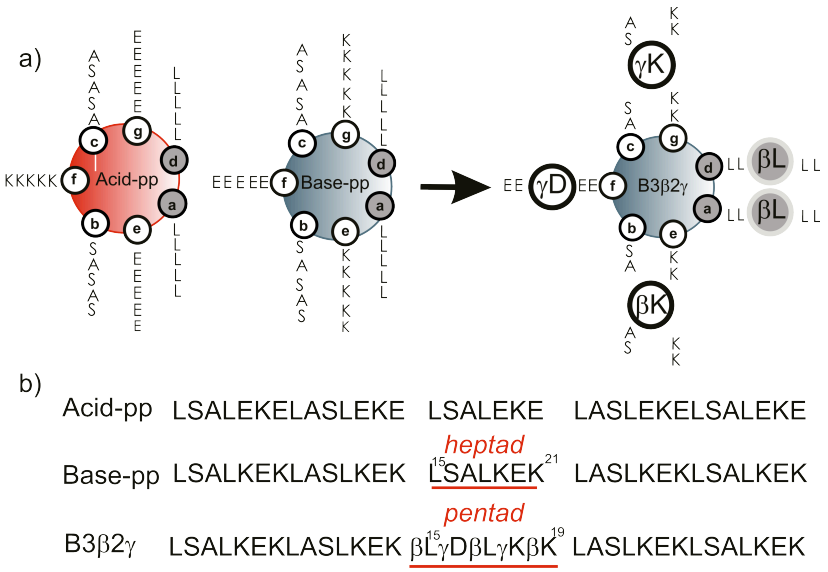

Figure 6.6 *a) Helical wheel presentations and b) Sequences of Acid-pp, Base-pp and the αβγ-chimera. The central heptad of Base-pp is substituted with a pentad in B3β2γ.*

While the homo-assembly of the peptides was shown to be destabilized through similarly charged residues at *e* and *g* positions, the CD spectrum of an equimolar mixture of Acid-pp and Base-pp indicates that the mixture is highly helical and stable with T_m value above 100 °C.[132] The side-chain methylene groups of residues at positions *e* and *g* pack against the predominantly hydrophobic residues at positions *a* and *d*, completing the hydrophobic interface, therefore the basic peptide with exclusive arrangement of the Lys residues at *e* and *g* positions is expected to have more hydrophobic support for the stability of the coiled coil. To this end the backbone modification was applied to the basic α-peptide sequence. We designed an αβγ-chimeric sequence by substitution of two central helical turns with an extended sequence of β- and γ-amino acids that forms highly stable coiled coil heterotetramer with the acidic α-peptide.[132]

In order to test our hypothesis, the impact of the backbone modification in a dimeric coiled coil assembly was futher tested experimentally in an investigated model system of Kim *et. al.*[147] The Kim system is composed of two peptides, Base-p1 and Acid-p1, inspired by studies of the Fos/Jun system[148, 149], a transcriptional activator involved in the signal transduction pathway, and the yeast transcription factor GCN4[150] (Figure 6.7). The designs

of both acidic and basic peptides are characterized with hydrophobic Leu arrangement and the e and g positions are predominantly occupied by charged residues. Adding an additional Leu residue to both Acid-p1 and Base-p1 compared to the original Kim design, we introduced more distance between the substituted β- and γ-amino acids and the C-terminus which is suggested not to substantially contribute to the helical structure.[151]

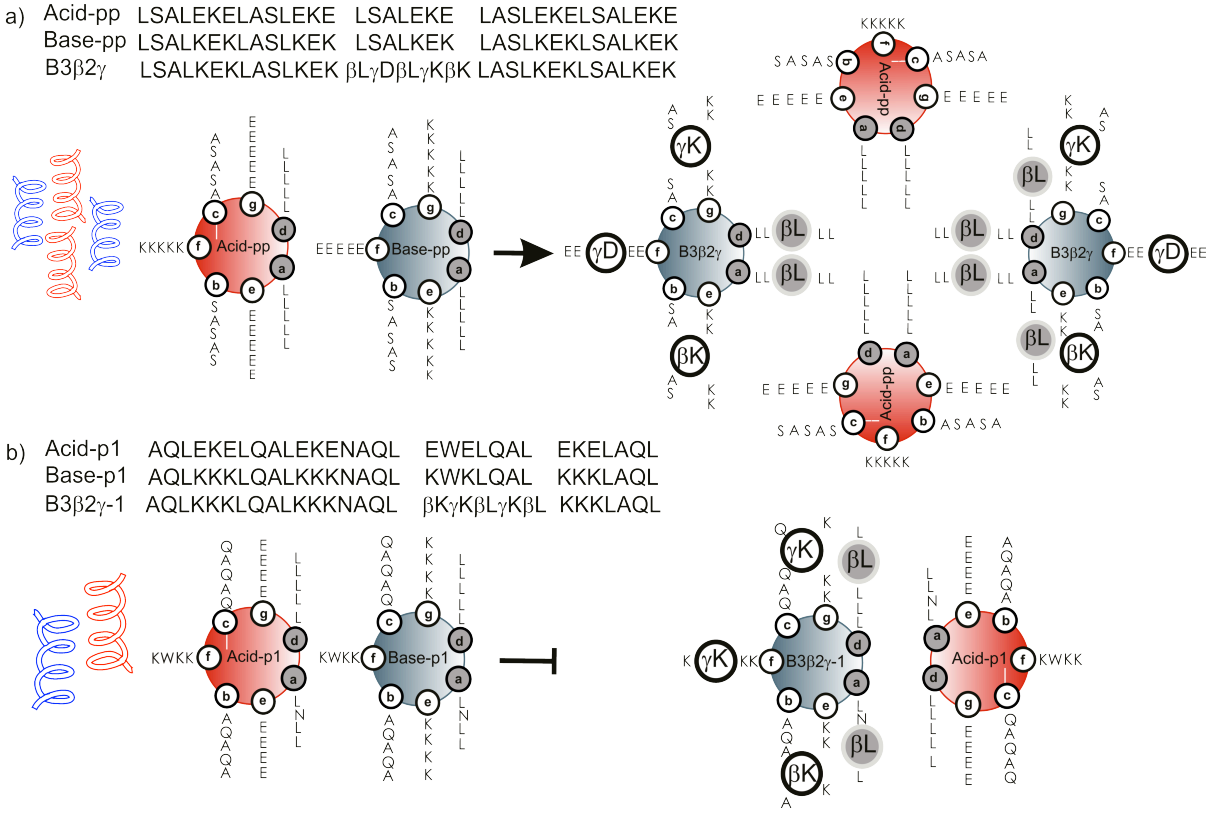

Figure 6.7 *a) Helical wheel representation of the tetrameric peptide component: Acid-pp, Base-pp and the modified chimera: B3β2γ b) Helical wheel representation of the dimeric peptide component: Acid-p1, Base-p1 and the modified chimera: B3β2γ-1. The peptide sequences are mentioned for all employed peptides on top of each panel.*

The dimeric state of the parent system reported by Kim *et al.*[152] and was further confirmed by size exclusion chromatography (data not shown). The two peptides differ only at positions *e* and *g* positions. Therefore, the homo-assembly of the peptides is expected to be destabilized through similarly charged residues at *e* and *g* positions. Similar to other investigated systems, the backbone modifications were applied to the Base-p1. This sequence is special due to the presence of asparagine residues at the hydrophobic core which has been shown to be a key element for the parallel dimeric structure formation. Because of such sequence encoded specialty in the central heptad, other heptad rather

the central one has been chosen. In B3β2γ-1, a complete heptad in the Base-p1 was substituted by an alternating sequence of β- and γ-amino acids. Isolated, each of the peptides Base-p1, Acid-p1 and the chimeric sequence of B3β2γ-1 are predominantly unfolded. However the biophysical behavior of the chimera in solution differs from that of the Base-p1.

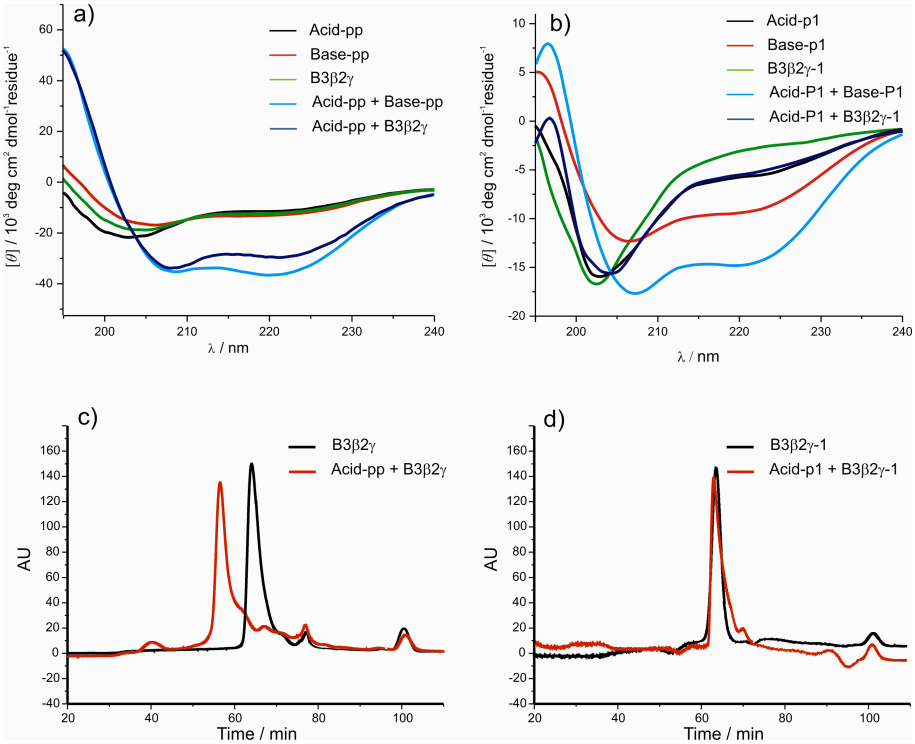

Figure 6.8 *a) CD spectra of B3β2γ at 20 μM, Acid-pp 20 μM, and an equimolar mixture (10 μM in each peptide). b) CD spectra of B3β2γ-1 at 200 μM, Acid-pp 200 μM, and an equimolar mixture (100 μM in each peptide). All measurements in Tris/HCl buffer solution at pH 7.4. c) and d) Size exclusion chromarograms of the isolated αβγ-peptides, and in an equimolar mixture with corresponding acidic α-peptides. The overall peptide concentration for c and d are 20 μM and 200 μM, respectively. The peak about 100 min is the internal reference (Abz-Gly).*

While the natural sequences associate in a parallel hetero-dimeric coiled coil[152], the assembly of the Acid-p1 and B3β2γ-1 was unsuccessful, as judged by the experimental data including CD spectrum and size exclusion chromatography (Figure 6.8). The impact of the same alteration in a tetrameric parent system is in marked contrast with the dimeric one. The comparison of the significant difference observed by CD and SEC for isolated B3β2γ and the 1:1 Acid-pp/ B3β2γ mixture clearly confirms the association of the chimera and α-peptide, apparently as a tetrameric helix bundle (Figure 6.8). The prodigious complementarities in side chain packing between the βγ segment and its α interaction

partner in a tetrameric α-helical coiled coil structure support the “scaffold-dependence” concept of such backbone modifications.

6.2.3 Further structural investigation of the hetero chimeric coiled coil folding motif

6.2.3.1 FRET studies

Despite the well-suited packing geometry of the tetrameric assembly of Acid-pp/Base-pp, as a scaffold for backbone engineering, this system lacks any selective element that directs the orientation of the helices toward each other. We wondered whether the insertion of the extra CH_2 groups into the backbone may provide such structural selectivity, therefore we carried out FRET experiments. Such studies have been shown to be of use in investigating the formation of the leucine zipper motif, as well as determining the preferred orientation. Here, the acceptor 3-nitrotyrosine (Y(NO_2); λ_{abs} = 420 nm) was introduced at the N-terminus of B3β2γ and the donor 4-aminobenzoic acid (Abz; λ_{ex} = 320 nm5) was incorporated into Acid-pp at either the primary amine of Lys34 or as an additional amino acid at the N-terminus. This strategy enables investigation of the heterooligomer with regard to a parallel or antiparallel arrangement of helices. The Förster radius R_0 of this particular donor-acceptor pair is 29-31 Å. In a tetrameric coiled coil this distance is about 30 Å (corresponding to its supercoil radius) which is in the range of the Förster radius. Therefore, intermolecular quenching is expected to occur upon hetero-tetrameric coiled coil formation. The resulting fluorescence spectra of N-terminally labelled Acid-pp-Abz in the presence of different concentrations of N-terminally labelled B3β2γ-Y(NO_2) is shown in Figure 6.9a. An increase in the concentration of B3β2γ-Y(NO2) results in a decrease in Abz fluorescence intensity, meaning that association can be demonstrated. These experiments were also carried out with C-terminally labelled Acid-pp-Abz and resulted to similar response. These results suggest that αβγ-Chimera, similar to parent peptide Base-pp, assembles with Acid-pp in both parallel and antiparallel binding modes.

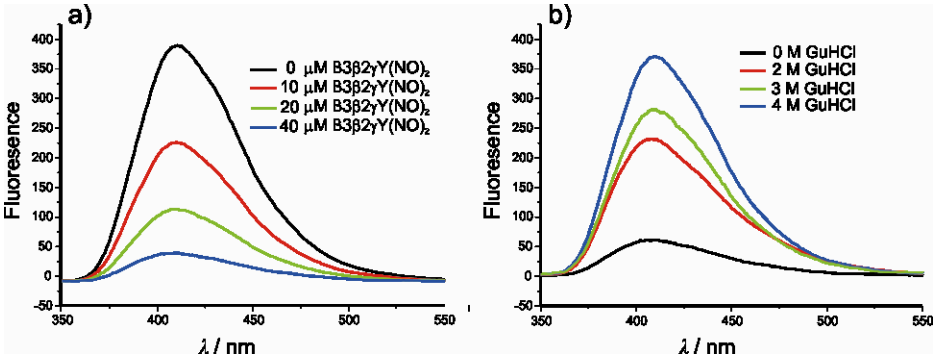

Figure 6.9 *a) Fluorescence spectra of 50 µM N-terminally labelled Acid-pp-Abz in the presence of different concentrations of N-terminally labelled B3β2γ-Y(NO_2). b) Fluorescence spectra of a mixture of 20 µM N-terminally labelled Acid-pp-Abz and 40 µM B3β2γ-Y(NO_2) at various GndHCl concentrations.*

Furthermore, GndHCl denaturation experiments clearly show that the Acid-pp/B3β2γ association is reversible. A considerable increase in donor fluorescence intensity at higher concentrations of denaturating agent is observed (Figure 6.9b) and is due to the exponential decrease in energy transfer efficiency as the spatial separation between the donor and the acceptor is increased.

6.2.3.2 The impact of high concentration on the structural behavior of the native and chimeric coiled coils

The parent system Acid-pp/Base-pp has shown to aggregate to α-fibres at concentrations above 100 µM, observed by TEM and AUC. This structural behaviour is imitated by B3β2γ/Acid-pp; the AUC result for the equimolar mixture of B3β2γ and Acid-pp (50 µM in each) is consistent with a state of aggregation and this observation provides additional strong evidence for the heteromeric association of these peptides. These assemblies are further specified by transmission electron microscopy as unbranched fibers of approximately 3 nm thickness (Figure 6.10a), and are similar in overall structural features to the fibers that result from equimolar mixture of Base-pp/Acid-pp (Figure 6.10b).

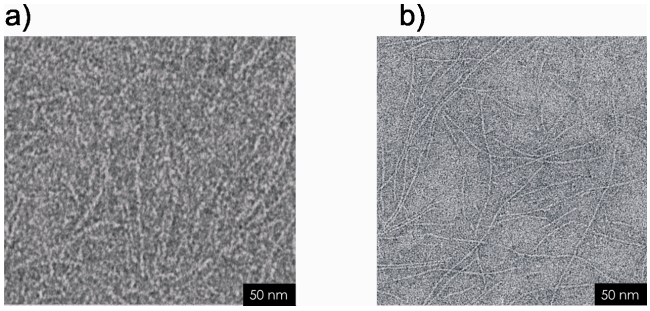

Figure 6.10 *a) and b) TEM of the equimolar mixture of Acid-pp/Base-pp and Acid-pp/B3β2γ at 250 µM.*

6.2.4 Selecting preferred interaction partners using combinatorial-screening methods

The pronounced fold stability of Acid-pp/B3β2γ is the result of prodigious complementarities in side chain packing between the βγ segment and its α interaction partner that leads to successful integration of the artificial fragment into an otherwise native-like α-helical coiled coil structure. However, the relatively lower thermal stability of the chimeric system compared to the natural system indicates the necessity for broadly surveying the optimized interaction properties. The availability of multiple, complementary β- and γ-amino acids may be necessary for generating a closer homogeneity to the native pattern, however, the number of the commercially or synthetically available β- and γ-residues is not sufficient for this goal. In contrast, the high availability of the α-building block facilitates the systematic empirical search for preferred interaction partners. Applying this approach, we assist the design of the foldameric pattern by finding the crucial contact elements, in order to improve the association of the unnatural pattern with the natural one. Whereas the rationally design of best interacting α-partners for chimeric sequence is highly limited to forehand selection of few analogous, the combinatorial chemical synthesis and analysis enables us to utilize and exploit the enormous amount of information generated by a large variety of target-interacting candidates. Therefore, two different techniques, the spot synthesis/analysis and the phage display technique, were used to identify sequences recognized by foldameric pattern and define the preferred composition of the corresponding artificial helix in respect to thermodynamic stability. These methods assist us to map α-residues on the natural peptide strand that interact with key β- and γ-amino acids on chimera.

6.2.4.1 Spot synthesis and analysis

Miniaturization and automation are the hallmarks of spot technology. This method provides for a huge number of probes and test samples that can be screened in ever shorter times, and markedly reducing assay dimensions and costs, as well as opening access to a very sensitive analysis. Such analysis has been shown to be useful for characterizing of the intermolecular domains[153] in general and coiled coils[154] in particular, at the amino acid level.

To this end, a wide range of the analogues of wild type α-partner (Acid-pp) were synthesized and analyzed in order to evaluate the influence of amino acid substitutions on association of the α-partner with the αβγ-chimeric backbone. Further, the stability and the stoichiometry of some preferred sequences were examined by CD and SEC in solution. First, we synthesized a peptide array comprising 1764 quadruple-substitution variants of Acid-pp (*wt*) sequence on cellulose membrane and probed it for binding to the chimeric sequence of B3β2γ, which was synthesized by standard solid-phase peptide synthesis and labeled at the N terminal with tetramethylrhodamine (TAMRA). As described above, chimera has its modified pentad (β- and γ-amino acids) at the centre of its 31-residue sequence (positions 15-19). Thus, the mutated positions are chosen from the complementary heptad of Acid-pp (positions 15-21), as designated in figure 6.11a, b. In order to investigate the crucial contacts at the interhelical domains of the corresponding coiled coils, the library included residues located close to and within the interhelical core (*adeg*) which are most responsible for molecular recognition. This means mutations were applied simultaneously to both hydrophobic (a^{15}, d^{18}) and electrostatic (e^{19}, g^{21}) residues (Figure 6.11a, b). The 35mer mutants on the membrane have a great identity in their sequences and only differ in positions interacting with β- and γ-residue side chains. Therefore, the binding of α-mutants to the αβγ-chimera can directly be attributed to unique interaction profile of the βγ-alternating pattern.

According to the fact that the hydrophobic residues drive mainly the hetero-oligomerization, the mutations at a^{15} and d^{18} positions incorporated only the hydrophobic amino acids including the sterically bulky ones (Figure 6.11a). For the e^{19} and g^{21} positions, aside from the complementary negative side chains of Glu and Asp, residues of a hydrophobic nature were included.

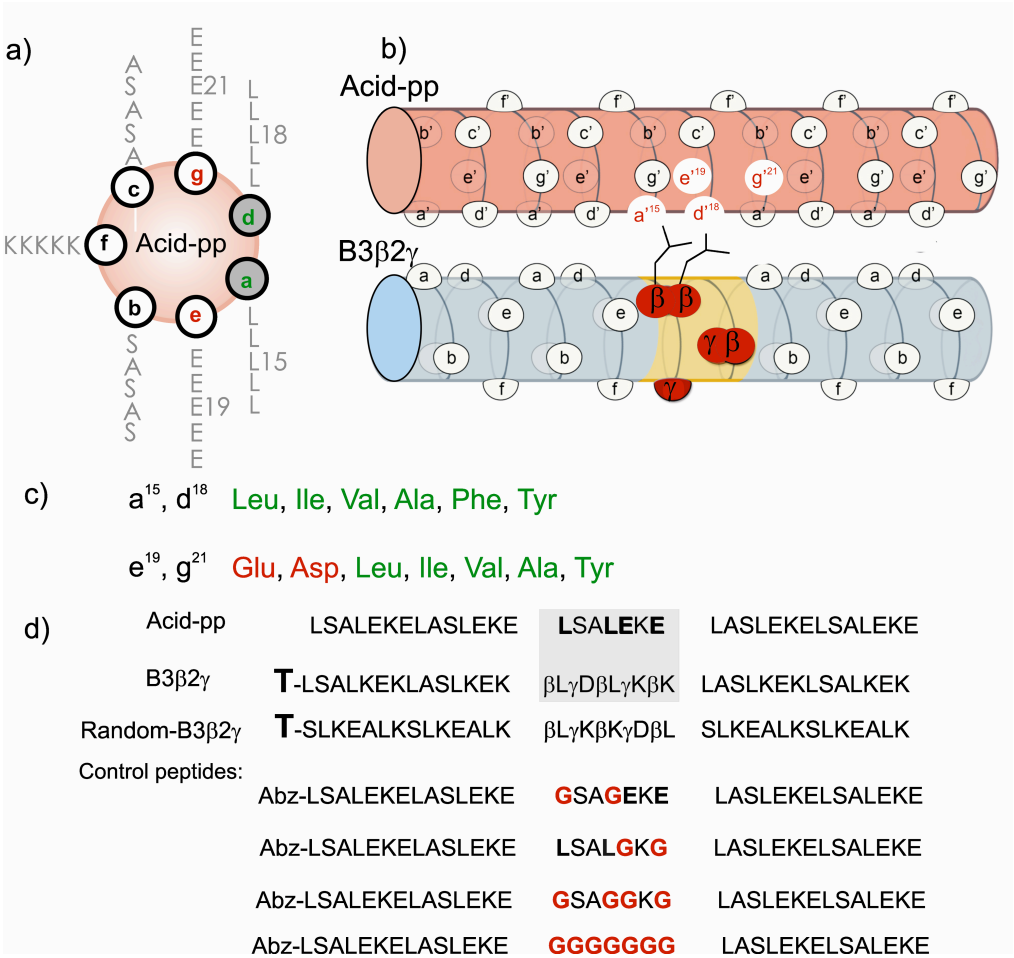

Figure 6.11 *a) Helical wheel representation of the Acid-pp (wt). The mutated positions are mentioned with their position number. The alternative hydrophobic and electrostatic amino acids are in green, and red, respectively. b) The cylindrical presentation of the Acid-pp and B3β2γ sequences. The mutated positions as well as the β- and γ-amino acids are presented in red color. c) The suggested amino acids for the hydrophobic and electrostatic positions. d) Sequences of Acid-pp (wt), B3b2g, randomly designed chimera: Random-B3β2γ, and control peptides.*

Interactions between the chimera and immobilized α-mutants were measured using a peptide array assay (described in methods and assays section). The peptide array was then incubated with fluorescently labeled chimera at a concentration of 10 μM. The measured intensities of the signals obtained from the TAMRA labeled modified sequence, interacting selectively with immobilized α-peptides, were classified due to signal intensities (SI) based on the observed Boehringer light units (BLUs). Remarkably, α-mutants exhibit diverse interaction properties in terms of binding to the chimera, despite their limited sequence variability (Figure 6.11c). Based on the SI values the α-mutants were classified in five different interacting groups. The sequences which have equal or slightly higher SI values compared to *wt* ($L^aL^dE^eE^g$) are classified as strong binders with only 22 members.

The second and third classes contain the mutants with SI values lower than the strong binders but still above 50% and 25% of *wt*, respectively. The poor binders have SI values below 25% of *wt*. The obtained SI values are summarized in sequence logos for the central heptad in *wt* (Figure 6.12), which show the frequency of selected residues at the mutated positions *a*, *d*, *e*, and *g*.

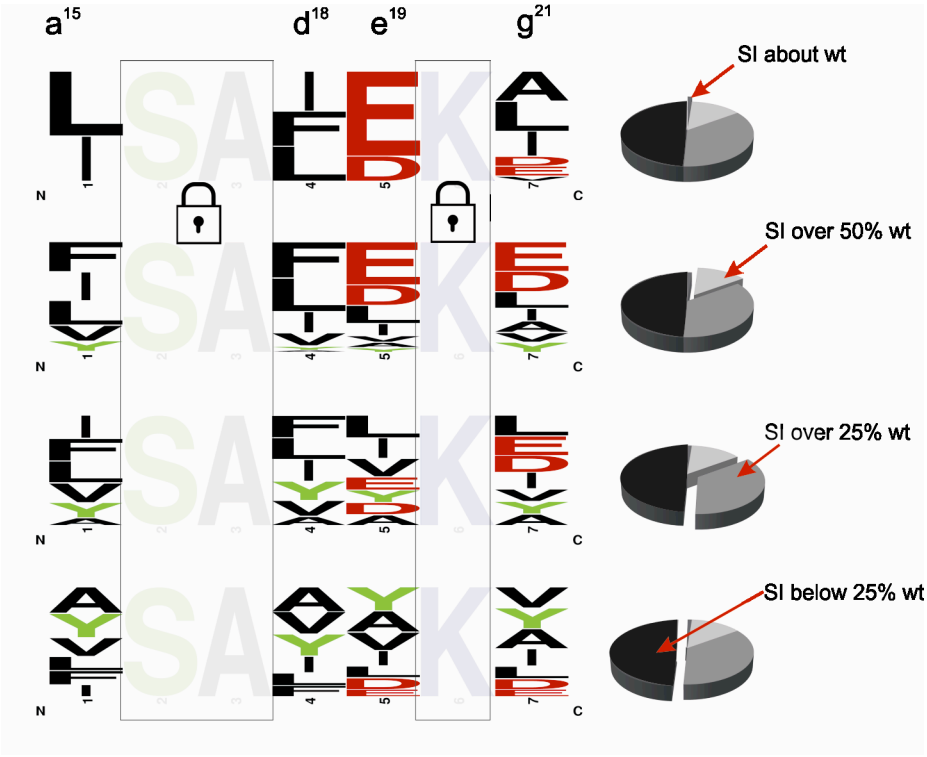

Figure 6.12 *The sequence logos (left) and the Pie charts (right) standing for a/d/e/g substitutions and summarizing heterospecific associations. The mutated positions a, d, e, g are designated by 1, 4, 5, 7 respectively. The logos and charts are classified due to signal intensity (SI).*

At each position the residues are arranged in order of predominance from top to bottom and the selected mutants are named after the combination of four mutated residues. Comparison of the sequence logos for all α-mutants reveals the high selectivity of strong binders for interacting with the chimera (hetero-selectivity). The frequency of specific side chains at the recognition domains suggests the preferred interactions between the β- and γ-amino acids and the complementary side chains of the natural α-partners (Figure 6.12, first logo on top).

The randomization of the type of side chains at a^{15}, d^{18}, e^{19} and g^{21} results in variety of different α-sequences, which are immobilized on the celloluse membrane via a βAla-βAla linker. Several types of sequencing were carried out to characterize an appropriate sequence optimally interacting with the βγ-foldameric pattern on the chimeric αβγ-

sequence. Some sequences helped to identify the key positions essential for recognition (the sequences that are involved in Gly-scan), and rest identified the preferred amino acid side chains that are allowed at each of the key positions (sequences that are involved in X-scan). Prior to spot analysis, the quality of the spot synthesis was examined by cleavage of few spots and characterization of the synthesized peptides by analytical HPLC and mass spectrometry.

As a negative control, the binding affinity of the modified sequences was tested against a randomly designed αβγ-chimeric sequence (Figure 6.11b), resulting in significantly poor binding profile. Interestingly, the sequences on the membrane show a remarkable selectivity in binding to B3β2γ, in contrast to the randomly designed αβγ-sequence (Random-B3β2γ) suggesting a direct relation between the observed light intensity and the possible hetero-association of chimera with mutants on the membrane. The rational binding of B3β2γ to the α-mutants on the membrane, in contrast to Random-B3β2γ, is an indication that the analyzed data are of good quality. Other indicative hallmarks are as follow:

- Interactions observed among the chimeric sequence and α-partners were highly consistent with previously published data.[132] In our previous study we reported a gradual destabilization of the chimeric coiled coil assembly by gradual truncation of the β- and γ-side chains at the hydrophobic core due to loss of hydrophobic interactions between αβγ-peptide and its native α-partner.[132] Similarly, the interactions between the peptide array and the chimera are lost by sequences presenting shorter side chains of Val and Ala at *a* and *d* positions.

- The negligible binding affinities between the chimera and the control sequences in which the hydrophobic and electrostatic residues were scanned with glycine residues (Figure 6.11b) indicate the rational selection of the mutants by B3β2γ based on a sufficient side chain-side chain contacts.

The peptide array detected many new side chain interactions, whose investigation provides us with useful insights about the complex contact-networks of a αβγ-chimeric folding motif, in the absence of high resolution structural data. The double mutation presentations of the mutants are shown in Figure 6.13. In such presentations three positions b, c and f at the outer face of central heptad in *wt* are considered constant and only the mutations are shown for either the hydrophobic (Figure 6.13a) or electrostatic (Figure 6.13b) domains. Regarding to figure 6.13a as well as the sequence logo for strong

binders, a higher peptide-peptide interaction was observed between chimeric pattern of B3β2γ and the α-mutants with large and bulky hydrophobic residues, including the aromatic Phe, long and bulky Leu, and β-branched Ile. In all helix bundles, there are buried cavities between helix-bundle components which are closely packed by hydrophobic side chains, and therefore they are usually water excluded.[118,146] The enlargement of the described cavity through positioning of the backbone extended amino acids in the core of the chimeric coiled-coil structure highlight the necessity of a compatible coverage for such cavity.

a)

LSALEKELASLEKE a[15]SAd[18]EKE LASLEKELSALEKE

d[18] \ a[15]	L	V	I	F	Y	A
L	20424.984	7793.704	10941.831	13737.3	11723.013	4069.144
V	9201.354	4487.474	7748.494	7686.152	2704.179	189.5977
I	15737.724	15205.1723	14911.99	13578.162	6629.298	2534.6982
F	15490.304	13385.7636	20267.119	13363.576	13616.249	3175.3204
Y	6679.6556	3517.7144	5386.138	7115.941	4750.984	511.1511
A	3236.2825	1324.0491	1791.734	4827.463	964.243	0

b)

LSALEKELASLEKE LSALe[19]K g[21] LASLEKELSALEKE

g[21] \ e[19]	L	V	I	Y	D	E	A
L	7851.372	6518.869	8638.414	5388.24	19113.994	20395.664	4902.384
V	6318.974	4843.249	5886.171	4220.864	17048.023	20796.744	4229.794
I	7323.554	3742.82	6498.388	3575.479	18424.553	21117.853	5317.494
Y	7697.191	5319.932	8183.929	8779.764	10789.644	16438.266	3842.829
D	11299.119	9306.264	12451.307	10396.715	7568.504	15830.153	5891.7987
E	10129.524	10162.404	10774.035	6647.009	14325.184	20424.984	9553.3516
A	4552.25	2932.792	5138.294	2567.102	16391.066	20557.504	2644.5285

Figure 6.13 *a) The mutation logo of the most frequently accepted residues by the strong α-binders. b) The signal intensities are translated into Boehringer light units (BLUs). Rows and columns represent the mutated positions. The selected mutations for further study in solution are highlighted.*

Therefore, it is likely that the steric side chains are well accommodated at these positions in order to avoid the packing frustration and destabilization of the assembly. Consequently, the bulky side chains (most frequently Phe and Leu residues) are preferred at the interior parts of the chimeric coiled coil bundle regarding to their space-filling character. The impact of these bulky hydrophobic residues can be compared following the double-mutation charts in which the *d* position in each case is occupied with Ile, Leu and Phe (Figure 6.12, 6.13a).

Interestingly, the preference of the hydrophobic residues is highly position dependant. The Phe is more favored at the *d* position while Leu is more selected in the *a* position. In spite of the size homogeneity between Phe and Tyr residues, they display prominent differences in coiled-coil formation, likely due to the destabilizing orientation of the polar hydroxyl group toward the hydrophobic core.[155]

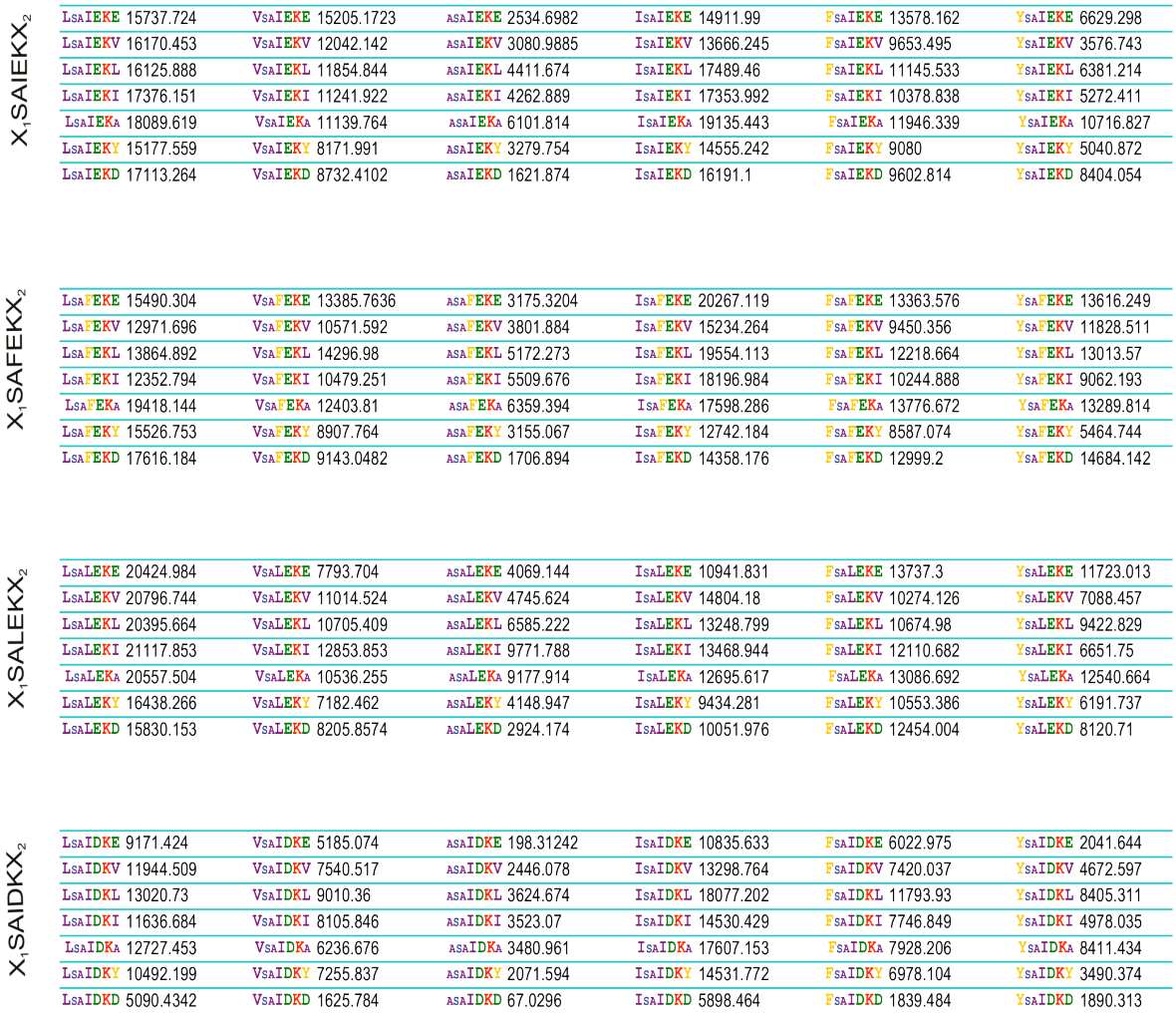

Figure 6.14 *Double mutation charts. The color codes are as follow: hydrophobic residues are in purple, the negatively charged ones are in green, positively charged are in red, tyrosine residue is in yellow and serine is presented in blue.*

The substitution of a single hydrophobic position by tyrosine ($L^{15}Y$) in $Y^aL^dE^eE^g$ mutant results in a significant reduction in the spot intensity compared to *wt* (Figure 6.12 and 6.13a). Subsequently, the mutants with two Phe residues in spite of providing sufficient hydrophobicity at the interhelical domain are among the weak binders. This is also true for the β-branched Ile; the substitution of two Ile residues results in medium binding affinity. This can be explained due to the fact that the chimeric hydrophobic core similar to the native coiled coils critically reacts to uncomfortable excess of side chain bulkiness.[155, 156] On the other hand the preference of specific hydrophobic side chains in *a* and *d* positions as well as unique combination of those evident that the selection of the residues at the hydropbobic core is not driven only by hydrophobicity of the side chains but also in respect to the side chain packing. Namely, the $I^aF^dE^eE^g$ mutant having Ile at a^{15} position in

combination with Phe at d^{18} is among the strong binders, whereas the SI value is significantly lower for a formally similar mutant with $F^aI^dE^eE^g$ pattern. Therefore, the side chain hydrophobicity and the preferred packing geometry are two different aspects, the combination of which can provide for the high stability of an artificial coiled coil.

These results additionally confirm the impact of the complementary electrostatic interactions at the *e* and *g* positions. The presentations of double mutations in these positions (Figure 6.13b) as well as the SI values of double mutated sequences X_1SAIDKX_2 and X_1SAIEKX_2 (Figure 6.14) show that shortening of the negatively charged, due to Glu^{e19}Asp exchange, results in a general decline in affinity for binding to the chimera for almost all presented mutants on the membrane. However, there is a discrepancy between the two core-flanking positions; the *e* position was found to be significantly higher in replacement sensitivity than the formally similar *g* position. The mutants with a broad spectrum of side chains at *g* position all have similar binding affinities for binding to chimeric pattern, suggesting that the g^{21} position is not the key element that influences the hetero-association. Oppositely, the comparison between the sequence logos confirms that the strong binding is highly dependent of the nature of the charged residue at *e* position. This fact was observed and reported as well in natural coiled coils.[154] Another interesting observation is the population of the hydrophobic residues at the core-flanking positions, which are interacting with leucine side chains of β-amino acids. This fact suggests the β-amino acids side chains contribution to the extended interhelical hydrophobic domain.[157-159] Further, to gain more insights into the interrelationship between hetero-selective binding and structure stability, some mutants from different classes were further studied in solution (Figure 6.15a). These sequences were synthesized on resin, purified, and finally investigated by CD (Figure 6.15) and size exclusion chromatography (Figure 6.16) measurements. We chose $I^aF^dE^eE^g$ as a representative of the strong binders to be tested in solution because of the frequently repeated positioning of Phe at the hydrophobic core, and more specifically at *d* position. The combination of Phe at *d* and Ile at *a* position resulted in significantly high binding affinity of $I^aF^dE^eE^g$ for assembling with the chimera. Moreover, the behavior of the $V^aV^dE^eE^g$ and $G^aG^dE^eE^g$ were tested in solution, which belong to medium and poor binder classes, respectively. The great similarity of these patterns with the *wt* sequence allows for studying the impact of substituents at *a* and *d* positions. As recognized from the efficient binding ability, $I^aF^dE^eE^g$ mutant is predicted to associate strongly with B3β2γ. This was confirmed in solution by a CD spectrum of an equimolar mixture of B3β2γ and the $I^aF^dE^eE^g$ mutant, which presented canonical minima at

222 and 208 nm of the α-helical coiled coil structure and the relatively high thermal stability (Figure 6.15b, c). In order to be able to quantitatively compare the thermal stability the melting process were carried out for the equmolar mixture solution of B3β2γ and each of the selected α-mutants, in presence of 2 M GndHCl.

The equimolar mixture of B3β2γ and $I^aF^dE^eE^g$ results in relatively high T_m values of 70°C, which is also close to that of equimolar mixture of B3β2γ and Acid-pp (T_m values of 74°C), (Figure 6.15c). In spite of the high affinity of $I^aF^dE^eE^g$ mutant for binding to the chimera on the membrane, B3β2γ/$I^aF^dE^eE^g$ has still lower thermal stability compared to parental system B3β2γ/Acidpp.

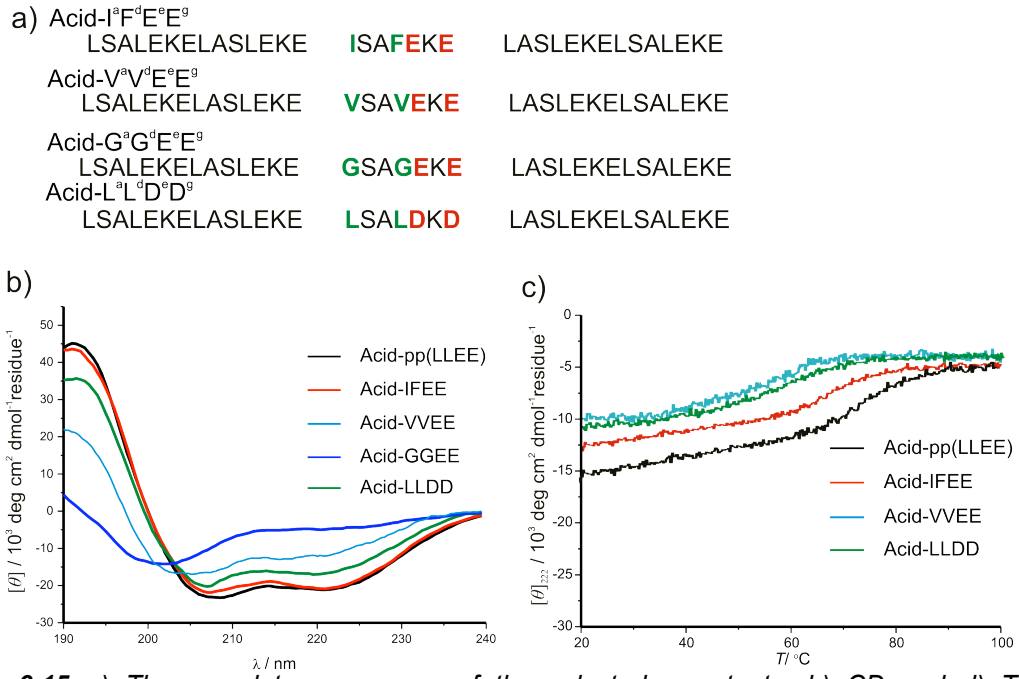

Figure 6.15 *a) The complete sequences of the selected α-mutants. b) CD and d) Thermal denaturation spectra of an equimolar mixture of B3β2γ with the α-mutants (10 μM in each peptide).*

Other selected mutant is $L^aL^dD^eD^g$, in which both Glu residues at e^{19} and g^{21} positions were substituted by Asp. The side chains at these positions are expected to interact with their complementary side chains of β^3-homoLys and γ^4-homoLys residues at βγ foldameric part of B3β2γ. Comparison of the melting point of B3β2γ/$L^aL^dD^eD^g$ with B3β2γ/Acid-pp (B3β2γ/$L^aL^dD^eD^g$ =64 °C, B3β2γ/Acid-pp =74 °C) demonstrates the impact of the electrostatic interactions between the natural and foldameric sequence on the stability of the resulting chimeric coiled coil.

In order to study the impact of the applied mutations on stoichiometry, the oligomerization state of the corresponding helix bundle of B3β2γ with each selected mutant was tested by SEC measurements (Figure 6.16). Expectedly, the $I^aF^dE^eE^g$ mutant having aromatic Phe residue at the interhelical interaction domain promotes higher states of oligomerization. The geometry of Phe residues at the hydrophobic core suggests the possibility for aromatic-aromatic interactions.[160] Phe exhibits the distinct feature of being largely indiscriminate in defining a specific oligomerization state at hydrophobic positions.[161] However, the major amount of the mixture solution (B3β2γ/ $I^aF^dE^eE^g$) is in tetrameric state, the broad shape of the chromatogram reveals a multi state assembly as well as an aggregation state (at 45 min). The SEC results demonstrate a tetrameric state for other two probed equimolar mixture solutions (B3β2γ/ $L^aL^dD^eD^g$ and B3β2γ/ $V^aV^dE^eE^g$), same as the B3β2γ/Acid-pp. The retention of the oligomeric state provides the opportunity for equally comparing the packing effects and burial of hydrophobic surface in different mutants. The equimolar mixture solution of the medium binders $L^aL^dD^eD^g$ and $V^aV^dE^eE^g$ with B3β2γ, display less intense minima at 222 nm an 208 nm, with T_m values much lower than melting point of *wt* (T_m B3β2γ/ $L^aL^dD^eD^g$ =64 °C and T_m B3β2γ/ $V^aV^dE^eE^g$ = 52°C*)*.

A more dramatic decrease in structure stability was observed in the B3β2γ/$G^aG^dE^eE^g$ mutant in which both Leu residues are mutated to glycine and the corresponding equimolar mixture solution is incapable of coiled coil formation. Therefore, we can conclude that the improved packing of the coiled coil structure could lead to an increase in thermal stability. Likewise in the natural α-helical coiled coil structure, the mutation of amino acids in the hydrophobic core of the chimeric coiled coil motif has much greater effects on the structure, when compared with the case of a mutation on the core-flanking positions. The replacement of Leu side chains in the *wt* sequence (Acid-pp) with Val in $V^aV^dE^eE^g$ has a more pronounced destabilizing effect compared to substitution of Glu side chains in the *wt* to Asp in $L^aL^dD^eD^g$ mutant. The difference in the impact of the applied mutations is also reflected in differences in spot intensity. As mentioned in Figure 6.13, the signal intensity of $L^aL^dD^eD^g$ mutant is almost half of the intensity observed by $V^aV^dE^eE^g$.

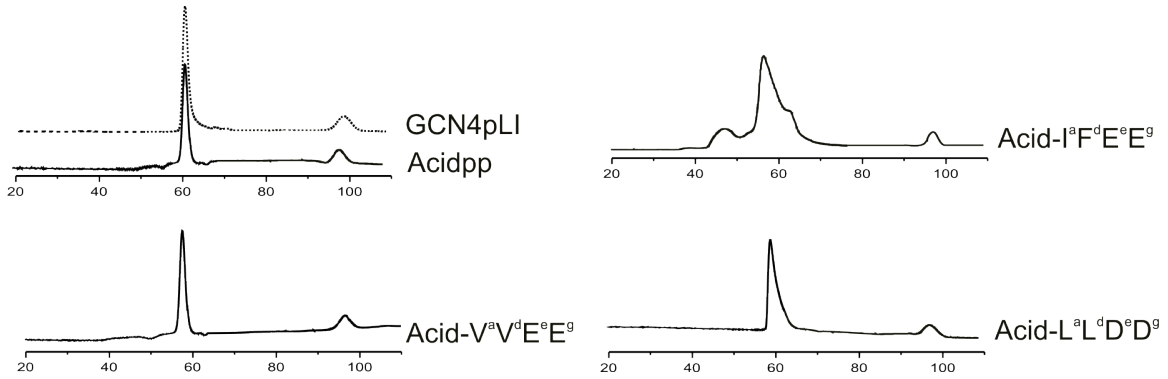

Figure 6.16 *Size exclusion chromatograms of an equimolar mixture of B3β2γ with the α-mutants (10 μM in each peptide). The chromatogram of tetrameric GCN4pLI is presented as reference for tetrameric structure. The comparison of the R_t value with GCN4pLI reveals a tetrameric structure for equimolar mixture of B3β2γ with Acid-pp (wt), as well as V^{a}V^{d}E^{e}E^{g} and L^{a}L^{d}D^{e}D^{g}, and a multi-state oligomerization for I^{a}F^{d}E^{e}E^{g}.*

Applying spot analysis, the interaction specificity of the B3β2γ has been studied by using coiled-coil arrays to assess the hetero-interactions with a wide range of α-peptides. However, this goal did not achieved and the systematic analysis did not lead to pattern(s) with greater affinity for binding to chimeric sequence compared to than wild-type (Acid-pp). The reason for that can be the limitation in number of mutations on the membrane. Nevertheless, these results suggest that the spot synthesis/analysis is a potentially powerful method to identify specific peptide partners that significantly assemble with an unnatural sequence. Interestingly, the coiled coil forming $\alpha\beta\gamma$-chimera exhibits a wide range of interaction profiles upon binding to immobilized α-mutants which are sometimes only differ gently in their patterns. Furthermore, this study determines the crucial residues forming the recognition epitop of the foldameric $\beta\gamma$-pattern. Dependence of the interaction affinities on side chain mutations in *a* and *d* positions as well as *e* position of interacting α-partners suggests the contribution of the complementary side chains on the $\beta\gamma$-foldameric pattern in the recognition process prior to coiled coil assembly. Therefore, the overall analysis of the interaction between the α-partners and B3β2γ provides for valuable information about possible interaction space accessible to chimera.

6.2.4.2 Phage display

Whereas, the mapping of the key positions by spot synthesis method is limited to a few types of α-amino acids due to restrictions in the number of derivatives that can be synthesized, the phage display method allows assaying the triggered heptad positions against all 20 coded amino acids. In phage display technique, artificial chemical evolution

is used to identify and isolate binding partners of a specific ligand out of a library of recombinantly produced peptides or proteins.[141,162,163] Screening peptide libraries for preferred interaction partners out of the pool of twenty canonical α-amino acids by this method facilitates to discover consensus sequence with less homology with parental epitope. This is one of great advantages of phage display to other screening methods with limited libraries and number of mutants. This screening approach provides valuable information about binding domains by creating sequences that show activities upon binding to βγ-foldameric pattern in B3β2γ. According to this method a particular type of amino acid is considered essential for binding if it is repeated frequently.

In the library the key positions (*a, d, e, g*) at the central heptad of Acid-pp (*wt*) were considered and therefore, randomized in DNA strands coding for *wt* by applying the $(NNK)_n$ strategy and displayed at the surface of a filamentous bacteriophage M13.[164] Two chimeric sequences of B3β2γ and a control variant, B3β2γ-variant1 (Figure 6.17) were synthesized and labeled by a biotin tag, and loaded on to Streptavidin magnetic particles. The previous studies have shown a drastic decrease in stability of the resulting hetero coiled coil assembly of Acid-pp/B3β2γ-variant1 compared to Acid-pp/B3β2γ, due to removal of two key side chains of β^3leucines in B3β2γ (please see section 6.1).[164]

Particles without peptide were used as a negative control and treated equally. Both chimeric sequences were screened in six panning rounds each followed by washing steps applying an increasing concentration of detergent (*Tween 20*). Additionally, the denaturing agent guanidinium hydrochloride was used in the final round. After each round, an aliquot of reinfected bacteria culture was titered on agar plates containing antibiotic (Carbenicillin) to only select infected bacteria. Colonies grown on the plates were counted and the overall colony number was calculated to assess the enrichment of colonies upon selective binding to the immobilized interacting sequence. Interestingly, our results showed a considerable enrichment of colonies for B3β2γ with a maximum in panning round 5 (Figure 6.18). These results reveal the significantly higher binding capacity (10000-fold higher colony number than its negative control without peptide) of expressed pIII fusion proteins on phage surfaces to B3β2γ on magnetic particles than its negative control without chimera. Whereas a significant enrichment of colonies was observed for B3β2γ, the screening of B3β2γ-variant1 resulted in a low colony number at the level of the background of unspecific bound phages found within the negative control, indicating the key role of the two β-amino acids at the hydrophobic core which are required for binding (Figure 6.18).

Starting from round 4, single colonies were picked from the plates and their phagemid vectors were isolated for DNA sequencing (Table 6.1).

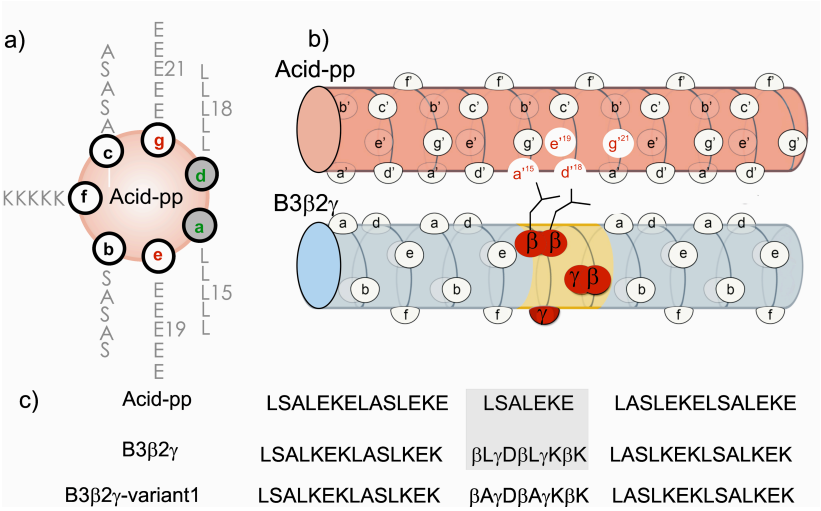

Figure 6.17 *a) Helical wheel representation of the Acid-pp (wt). The mutated positions are mentioned with their position number. The alternative hydrophobic and electrostatic amino acids are in green, and red, respectively. b) The cylindrical presentation of the Acid-pp and B3β2γ sequences. The mutated positions on Acid-pp as well as the β- and γ-amino acids on the chimera are presented in red color. c) Sequences of Acid-pp (wt), B3β2γ, B3β2γ-variant1.*

Several rounds of selection provide a short list of peptide sequences that bind selectively with B3β2γ. The comparison of the selected phage insert amino acid sequences reveals the most important positions and appropriate residues that improve the binding activities (Table 6.1). The trends within the amino acids at the randomized positions in all preferred clones are highly similar, suggesting that the hetero selective interactions between chimera and its natural α-partner are highly specific. Of all isolated binding clones, clone1 ($C^aF^dL^eE^g$) is the most repeated and therefore interesting one, which is confirmed by both genotype and phenotype sequences (refers to clone1 and 2). $I^aC^dE^eF^g$ (refers to clone4) and $V^aL^dL^eD^g$ (refers to clone5) are other two mostly repeated sequences (Table 6.1). The $C^aF^dL^eD^g$ sequence (refers to clone3) is also among the preferred sequences which has a high structural homology to clone1. Markedly, the applied rounds of selections led to convergence on the cysteine residue in the hydrophobic core, either at a^{15} or d^{18} positions. Importantly, the selected sequences are unrelated to parental sequence (central heptad of acid-pp). Therefore truly different physicochemical properties from the newly suggested side chain packing at the interhelical core of the chimeric coiled coil should be expected.

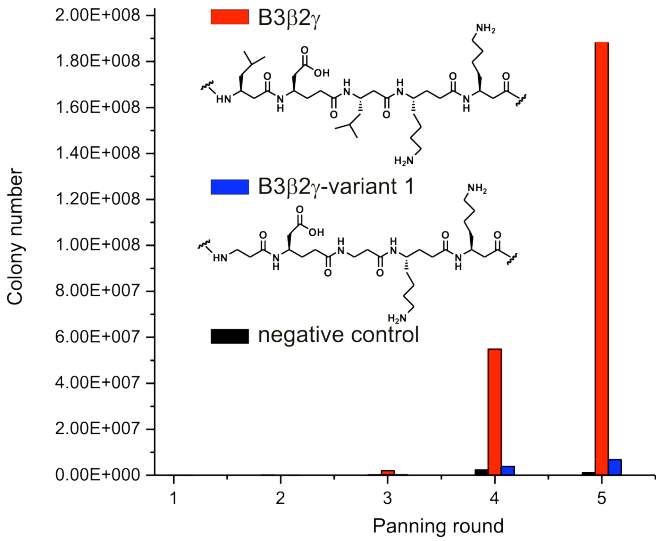

Figure 6.18 *Colony numbers throughout each panning round with* B3β2γ *and* B3β2γ*-variant 1 and negative control. The structures of the βγ- foldameric part of the chimeras is shown.*

It is also important to note that the coiled-coil pairing selectivity is profoundly influenced by core flanking side-chain interactions. This can be recognized due to intolerance of these positions to be substituted by a variety of amino acids. The hydrophobic Leu residues as well as negatively charged glutamic acid are the frequently selected amino acids at these positions.

Comparing the selected amino acid by means of phage display at each of four randomized positions, identified an interesting similarities to the trends found by spot analysis (please see section 6.2.4.1). According to both methods, the steric and bulky hydrophobic residues are well preferred at the chimeric hydrophobic core. This similarity can be seen also in positioning of the key side chains, e.g. Ile at a^{15} and Phe residue appears often at d^{18}. The resemblance in the observations is also followed by the core flanking positions; these residues mainly tolerate negatively charged Glu and hydrophobic side chains. However, according to the phage display screening one can not observe the discrepancy between the two core-flanking positions, as was the case in the spot analysis. This can be attributed to the technical differences in the presentation of the targeted peptide in two methods.[165]

Table 6.1 *Sequencing resulted from mutation-free vectors for B3β2γ. The amino acids at the mutated positions for the selected sequences interacting with B3β2γ. as well as the negative control peptides and wild-type are shadowed in light grey.*

Positions / Sequences	a^{15}	d^{18}	e^{19}	g^{21}
Clone1	TGT (Cys)	TTT(Phe)	CTT(Leu)	GAG(Glu) x2
Clone2	TGT (Cys)	TTT(Phe)	TTG(Leu)	GAG(Glu)
Clone3	TGT(Cys)	TTT(Phe)	CTT(Leu)	GAT(Asp)
Clone4	ATT(Ile)	TTG(Cys)	GAG(Glu)	TTT(Phe) x2
Clone5	GTT(Val)	CTG(Leu)	TTG(Leu)	GAT(Asp)
Acidpp (*wt)*	Leu	Leu	Glu	Glu
$C^aF^dL^eD^g$(selected)	Cys	Phe	Leu	Ile
$I^aF^dL^eE^g$(control)	Ile	Phe	Leu	Ile
$I^aC^dE^eF^g$(selected)	Ile	Cys	Glu	Phe
$I^aV^dE^eF^g$(control)	Ile	Val	Glu	Phe
$V^aL^dL^eD^g$(selected)	Val	Leu	Leu	Asp

It is also important to note that in contrast to B3β2γ, the evaluation of sequenced phagemid vectors from panning with B3β2γ-Variant 1 revealed a completely random distribution of different amino acids throughout all positions (Table 6.2). This fact indicates that there is no observable trend for the selection of particular residues at any of the randomized position and in turn reveals the critical contribution of the hydrophobic side chains in the βγ-segment in hetero-selection of the clones bound to phages. These observations suggest that an optimum packing between two β^3Leu side chains and those of the selected α-peptide requires a compromise in interactions of both contributing sequences at the characteristic interhelical domains.

The selected peptides were synthesized and the influence of amino acid substitutions on the association of equimolar mixture of the selected peptides with B3β2γ are tested in solution. Additionally, control sequences $I^aF^dL^eE^g$ and $I^aV^dE^eF^g$ were studied as structure-homologues of $C^aF^dL^eE^g$ and $I^aC^dE^eF^g$, respectively, in order to judge the impact of Cys residues on the entire structure stability.

Table 6.2 *Sequencing results of mutation-free vectors and selected peptides interacting with B3β2γ-variant1.*

Positions / Sequences	a^{15}	d^{18}	e^{19}	g^{21}
Clone1	Ala(GCT)	Ser(TCT)	Gln(TAG)	Ser(TCG)
Clone2	Gln (TAG)	Var(GTG)	Tyr(TAT)	Ala(GCG)
Clone3	Leu(CTT)	Cys(TGT)	Asn(AAT)	Val(GTG)
Clone4	Thr (ACG)	Ser(AGT)	Leu(CTG)	Val(GTT)
Clone5	Gly(GGT)	Pro(CCG)	Pro(CCG)	Ser(TCG)

Interestingly, the peptides follow the same trend as found by selected phages, in solution. The increased hydrophobic core packing of $I^aC^dE^eF^g$ and $C^aF^dL^eE^g$ sequences is reflected in their higher thermal stability compared to Acidpp/B3β2γ bundle (Figure 6.18a). While $C^aF^dL^eE^g$ /B3β2γ has a significantly higher T_m value (85°C) compared to Acidpp/B3β2γ (71°C), the equimolar mixture of $I^aC^dE^eF^g$ /B3β2γ starts melting above 90°C. The prodigious stability of $I^aC^dE^eF^g$ /B3β2γ resembles closely the native parental system Acidpp/Basepp system (Figure 6.19a). Hetero-assembly of $V^aL^dL^eD^g$ with B3β2γ however is not resulting in higher stability but equally stable structure (T_m value of 72°C) compared to Acidpp/B3β2γ.

The frequent selection of Cys is observed at the hydrophobic core of the corresponding coiled coil, as well as the pronounced stability induced by Cys containing sequences, suggest this residue being a key element for packing and therefore the mutation of thiol side chain is expected to affect the stability of the entire motif. This hypothesis can be easily studied by comparing the behavior of this sequence with control variants in which Cys is substituted by other relevant residues. Therefore, $I^aF^dL^eE^g$ was synthesized which has high sequence similarity to the most frequently selected clone (clone 1, refers to $C^aF^dL^eE^g$). The substitution of Cys with Ile results in a less stable hetero coiled coil structure (T_m value of 73 °C). The decrease in stability can be attributed to side chain

steric mismatching at the hydrophobic core compared to optimum packing (combination of one small and one large side chain) in $C^aF^dL^eE^g$. According to the hydropathy scale and valume, cysteine is intermediate between alanine and valine.[166] The optimum size of Cys compared to Ile reasons the steric matching with bulky side chains like Phe in $C^aF^dL^eE^g$ or Ile in $I^aC^dE^eF^g$. The significance of steric matching of the hydrophobic core side chains in controlling specificity of the corresponding coiled coil has been explored by several groups. Such side chain matching can be seen also by other preferred sequences; in $I^aC^dE^eF^g$ and $V^aL^dL^eD^g$, Cys and Val are paired with branched Ile and Leu, respectively. Apparently, the resulting well hydrophobic packing is the origin of pronounced thermal stabilities observed by the corresponding chimeric coiled coils.

Other designed control peptide $I^aV^dE^eF^g$ showed considerably less stability in solution (T_m value of 77°C) compared to $I^aC^dE^eF^g$, despite a large structural homology to each other (Figure 6.19b). This result confirms further the crucial role of Cys amino acid on stability of the fold. Albeit valine has a close mean volume to Cys, Cys[15]Val mutation is not well tolerated, which indicates the functional role of cysteine side chain as another stabilizing factor in addition to its physical character (size and hydropathy). Considering a less-ideal helical structure of the βγ-foldameric pattern compared to the native one, the intermolecular H-bonding between backbone carbonyl on the chimeric peptide and the Cys thiol of the α-partner is highly favored in the resulted hetero-assembly. Such hydrogen bond formations have been shown to contribute in a large extent to structural stability.[167, 168] It can be predicted that the close proximity of the functional groups at the interior part of chimeric coiled coil assembly allows for such strong H-bond formation similar to the native one.[168] Regarding the H-bonding ability, Ser and Thr are other reasonable choices that offer stronger H-bonds due to a higher pKa value of alcohol compared to thiol functional group, though none of these polar residues was selected among preferred clones.[169] It appears that the polarity introduced by these residues in the hydrophobic core destabilizes further less ideally packed chimeric coiled coil. In contrast, the physicochemical properties of cysteine residue such as its hydrophobicity and the appropriate size and volume as well as stabilizing intermolecular hydrogen bond makes this residue the most abundant side chain found in the hydrophobic core of B3β2γ/Acid-pp. Considering the native-like stability of the cysteine containing sequences in general and that of $I^aC^dE^eF^g$ in particular, one can conclude that the combination of hydrophobic Cys side chain with a complementary bulky residue fulfill the inquiries of the βγ-pattern in order to form an ideally formed helical construct.

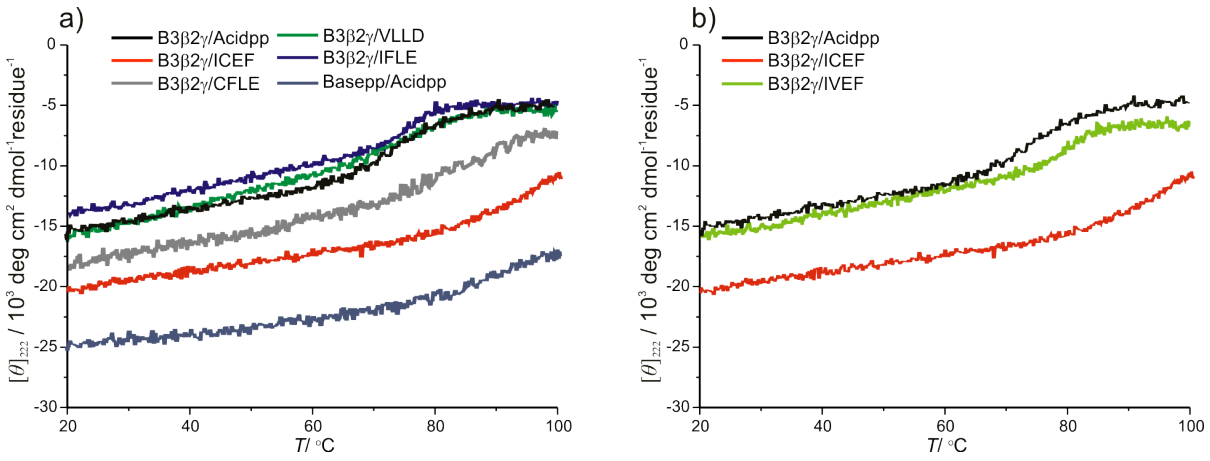

Figure 6.19 *Thermal denaturation spectra of the equimolar mixture of the chimera and selected partners. The spectrum of native parental system is shown for comparison.The peptide total concentration is 20 μM. The spectra were recorded at pH 7.4 and in presence of 1.5M GndHCl.*

Other known functionality of cysteine residues is the ability of disulfide bond formation which has shown to have a great contribution in coiled coil stability[169]; however, it requires optimal sites that are compatible with the strict stereochemical requirements of the disulfide bond in the closely packed interior of a protein. Both local structure and flexibility of the region in which the Cys residue is located affect the rate of formation of the disulfide bond.

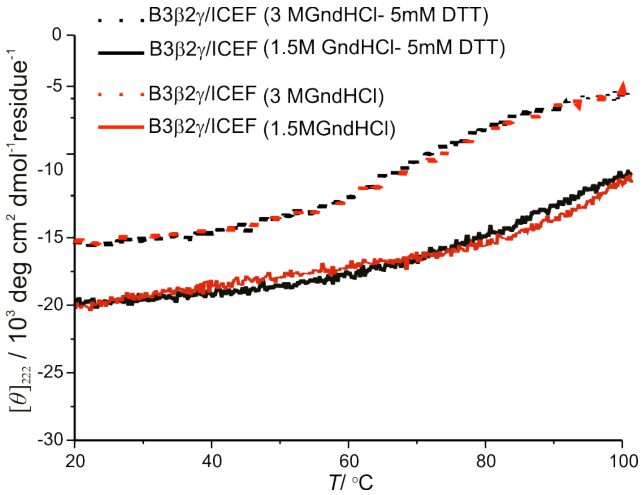

Figure 6.20 *Thermal denaturation spectra of the equimolar mixture of B3β2γ/ICEF. The specta are shown before and after treatment with DTT. The specta are in presence of 1.5 and 3M GndHCl.*

The oxidation rate of thiols located at the rigid hydrophobic core in the central heptad of a 35-mer sequence is expected to be very low, and therefore is less probable to be the basic

of the selection during the bio-panning procedures. However, this concern was explored experimentally by comparison of the CD specta of 1:1 B3β2γ/ $I^aC^dE^eF^g$ before and after incubation with DTT as reducing agent (Figure 6.20).[169] Additionally the samples were heated up to 60 °C in order to facilitate the decline of the disulfide bridges at the interior part of assembly. The resemblance of the obtained spectra indicates that the stability of heterooligomeric coiled coil formation is exclusively a consequence of non-covalent interactions between the monomers.

Further the stoichiometry of the corresponding hetereo coiled coils with chimera was examined by SEC (Figure 6.21). Whereas, the oligomerization state of the 1:1 mixture of B3β2γ and $I^aC^dE^eF^g$ and $V^aL^dL^eD^g$ are similar to a tetrameric state of B3β2γ/Acidpp, the retention time of the hetero-bundles of $C^aF^dL^eE^g$ as well as $I^aF^dL^eE^g$ is consistent with multi-state of oligomerization. This is likely due to stacking of aromatic side chains at the interhelical domains favoring higher orders of oligomerizations, however, tetramers present the major species. Considerably, the Cys[15]Val mutation in $I^aV^dE^eF^g$ affects not only the stability of the fold but also the aggregation state. This mutant presents a mixture of tetramer-trimer oligomeric state.

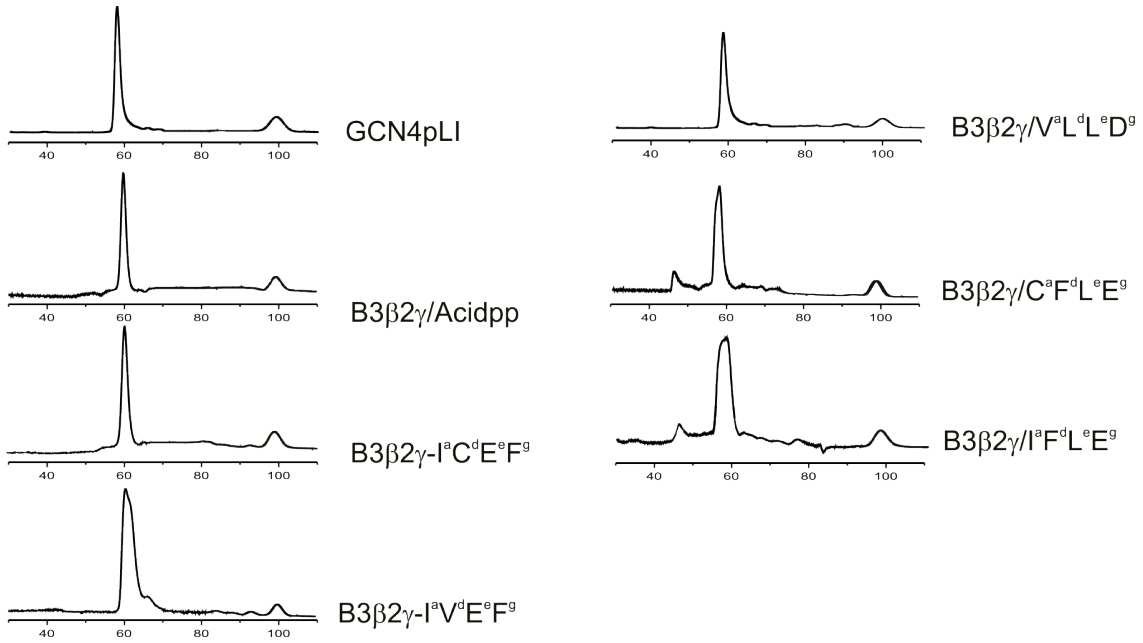

Figure 6.21 *Size exclusion chromatograms of an equimolar mixture of B3β2γ with the α-mutants (10 μM in each peptide). The chromatogram of tetrameric GCN4pLI is presented as reference. The comparison of the R_t value with GCN4pLI reveals tetrameric structure for equimolar mixture of B3β2γ with Acid-pp (wt), as well as $I^aC^dE^eF^g$ and $V^aL^dL^eD^g$, and a multi-state oligomerization for $I^aF^dL^eE^g$, $C^aF^dL^eE^g$ and $I^aV^dE^eF^g$.*

The phage display technique was used to identify sequences recognized by B3β2γ, one of the few coiled coil forming chimeras. These results are further confirmed in solution applying CD and SEC. The few number of selected clones and the close similarity between their sequences show that the functional groups on chimeric site, namely hydrophobic and electrostatic positions require precise physical (size, volume, packing, polarity) and chemical properties (side chain reactivity) in order to bind to α-partner with high selectivity and stability. These results defined hetero coiled coil forming α-partners with the lowest sequence homology with parental *wt* and high affinity to assemble with B3β2γ. Applying this method, chimeric coiled coil motif with significantly higher stability was achieved. Interestingly some of the most selected sequences by phage display screening also resemble the oligomerization state of the native parental system (Acidpp/Basepp). Finally, these observations provide lines of evidences for the reliability of phage display as an excellent technique to generate the natural sequences that suitably interact with unknown artificial coiled coil forming patterns.

6.3 Publication II: A helix-forming αβγ-chimeric peptide with catalytic activity: a hybrid peptide ligase

Raheleh Rezaei Araghi, Beate Koksch, *ChemCommun*, **2011**, 47, 3544 – 3546.

The original paper with supporting information is available at:

http://dx.doi.org/10.1039/C0CC03760E

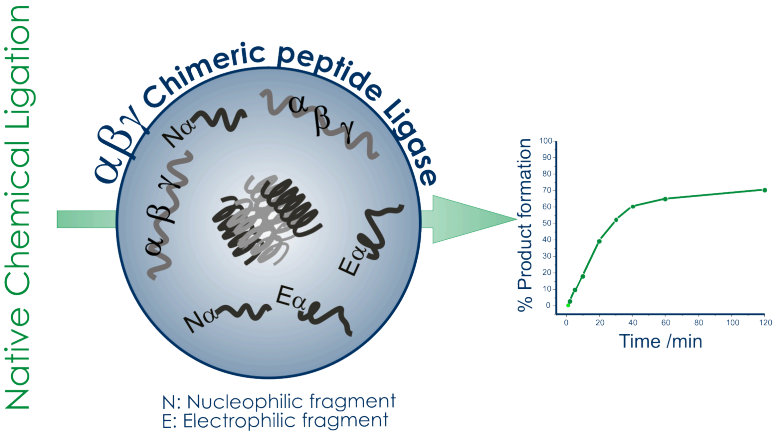

6.3.1 Concept

The unique capabilities of enzymes, which stem from their well-defined three-dimensional structures, have been a source of inspiration for the design and synthesis of unnatural catalysts ranging from synthetic to polypeptide-based molecules. In order to bring the essential functional groups together and present a well-formed catalytic site, a biopolymer catalyst has to suitably mimic the natural folded state in order to enable catalysis to take place. On the other hand, the application of natural peptides in catalyst design is highly limited due to the chain length dependent activity as well as limited structural motifs and α-amino acid library. This fact has inspired the design of foldamer-based catalysts.[170-172] Extensive efforts over the past decade have led to the identification of many families of nonnatural oligomers, also termed foldamers or chimeras that display a variety of specific secondary, tertiary, and quaternary structures. Despite the structural diversity in foldamer design, the rational design of molecules possessing catalytic activity is however still limited to few examples. The challenging factor in foldamer-based design is the mimicry of a well-

formed catalytic site that enables the attachment of catalytic centers at defined locations on the foldamric scaffold for optimal performance.

The previous results revealed that the αβγ-chimeric structure presents arrays of discrete side-chain functional groups in the context of the α-helical coiled coil folding motif. This fact suggests the unique artificial scaffolds of αβγ-chimera for effective engineering of a coiled coil peptide-based catalytic activity. As a case study, peptide ligation phenomenon is selected. In the templated-directed native chemical ligation[173], a coiled coil forming peptide sequence acts as a template to preorganize other peptide fragments in order to form a peptide bond.[174-177] The feasibility of peptide replication has led to the discovery of a wide range of autocatalytic and cross-catalytic systems, all based on the α-helical coiled coil, which is one of the best conserved oligomeric folding motifs in nature. Coiled coils even without any larger scale assembly can be highly functional; one such unique function is the catalysis. As it has been described in section 3.6, the combination of hydrophobic and van der Waals interactions providing the "knobs-into-holes" packing is the primary driving forces for coiled coil formation. Charged residues mainly at positions e and g form the second molecular recognition motif, stabilized by interhelical Coulomb interactions. The combination of these two recognition domains imparts coiled coil peptides with high binding selectivity, a property which has been shown to influence the catalytic efficiency of de novo designed peptide ligases in template-directed peptide ligation.

The native chemical ligation is a chemoselective reaction in which an unprotected peptide-thioester is reacted with a second unprotected peptide containing an N-terminal cysteine residue (Figure 6.22a).[173] This reaction is initiated by reversible exchange of the thioester with the thiol moiety of the N-terminal cysteine side chain. The second step is a rapid and irreversible intramolecular rearrangement, forming the thermodynamically favored amide bond at the ligation site in relatively high yield. The ability of the ligase peptide to anneal with two peptide fragments is mediated by presenting a surface for substrate assembly via formation of a hydrophobic core at the peptide interface (Figure 6.22b).[174, 176, 177] Charged residues flanking the core provide additional binding specificity through electrostatic complementarity. The combination of these two recognition domains imparts coiled coil peptides with high binding selectivity, a property which has been shown to influence the catalytic efficiency of de novo designed peptide ligases. While the annealing of electrophilic and nucleophilic peptides with a complementary full-length template is driven by intermolecular interactions, their condensation is facilitated by the template, due to the

increase in effective concentration in the substrate-template complex including template and the ligating fragments. In order for the catalytic cycle to continue, the peptides must dissociate once the chemoselective ligation has occurred. Therefore, the product inhibits the reaction process by time and the turnover rate is highly dependent on the stability of the product-template complex (Figure 6.22c).

To accelerate this catalytic process, peptides with less ideally packed coiled coil structure are suggested. Out of this particular point, the backbone or side chain modified motifs with relatively less stable binding sites are potentially great candidates for such catalytic activity. Other strategies, such as reducing the number of heptad repeats or creating a proline kink were examined as well as accelerating the coiled coil-mediated ligation reaction.[178,179] Additionally, the incorporation of complementary charges at the e and g positions was shown to enhance substrate binding to the template, therefore it is expected that the environmental conditions will play a role in the ligase selectivity and efficiency upon pH or ionic strength changes.

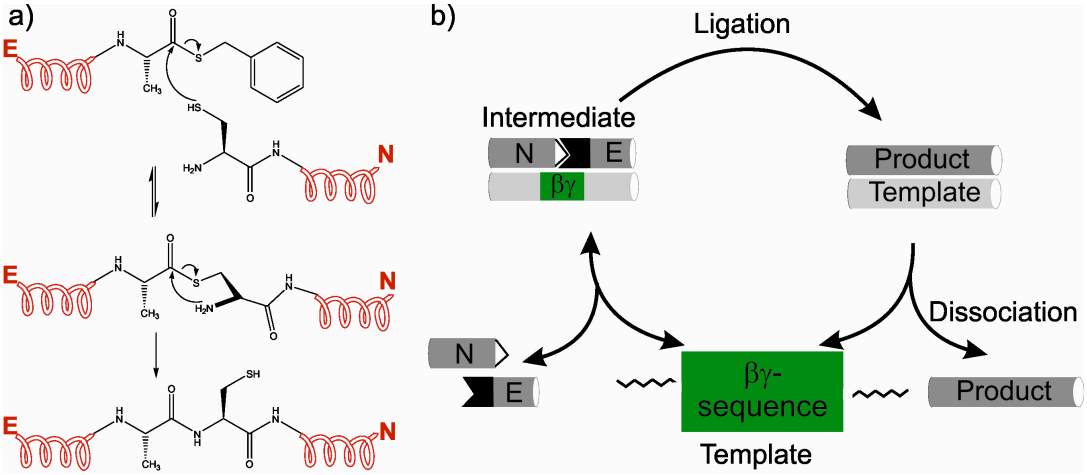

Figure 6.22 *a) Scheme of the native chemical based on the Kent strategy.[173] b) Template-ditected cross-catalyzed peptide ligation and the contribution of β- and γ-amino acids (in green) to the ligation site. The electrophilic and nucleophilic peptides are designated by E and N respectively.*

Similarly, for the αβγ-chimera to act as template, βγ chimeric backbone should provide for the spatial arrangement of all functional groups involved in the formation of the catalytic site to allow efficient catalysis to take place. Hence, the catalytic performance can also assess the structure/stability relationship. To this end, we describe the native-like catalytic activity of the first artificial peptide ligase containing a foldameric sequence of β- and γ-

amino acids, whereas all the de novo designed peptide ligases reported to date consist of exclusively α-amino acids.

6.3.2 Summary

The present study was motivated particularly by the exploration of a heterotetrameric artificial coiled coil (Acid-pp/B3β2γ), applying an exclusive leucine interface. In order to study the impact of the β- and γ-amino acid side chains on the resulting catalytic activity, B3β2γ was selected to act as the α-helical template, while the Acid-pp sequence contains the ligation site. Thus, positions b^{16} and c^{17} in original sequence of Acid-pp were substituted by Ala in the electrophilic thioester fragment (E) and Cys in the nucleophilic fragment (N), respectively. The electrostatic recognition interface of the αβγ-chimeric sequence is occupied by lysine, while those of the natural E and N fragments contain glutamic acids. The annealing of the fragments on the chimeric template is driven mainly by the hydrophobic intermolecular interactions.[177] Furthermore, the incorporation of complementary charges at the e and g positions was expected to enhance substrate binding while disrupting the inhibitory homomeric assemblies.[177] The catalytic power of the chimeric template was determined by measuring initial rates of product formation in the reaction of equimolar solutions of [E] and [N] (Figure 6.23a).

While product formation was negligible in the absence of the ligase, there was a significant increase in the initial rate of ligation upon addition of 50 μM B3β2γ demonstrating the catalytic activity of the chimera, albeit with slightly reduced activity when compared to native Base-pp. Considering the high sensitivity of template-directed ligation to any structural modification applied to the template, near the ligation site, the slight drop in activity has its origin in the modest difference between side chain interactions within the helical structure of B3β2γ compared to the native Base-pp.

The declined catalytic activity of the chimera due to the titration with a denaturating agent confirmed further the structure dependence of the observed catalytic efficiency. In further experiments, we examined the catalytic effect of two control basic peptides, Base-7G and B3β2γL15,17A (Figure 6.23b). Providing a glycine-linker in Base-7G, right at the same region that the chimeric backbone in B3β2γ is extended, and the truncation of the long isopropyl side chains of both hydrophobic β-residues through β^3Leu→β^3Ala mutation in B3β2γL15,17A, resulted in a clear reduction of the initial rate and rate enhancement.

These results provide strong evidence for the contribution of the βγ-sequence to the formation of the interface of the four-helix bundle Acid-pp/B3β2γ by specific orientation of hydrophobic and charged βγ-amino acid side chains, as well as by maintenance of the α-helix-like backbone conformation. The surprisingly similar concentration of Acid-pp needed for the inhibition of the ligation catalysis by Base-pp and B3b2g suggests that the binding affinities of these templates with the complementary acidic peptide in the corresponding coiled coils are also similar. The αβγ-chimeric ligase substantially mimics the substrate selectivity and catalytic efficiency of the natural alpha-peptide. The ability of αβγ-foldameric sequence to form a quaternary structure and mimic the function of the native heptad repeat pattern demonstrates the great potential of this class of chimeric peptides in the development of artificial enzymes.

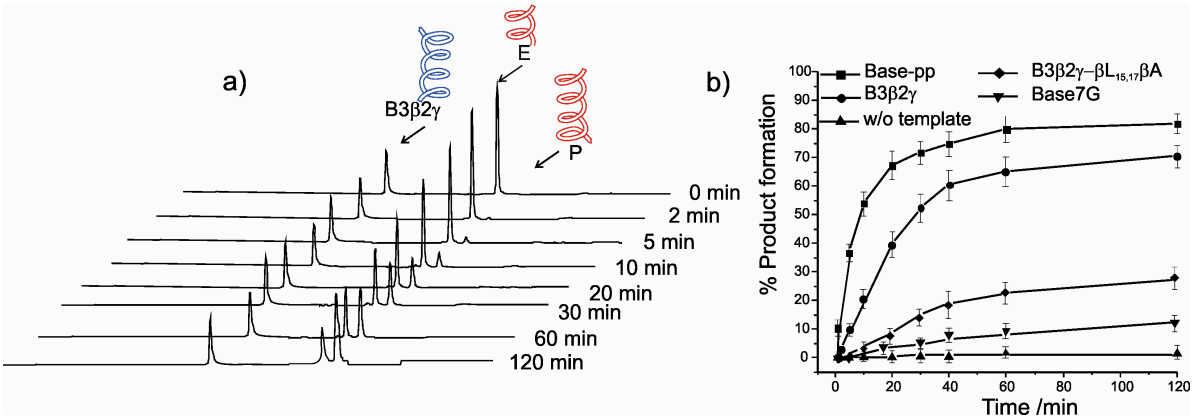

Figure 6.23 *a) HPLC analysis of species observed upon incubation of reaction mixture containing equimolar mixture of E and N fragments = 150 μM and 50 μM of B3β2γ at pH 7.4 and 25°C in redox buffer over 120 min. P indicates product (the ligated peptide chain).b) Product formation as a function of time. The product formation in absence of the template is shown for reference (up-pointing triangles). Error bars show standard deviations of three independent runs.*

Author contributions

All experimental investigations are part of this thesis and carried out by author.

6.4 Publication III: A Systematic Study of Fundamentals in α-Helical Coiled Coil Mimicry by Alternating Sequences of β- and γ-Amino Acids

- **Raheleh Rezaei Araghi**, Carsten Baldauf, Ulla I. M. Gerling, Cosimo Damiano Cadicamo, Beate Koksch, *Amino Acids,* **2011**, 41, 733 -.742**.**

The original paper with supporting information is available at:

http://dx.doi.org/10.1007/s00726-011-0941-z

6.4.1 Concepts

Numerous studies on coiled-coils have led to an understanding of the factors affecting coiled-coil stability. Of these effects, the burial of the hydrophobic core (hydrophobic effect) and packing effect are the major contributors to coiled-coil stability; therefore modifications leading to non sufficient van der Waals interactions at the interior part of helix-bundle fail to suitably adopt this particular folding motif. Harbury *et al.* have shown the role of these buried hydrophobic residues in determining the structural stability and the oligomerization state of the corresponding coiled coils by studying mutants of the GCN4 leucine zipper (a basic leucine zipper protein, and the primary regulator of the transcriptional response to amino acid starvation).[118] The formation of different oligomerization states of coiled coils was explained in terms of packing geometries of the *a* and *d* position amino acid side chains in the hydrophobic core. Additionally, there are also stabilizing factors other than stability contributions from residues in the hydrophobic core (*a* and *d*) positions, such as side-chain van der Waals packing effects, including polypeptide chain length, interchain and intrachain electrostatic interactions, H-bonding and side-chain helical propensities.[180]

6.4.2 Summary

The preliminary structural investigation reveals the great potential of a βγ-pattern to adopt a favorable geometry for α-helical packing in a heteromeric coiled coil model system.[132-133] In a next step, based on a biologically inspired molecule, GCN4pLI (tetrameric variant of GCN4 p1), we designed a αβγ-chimeric structure that exerts native-like interhelical interactions, promoting its self-assembly. Nevertheless, such backbone modification is

accompanied by the loss of one peptide bond and therewith one H-bond donor and one H-bond acceptor per αααα→βγ isosteric substitution.

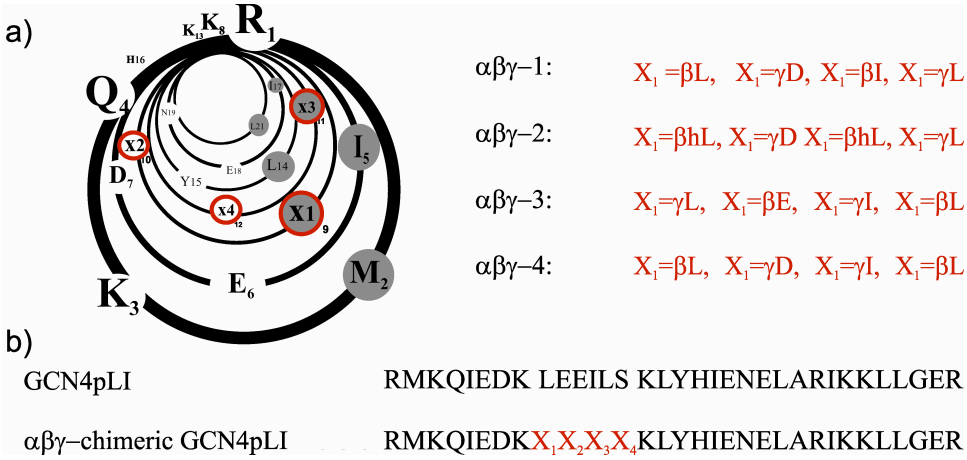

Figure 6.24 *a) The helical representation of 21 N-terminal amino acids in αβγ-chimeric variants of GCN4pLI. The amino acids at the hydrophobic core are highlighted in grey. The substituted β- and γ-amino acids in the αβγ-chimeric sequences are designated in X1-X4 and are surrounded by red circles. b) The primary structure of the GCN4pLI and general sequence of αβγ-chimera.*

However, we hypothesize that the loss of this peptide bond is not sufficient to cause considerable disorder in the entire modified interhelical domain, unless it is accompanied by other perturbative structural consequences such as disruption in local packing or conformational chaos due to the further loss of H-bonds. To test this hypothesis, we first focused on understanding of the features destabilizing the quaternary structure by designing αβγ-chimeric sequences (alternating βγβγ, γβγβ and mixed βγγβ sequences) (Figure 6.24). The self- and hetero-assembly of αβγ-chimeric sequences was investigated by means of molecular dynamics, circular dichroism, and a disulfide exchange assay. The βγ-substituted patterns in the αβγ-variants are different in the type of backbone that contributes to hydrophobic core (βγβγ: two β-residues, γβγβ: two γ-residues and in βγγβ: one β- and one γ-residues) . The further loss of H-bonding contact in the mixed pattern of γββγ results in a significant thermal destabilization compared with other αβγ-chimeras with alternating patterns (βγβγ and γβγβ) (Figure 6.25). This fact is further confirmed by results of MD simulations and molecular modeling. In addition, the theoretical and experimental results indicate that the αβγ-chimeras with alternating βγβγ and γβγβ substitution patterns do not equally mimic the structural behavior of the native parent peptide in solution. According to the melting points of the related chimeric helix bundles, the γ-amino acids are less preferred at the hydrophobic core than β-amino acids mainly due to a less buried hydrophobic surface area (Figure 6.24).

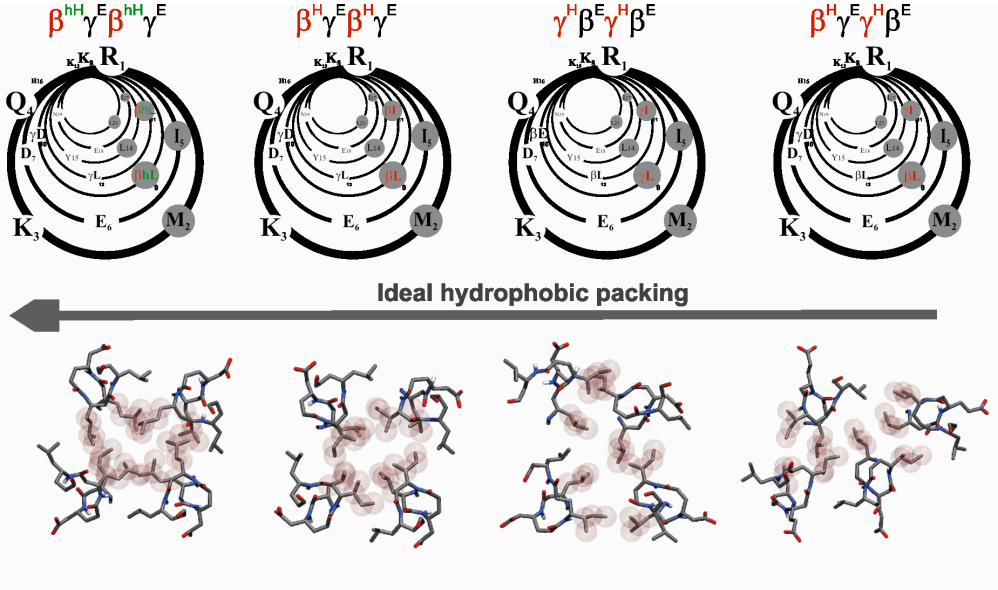

Figure 6.25 *The helical wheel presentation of first 21 N-terminally amino acids in chimeric structures as well as the hydrophobic side chain carbone contributions into the hydrophobic core presented by transparent van der Waals spheres. H, hH and E designate hydrophobic, hyper hydrophobic and electerostatic side chains, respectively.*

In a further step, we showed that the quaternary structure stability improves due to well-buried hydrophobic surface area by positioning hyperhydrophobic side chains; namely sufficiently long and bulky, on the backbone of β-residues (Figure 6.25). Apparently, the substitution of βleu residues with βhomoleu at the hydrophobic core of βγβγ-variant has increased the thermal stability. Therefore, a careful choice of non natural residues can provide key residue contacts such as van der Waals interactions and intrahelical H-bonding to compensate for the replacement of the natural α-amino acids. Furthermore, the results of the disulfide exchange assay indicate that only the specific substitution pattern with sufficient contact elements provides appropriate packing parameters required for the assembly of the chimera with native GCN4-derived molecule.

Author contributions

The experimental investigations including SPPS, CD spectroscopy, thermodynamic analysis, disulfide bridge assay are part of this thesis and carried out by the author. MD simulations were conducted by Dr. C. Baldauf (Fritz-Haber-Institut der Max-Planck-Gesellschaft). Data evaluation of sedimentation velocity and sedimentation equilibrium experiments was supported by M. Sc. U. Gerling. Dr. C. D. Cadicamo synthesized N-Fmoc βhomoLeu.

7. Summary

This thesis provides the first insight into the design and structural characterization of an otherwise natural α-helical coiled coil motif, which includes a foldameric pattern of β- and γ-amino acids. The obtained results indicate that one characteristic heptad repeat in native α-helical coiled coils, comprising two hydrogen-bonded turns can modularly be substituted by an extended βγ pattern with retention of helix dipole, global conformation and stability of fold. The systematic substitution of βγ-foldameric pattern in an α-peptide sequence results in an αβγ-chimeric sequenece. In this thesis, the design and structural characteristics of this newly designed chimeria are studied. The summary of each indevidual sections are as follow:

Part I

Two central turns of a hetero-assembling parent peptide (Base-pp) were replaced by a pentad of alternating β- and γ-amino acid residues in the chimera B3β2γ. Similar to its parent peptide, the assembly of the αβγ-chimera into a heteromeric leucine zipper with an exclusively natural oppositely charged α-peptide is driven only by noncovalent interactions and the resulting folded structure is highly thermostable. The several side chains scanning reveal that β- and γ-amino acids participate in the formation of the characteristic interaction domains of the α-helical coiled-coil folding motif similar to those of the natural system. The SEC and AUC results reveal the tetrameric oligomerization state for the natural (Acid-pp/Base-pp) and the chimeric (Acid-pp/B3β2γ) model systems.

Part II

Next, in order to improve the structure stability as well as a selective interaction of the αβγ-chimera with the natural partner, an extensive screening of preferred interacting side chains was performed by means of Spot analysis and phage display screening. In both methods, a large set of quadruple-substitution (a^{15}, d^{18}, e^{19}, g^{21}) variants of Acid-pp (*wt*) was probed for binding to the chimeric sequence of B3β2γ. The 35mer α-mutants on the membrane have a great identity in their sequences and only differ in the type of the side chains at positions interacting with β- and γ-residue side chains.

- Spot analysis showed that steric and bulky hydrophobic residues are well preferred at the chimeric hydrophobic core. These results also support the importance of the core flanking positions; these positions tolerate either negatively charged Glu interacting with positively charged Lys on the chimera, or hydrophobic side chains. The stability of the resulting hetero-assemblies between the selected sequences and αβγ-chimera was further confirmed in solution by CD and thermal denaturation. However, according to these results, the resulted coiled coils (B3β2γ/preferred mutant) reveal similar, but not higher, thermal stabilities and helical contents compared to B3β2γ/Acidpp.

- The phage display method allows the key heptad positions (a^{15}, d^{18}, e^{19}, g^{21}) to be assayed against all 20 coded amino acids. Several rounds of selection provide a short list of peptide sequences that bind selectively with B3β2γ. The comparison of the selected sequences reveals the most appropriate residues that improve the binding activity. The trends within the amino acids at the randomized positions in all preferred clones are highly similar, suggesting that the hetero-selective interactions between chimera and its natural α-counterpart has highly specific requirements. In particular, phage display revealed unpredictable side chain compositions that have low sequence homology to the parental sequence (central heptad of Acid-pp). Particularly, the applied rounds of selections led to a convergence on the cysteine residue in the hydrophobic core, either at the a^{15} or d^{18} position. The substitution of Cys by another size-relevant hydrophobic residue results in a pronounced drop in stability, indicating the role of thiol functionality on the stability of the fold. The possible inter or intramolecular hydrogen bonding between the thiol group of Cys and a proximate backbone carbonyl is expected to largely contribute to the pronounced stability of the resulted coiled coil structures by cysteine containing sequences. The physicochemical properties of cysteine residues make it well-suited for positioning at the hydrophobic core of chimeric coiled coils. In addition, the “steric matching” of relatively small Cys residue with bulky side chains of Phe and Ile provides for the optimal interacting side chain composition found by phages. While other selected sequences have multiple states of oligomerization in solution, the SEC result of the $I^aC^dE^eF^g$ variant distinctly shows tetramers as the only type of species in solution, similar to B3β2γ/Acidpp.

Part III

Additionally, the discrete side-chain functional groups of β- and γ-amino acids in the context of the α-helical coiled coil folding motif provides a unique artificial scaffold for effective catalyzing templat-directed native chemical ligation. In order to act similar to an α-peptide ligase, the βγ foldameric backbone provided for the spatial arrangement of all functional groups involved in the formation of the catalytic site. Hence the catalytic performance further assessed the structure/stability relation. Although the number of main chain hydrogen bonds providing α-helicity in the native peptide is reduced for B3β2γ, the positioning of β- and γ-side chains is compatible with the coiled coil structure and, thus, function. According to both the initial rate and the turnover of the reactions, the αβγ-chimeric ligase substantially mimics the substrate selectivity and catalytic efficiency of the natural α-peptide.

Part IV

Finally, aimed at understanding the structural features crucial for the integrity of α-helical mimicry by βγ-sequences, two turns of the α-helical structure in a self-assembling GCN4-derived sequence were substituted by differently arranged βγ-sequences. The design of homo-assembling αβγ-chimeric variants of GCN4pLI led to interhelical packing interactions driven locally by extended backbone amino acids. Despite the native-like behavior of βγ alternating sequences such as retention of α-helix dipole and the formation of 13-membered α-helix turns, the different βγ substitution patterns do not equally mimic the features necessary for α-helical coiled coil interaction. The preservation of the key residue contacts such as van der Waals interactions and intra-helical H-bonding, which can be met obviously only by a particular substitution pattern, thermodynamically favor the adoption of the coiled coil folding motif. These results show how successfully the destabilizing structural consequences of α→βγ modification, due to the loss of H-bonding, can be harnessed by reducing the solvent-exposed hydrophobic surface area and placing of hyperhydrophobic side chains at the hydrophobic core. These results show that the presence of β-amino acids, in contrast to γ-residues, at the hydrophobic core with sufficiently long and bulky side chains, provides key van der Waals interactions to compensate for the replacement of the natural α-amino acids. In addition, these results show that hetero-association of the αβγ-chimeric sequence with the native GCN4pLI is

also thermodynamically allowed only in the case of an ideal arrangement of β- and γ-residues.

8. Outlook

Supported by a long line of evidence, the design of an artificial folding motif was achieved, involving an extended domain of non-proteinogenic β- and γ-amino acids. However, systematic NMR studies are still needed in order to provide the high-resolution structural information about the unprecedented features of the αβγ-chimeric quaternary structure. Such studies are already under way.

With regard to the coiled coil-based hetero-assembling chimera, the formation of the helix in solution and the stability of the helical folding motif strongly depend on perfect interactions between the peptidic and non-peptidic components. Therefore, having a well-designed and characterized chimeric coiled coil provides an exciting opportunity to probe sequence features that influence both the structural and interaction specificity of the modified oligomer. However, the high oligomerization state of the presented chimeric coiled coils is expected to complicate any further thermodynamic and kinetic studies as well as the potential biological applications. Therefore, improvements of the parental model system regarding the oligomerization state and folding stability must be considered. As described in section 2.3, many stabilizing strategies can be applied to control and further improve the stability and selectivity of dimeric coiled coil systems to be able to host the extended unnatural peptidic sequence without considerable loss of folding stability. Next, the partial decline in stability of the entire quaternary structure due to the loss of H-bonding raises the motivation to apply β- and γ-amino acids with functionalized backbones, which offer extra H-bond donor/accepters. The frequent selection of H-donor Cys residues, which was detected by phage display screening, further may support this suggestion. Moreover, the application of homologous amino acids with hyperhydrophobic side chains can potentially improve the interhelical packing of the chimeric coiled coil. Other types of β- and γ-amino acid variation in respect to stiochiometry and side chain positioning may also advance the stability of the artificial folding motif.

The ability of αβγ-chimera to mimic α-helical interfaces in aqueous solution together with the proteolytic stability of β- and γ-amino acids provides for the application of this new

class of coiled coil forming chimeras for selective interactions with peptides and proteins. Considering this advantage, a new line of research may involve replacement of protein modules with this particular chimeric subunit. In this endeavor, bZIPs are attractive coiled coil based targets, which participate in a wide range of important biological processes and pose attractive targets for selective inhibition. The bZIPs family possesses homo- and/or hetero-dimerizing coiled coil domains involved in regulation of transcription and can be a subject to structural modifications. To this end, an extended α-sequence in a basic bZip structural motif can modularly be substituted by alternating β- and γ-amino acids. The investigation of best interacting native partner for the modified biologically-derived sequence can further be identified by means of phage display technology. Additionally, the compatibility of foldameric $\beta\gamma$ pattern in native α-helical constructs can be assessed regarding the preservation of DNA binding affinity. Moreover, the optimized helical conformation of $\alpha\beta\gamma$-sequences can potentially present a great candidate to effectively recapitulate the binding surface of known helical α-peptide inhibitors.

9. References

1. Gellman, S. H., *Accounts of Chemical Research* **1998,** 31, (4), 173-180.
2. Speakman, P. T., *Nature* **1971,** 229, (5282), 241-243.
3. Reznikoff, W. S.; Winter, R. B.; Hurley, C. K., *Proceedings of the National Academy of Sciences of the United States of America* **1974,** 71, (6), 2314-2318.
4. Sattler, M.; Liang, H.; Nettesheim, D.; Meadows, R. P.; Harlan, J. E.; Eberstadt, M.; Yoon, H. S.; Shuker, S. B.; Chang, B. S.; Minn, A. J.; Thompson, C. B.; Fesik, S. W., *Science* **1997,** 275, (5302), 983-986.
5. Wallace, B. A., *Biophysical journal* **1986,** 49, (1), 295-306.
6. Siu, S. W. I.; Böckmann, R. A., *Journal of Structural Biology* **2007,** 157, (3), 545-556.
7. Hill, D. J.; Mio, M. J.; Prince, R. B.; Hughes, T. S.; Moore, J. S., *Chemical Reviews* **2001,** 101, (12), 3893-4012.
8. Wender, P. A.; Mitchell, D. J.; Pattabiraman, K.; Pelkey, E. T.; Steinman, L.; Rothbard, J. B., *Proceedings of the National Academy of Sciences of the United States of America* **2000,** 97, (24), 13003-13008.
9. Fillon, Y. A.; Anderson, J. P.; Chmielewski, J., *Journal of the American Chemical Society* **2005,** 127, (33), 11798-11803.
10. Liu, D.; DeGrado, W. F., *Journal of the American Chemical Society* **2001,** 123, (31), 7553-7559.
11. Porter, E. A.; Wang, X.; Lee, H.-S.; Weisblum, B.; Gellman, S. H., *Nature* **2000,** 404, (6778), 565-565.
12. Bautista, A. D.; Craig, C. J.; Harker, E. A.; Schepartz, A., *Current Opinion in Chemical Biology* **2007,** 11, (6), 685-692.
13. Cheng, R. P.; Gellman, S. H.; DeGrado, W. F., *Chemical Reviews* **2001,** 101, (10), 3219-3232.
14. Karle, I. L.; Pramanik, A.; Banerjee, A.; Bhattacharjya, S.; Balaram, P., *Journal of the American Chemical Society* **1997,** 119, (39), 9087-9095.
15. Vasudev, P. G.; Ananda, K.; Chatterjee, S.; Aravinda, S.; Shamala, N.; Balaram, P., *Journal of the American Chemical Society* **2007,** 129, (13), 4039-4048.
16. Andrews, M. J. I.; Tabor, A. B., *Tetrahedron* **1999,** 55, (40), 11711-11743.
17. Cooley, R. B.; Arp, D. J.; Karplus, P. A., *Journal of Molecular Biology* 404, (2), 232-246.
18. Aurora, R.; Creamer, T. P.; Srinivasan, R.; Rose, G. D., *Journal of Biological Chemistry* **1997,** 272, (3), 1413-1416.
19. DeGrado, W. F.; Summa, C. M.; Pavone, V.; Nastri, F.; Lombardi, A., *Annual review of biochemistry* **1999,** 68, 779-819.
20. Munoz, V.; Serrano, L., *Proteins: Structure, Function, and Bioinformatics* **1994,** 20, (4), 301-311.
21 Nick Pace, C.; Martin Scholtz, J., *Biophysical journal* **1998,** 75, (1), 422-427.
22. Kurochkina, N., *Journal of Theoretical Biology* 264, (2), 585-592.
23. Patgiri, A.; Jochim, A. L.; Arora, P. S., *Accounts of Chemical Research* **2008,** 41, (10), 1289-1300.
24. Zhao, L.; Chmielewski, J., *Current Opinion in Structural Biology* **2005,** 15, (1), 31-34.
25. Seebach, D.; Gardiner, J., *Accounts of Chemical Research* **2008,** 41, (10), 1366-1375.
26. Wu, Y. D.; Gellman, S., *Accounts of Chemical Research* **2008,** 41, (10), 1231-1232.

27. Horne, W. S.; Gellman, S. H., *Accounts of Chemical Research* **2008,** 41, (10), 1399-1408.
28. Pierret, B.; Virelizier, H.; Vita, C., *International Journal of Peptide and Protein Research* **1995,** 46, (6), 471-479.
29. Jackson, D. Y.; King, D. S.; Chmielewski, J.; Singh, S.; Schultz, P. G., *Journal of the American Chemical Society* **1991,** 113, (24), 9391-9392.
30. Campbell, R. M.; Bongers, J.; Felix, A. M., *Biopolymers* **1995,** 37, (2), 67-88.
31. Phelan, J. C.; Skelton, N. J.; Braisted, A. C.; McDowell, R. S., *Journal of the American Chemical Society* **1997,** 119, (3), 455-460.
32. Yu, C.; Taylor, J. W., *Tetrahedron Letters* **1996,** 37, (11), 1731-1734.
33. Ghadiri, M. R.; Fernholz, A. K., *Journal of the American Chemical Society* **1990,** 112, (26), 9633-9635.
34. Orner, B. P.; Ernst, J. T.; Hamilton, A. D., *Journal of the American Chemical Society* **2001,** 123, (22), 5382-5383.
35. Davis, J. M.; Tsou, L. K.; Hamilton, A. D., *Chemical Society Reviews* **2007,** 36, (2), 326-334.
36. Kritzer, J. A.; Lear, J. D.; Hodsdon, M. E.; Schepartz, A., *Journal of the American Chemical Society* **2004,** 126, (31), 9468-9469.
37. Cheng, R. P., *Current Opinion in Structural Biology* **2004,** 14, (4), 512-520.
38. Dervan, P. B., *Science* **1986,** 232, (4749), 464-471.
39. Dervan, P. B.; Bürli, R. W., *Current Opinion in Chemical Biology* **1999,** 3, (6), 688-693.
40. Hamuro, Y.; Geib, S. J.; Hamilton, A. D., *Journal of the American Chemical Society* **1997,** 119, (44), 10587-10593.
41. Hamuro, Y.; Geib, S. J.; Hamilton, A. D., *Journal of the American Chemical Society* **1996,** 118, (32), 7529-7541.
42. Hamuro, Y.; Geib, S. J.; Hamilton, A. D., *Angewandte Chemie International Edition in English* **1994,** 33, (4), 446-448.
43. Wu, C. W.; Kirshenbaum, K.; Sanborn, T. J.; Patch, J. A.; Huang, K.; Dill, K. A.; Zuckermann, R. N.; Barron, A. E., *Journal of the American Chemical Society* **2003,** 125, (44), 13525-13530.
44. Burkoth, T. S.; Beausoleil, E.; Kaur, S.; Tang, D.; Cohen, F. E.; Zuckermann, R. N., *Chemistry & biology* **2002,** 9, (5), 647-654.
45. Scott Lokey, R.; Iverson, B. L., *Nature* **1995,** 375, (6529), 303-305.
46. Nelson, J. C.; Saven, J. G.; Moore, J. S.; Wolynes, P. G., *Science* **1997,** 277, (5333), 1793-1796.
47. Eschenmoser, A.; Loewenthal, E., *Chemical Society Reviews* **1992,** 21, (1), 1-16.
48. Eschenmoser, A., *Science* **1999,** 284, (5423), 2118-2124.
49. Uhlmann, E.; Peyman, A.; Breipohl, G.; Will, D. W., *Angewandte Chemie International Edition* **1998,** 37, (20), 2796-2823.
50. Nielsen, P. E.; Egholm, M.; Berg, R. H.; Buchardt, O., *Science* **1991,** 254, (5037), 1497-1500.
51. Horne, W. S.; Price, J. L.; Keck, J. L.; Gellman, S. H., *Journal of the American Chemical Society* **2007,** 129, (14), 4178-4180.
52. Zornik, D.; Meudtner, R. M.; El Malah, T.; Thiele, C. M.; Hecht, S., *Chemistry – A European Journal* 17, (5), 1473-1484.
53. Constable, E. C.; Elder, S. M.; Tocher, D. A., *Polyhedron* **1992,** 11, (20), 2599-2604.
54. Seebach, D.; Beck, A. K.; Bierbaum, D. J., *Chemistry & Biodiversity* **2004,** 1, (8), 1111-1239.
55. Soth, M. J.; Nowick, J. S., *Current Opinion in Chemical Biology* **1997,** 1, (1), 120-129.

56. Seebach, D.; L. Matthews, J., *Chemical Communications* **1997**, (21), 2015-2022.
57. DeGrado, W. F.; Schneider, J. P.; Hamuro, Y., *Journal of Peptide Research* **1999,** 54, (3), 206-217.
58. Hintermann, T.; Gademann, K.; Jaun, B.; Seebach, D., *Helvetica Chimica Acta* **1998,** 81, (5-8), 983-1002.
59. Vasudev, P. G.; Chatterjee, S.; Shamala, N.; Balaram, P., *Chemical Reviews*.
60. Olson, G. L.; Bolin, D. R.; Bonner, M. P.; Bos, M.; Cook, C. M.; Fry, D. C.; Graves, B. J.; Hatada, M.; Hill, D. E., *Journal of Medicinal Chemistry* **1993,** 36, (21), 3039-3049.
61. Abele, S.; Seebach, D., *European Journal of Organic Chemistry* **2000,** 2000, (1), 1-15.
62. Murer, P.; Rheiner, B.; Juaristi, E.; Seebach, d., *Heterocycles* **1994,** 39, 319-344.
63. Brenner, M.; Seebach, D., *Helvetica Chimica Acta* **2001,** 84, (5), 1181-1189.
64. Seebach, D.; Schaeffer, L.; Brenner, M.; Hoyer, D., *Angewandte Chemie International Edition* **2003,** 42, (7), 776-778.
65. Kleinkauf, H.; Von Döhren, H., *European Journal of Biochemistry* **1996,** 236, (2), 335-351.
66. Kawata, S.; Ashizawa, S.; Hirama, M., *Journal of the American Chemical Society* **1997,** 119, (49), 12012-12013.
67. Pettit, G. R.; Kamano, Y.; Kizu, H.; Dufresne, C.; Herald, C. L.; Bontems, R. J.; Schmidt, J. M.; Boettner, F. E.; Nieman, R. A., *Heterocycles* **1989,** 28, (2), 553-558.
68. Grammel, N.; Pankevych, K.; Demydchuk, J.; Lambrecht, K.; Saluz, H. P.; Ullrich, K.; Krügel, H., *European Journal of Biochemistry* **2002,** 269, (1), 347-357.
69. Vasudev, P. G.; Chatterjee, S.; Shamala, N.; Balaram, P., *Chemical Reviews* 111, (2), 657-687.
70. Bestian, H., *Angewandte Chemie International Edition in English* **1968,** 7, (4), 278-285.
71. Venkatraman, J.; Shankaramma, S. C.; Balaram, P., *Chemical Reviews* **2001,** 101, (10), 3131-3152.
72. Appella, D. H.; Christianson, L. A.; Karle, I. L.; Powell, D. R.; Gellman, S. H., *Journal of the American Chemical Society* **1996,** 118, (51), 13071-13072.
73. Appella, D. H.; Christianson, L. A.; Karle, I. L.; Powell, D. R.; Gellman, S. H., *Journal of the American Chemical Society* **1999,** 121, (26), 6206-6212.
74. Appella, D. H.; Christianson, L. A.; Klein, D. A.; Richards, M. R.; Powell, D. R.; Gellman, S. H., *Journal of the American Chemical Society* **1999,** 121, (33), 7574-7581.
75. Gademann, K.; Seebach, D., *Helvetica Chimica Acta* **2001,** 84, (10), 2924-2937.
76. Arvidsson, P. I.; Frackenpohl, J.; Ryder, N. S.; Liechty, B.; Petersen, F.; Zimmermann, H.; Camenisch, G. P.; Woessner, R.; Seebach, D., *ChemBioChem* **2001,** 2, (10), 771-773.
77. Schmitt, M. A.; Weisblum, B.; Gellman, S. H., *Journal of the American Chemical Society* **2004,** 126, (22), 6848-6849.
78. van den Elsen, J. M. H.; Kuntz, D. A.; Hoedemaeker, F. J.; Rose, D. R., *Proceedings of the National Academy of Sciences* **1999,** 96, (24), 13679-13684.
79. Hayen, A.; Schmitt, M. A.; Ngassa, F. N.; Thomasson, K. A.; Gellman, S. H., *Angewandte Chemie International Edition* **2004,** 43, (4), 505-510.
80. Seebach, D.; Overhand, M.; Kühnle, F. N. M.; Martinoni, B.; Oberer, L.; Hommel, U.; Widmer, H., *Helvetica Chimica Acta* **1996,** 79, (4), 913-941.
81. Frackenpohl, J.; Arvidsson, P. I.; Schreiber, J. V.; Seebach, D., *ChemBioChem* **2001,** 2, (6), 445-455.

82. Hook, D. F.; Gessier, F.; Noti, C.; Kast, P.; Seebach, D., *ChemBioChem* **2004,** 5, (5), 691-706.
83. Porter, E. A.; Weisblum, B.; Gellman, S. H., *Journal of the American Chemical Society* **2002,** 124, (25), 7324-7330.
84. Dado, G. P.; Gellman, S. H., *Journal of the American Chemical Society* **1994,** 116, (3), 1054-1062.
85. James Iii, W. H.; MuÌˆller, C. W.; Buchanan, E. G.; Nix, M. G. D.; Guo, L.; Roskop, L.; Gordon, M. S.; Slipchenko, L. V.; Gellman, S. H.; Zwier, T. S., *Journal of the American Chemical Society* **2009,** 131, (40), 14243-14245.
86. Sengupta, A.; Roy, R. S.; Sabareesh, V.; Shamala, N.; Balaram, P., *Organic & Biomolecular Chemistry* **2006,** 4, (6), 1166-1173.
87. Krauthäuser, S.; Christianson, L. A.; Powell, D. R.; Gellman, S. H., *Journal of the American Chemical Society* **1997,** 119, (48), 11719-11720.
88. Seebach, D.; Abele, S.; Gademann, K.; Jaun, B., *Angewandte Chemie International Edition* **1999,** 38, (11), 1595-1597.
89. Chen, F.; Lepore, G.; Goodman, M., *Macromolecules* **1974,** 7, (6), 779-783.
90. Rueping, M.; Jaun, B.; Seebach, D., *Chemical Communications* **2000**, (22), 2267-2268.
91. Cheng, R. P.; DeGrado, W. F., *Journal of the American Chemical Society* **2001,** 123, (21), 5162-5163.
92. Hart, S. A.; Bahadoor, A. B. F.; Matthews, E. E.; Qiu, X. J.; Schepartz, A., *Journal of the American Chemical Society* **2003,** 125, (14), 4022-4023.
93. Koert, U., *Angewandte Chemie* **1997,** 109, (17), 1922-1923.
94. Bode, K. A.; Applequist, J., *Macromolecules* **1997,** 30, (7), 2144-2150.
95. Hanessian, S.; Luo, X.; Schaum, R., *Tetrahedron Letters* **1999,** 40, (27), 4925-4929.
96. David, R.; GuÌˆnther, R.; Baumann, L.; LuÌˆhmann, T.; Seebach, D.; Hofmann, H.-J. r.; Beck-Sickinger, A. G., *Journal of the American Chemical Society* **2008,** 130, (46), 15311-15317.
97. Sadowsky, J. D.; Schmitt, M. A.; Lee, H. S.; Umezawa, N.; Wang, S.; Tomita, Y.; Gellman, S. H., *Journal of the American Chemical Society* **2005,** 127, (34), 11966-11968.
98. Schmitt, M. A.; Choi, S. H.; Guzei, I. A.; Gellman, S. H., *Journal of the American Chemical Society* **2005,** 127, (38), 13130-13131.
99. Schmitt, M. A.; Choi, S. H.; Guzei, I. A.; Gellman, S. H., *Journal of the American Chemical Society* **2006,** 128, (14), 4538-4539.
100. Guo, L.; Chi, Y.; Almeida, A. M.; Guzei, I. A.; Parker, B. K.; Gellman, S. H., *Journal of the American Chemical Society* **2009,** 131, (44), 16018-16020.
101. Guo, L.; Almeida, A. M.; Zhang, W.; Reidenbach, A. G.; Choi, S. H.; Guzei, I. A.; Gellman, S. H., *Journal of the American Chemical Society* **2010***,* 132, (23), 7868-7869.
102. Guichard, G.; Huc, I., *Chemical Communications* 47, (21), 5933-5941.
103. Baldauf, C.; Günther, R.; Hofmann, H. J. r., *The Journal of Organic Chemistry* **2006,** 71, (3), 1200-1208.
104. Sharma, G. V. M.; Jadhav, V. B.; Ramakrishna, K. V. S.; Jayaprakash, P.; Narsimulu, K.; Subash, V.; Kunwar, A. C., *Journal of the American Chemical Society* **2006,** 128, (45), 14657-14668.
105. Rueping, M.; Schreiber, J. V.; Lelais, G.; Jaun, B.; Seebach, D., *Helvetica Chimica Acta* **2002,** 85, (9), 2577-2593.
106. De Pol, S.; Zorn, C.; Klein, C. D.; Zerbe, O.; Reiser, O., *Angewandte Chemie International Edition* **2004,** 43, (4), 511-514.

107. Hecht, S.; Huc, I., *Foldamers : structure, properties, and applications*. Wiley-VCH: Weinheim, 2007.
108. Parry, D. A. D., *Bioscience Reports* **1982,** 12, (2), 1017-1024.
109. Crick, F. H. C., *Acta Crystallographica* **1953,** 6, 689-697.
110. Lupas, A. N.; Gruber, M.; David A. D. Parry, a. J. M. S., The Structure of [alpha]-Helical Coiled Coils. In *Advances in Protein Chemistry*, Academic Press: 2005; Vol. Volume 70, pp 37-38.
111. Woolfson, D. N.; David A. D. Parry, a. J. M. S., The Design of Coiled-Coil Structures and Assemblies. In *Advances in Protein Chemistry*, Academic Press: 2005; Vol. Volume 70, pp 79-112.
112. Robson Marsden, H.; Kros, A., *Angewandte Chemie International Edition* 49, (17), 2988-3005.
113. Lupas, A. N., *Trends Biochem Sci* **1996,** 21, (10), 375-382.
114. Betz, S. F.; Liebman, P. A.; DeGrado, W. F., *Biochemistry* **1997,** 36, (9), 2450-2458.
115. Cohen, C.; Parry, D. A. D., *Proteins: Structure, Function, and Genetics* **1990,** 7, (1), 1-15.
116. Hodges, R. S., *Biochemistry and Cell Biology* **1996,** 74, (2), 133-154.
117. Schnarr, N. A.; Kennan, A. J., *Journal of the American Chemical Society* **2001,** 123, (44), 11081-11082.
118. Harbury, P. B.; Zhang, T.; Kim, P. S.; Alber, T., *Science* **1993,** 262, (5138), 1401-1407.
119. Fairman, R.; Chao, H. G.; Lavoie, T. B.; Villafranca, J. J.; Matsueda, G. R.; Novotny, J., *Biochemistry* **1996,** 35, (9), 2824-2829.
120. Gonzalez, L.; Plecs, J. J.; Alber, T., *Nature Structural Biology* **1996,** 3, (6), 510-515.
121. Lin, R. C.; Scheller, R. H., *Annual Review of Cell and Developmental Biology* **2000,** 16, 19-49.
122. Diss, M. L.; Kennan, A. J., *The Journal of Organic Chemistry* **2008,** 73, (24), 9752-9755.
123. Son, S.; Tanrikulu, I. C.; Tirrell, D. A., *ChemBioChem* **2006,** 7, (8), 1251-1257.
124. Tang, Y.; Ghirlanda, G.; Vaidehi, N.; Kua, J.; Mainz, D. T.; Goddard, W. A.; DeGrado, W. F.; Tirrell, D. A., *Biochemistry* **2001,** 40, (9), 2790-2796.
125. Horne, W. S.; Yadav, M. K.; Stout, C. D.; Ghadiri, M. R., *Journal of the American Chemical Society* **2004,** 126, (47), 15366-15367.
126. Raguse, T. L.; Lai, J. R.; LePlae, P. R.; Gellman, S. H., *Organic Letters* **2001,** 3, (24), 3963-3966.
127. Cheng, R. P.; DeGrado, W. F., *Journal of the American Chemical Society* **2002,** 124, (39), 11564-11565.
128. Qiu, J. X.; Petersson, E. J.; Matthews, E. E.; Schepartz, A., *Journal of the American Chemical Society* **2006,** 128, (35), 11338-11339.
129. Price, J. L.; Horne, W. S.; Gellman, S. H., *Journal of the American Chemical Society* **2007,** 129, (20), 6376-6377.
130. Goodman, J. L.; Petersson, E. J.; Daniels, D. S.; Qiu, J. X.; Schepartz, A., *Journal of the American Chemical Society* **2007,** 129, (47), 14746-14751.
131. Price, J. L.; Horne, W. S.; Gellman, S. H., *Journal of the American Chemical Society* **2010,** 132, (35), 12378-12387.
132. Rezaei Araghi, R.; Jäckel, C.; Cölfen, H.; Salwiczek, M.; Völkel, A.; Wagner, S. C.; Wieczorek, S.; Baldauf□, C.; Koksch, B., *ChemBioChem* **2010,** 11, (3), 335-339.
133. Rezaei Araghi, R.; Koksch, B., *Chemical Communications* 47, (12), 3544-3546.
134. Rezaei Araghi, R.; Baldauf, C.; Gerling, U. I. M.; Cadicamo, C. D.; Koksch, B., *Amino Acids* **2011**.

135. Fasman, G. D., *Circular dichroism and the conformational analysis of biomolecules*. Plenum Press: New York, 1996.
136. Chen, Y.-H.; Yang, J. T.; Chau, K. H., *Biochemistry* **1974,** 13, (16), 3350-3359.
137. Luidens, M. K.; Figge, J.; Breese, K.; Vajda, S., *Biopolymers* **1996,** 39, (3), 367-376.
138. Lebowitz, J.; Lewis, M. S.; Schuck, P., *Protein Science* **2002,** 11, (9), 2067-2079.
139. Laue, T. M.; Stafford, W. F., III, *Annual Review of Biophysics & Biomolecular Structure* **1999,** 28, (1), 75.
140. Frank, R., *Journal of Immunological Methods* **2002,** 267, (1), 13-26.
141. Kehoe, J. W.; Kay, B. K., *Chemical Reviews* **2005,** 105, (11), 4056-4072.
142. Barbas, C. F., *Phage display : a laboratory manual*. Cold Spring Harbor Laboratory Press: Cold Spring Harbor, NY, 2001.
143. García-Echeverría, C., *Bioorganic & Medicinal Chemistry Letters* **1997,** 7, (13), 1695-1698.
144. Garcia-Echeverria, C., *Journal of the American Chemical Society* **1994,** 116, (13), 6031-6032.
145. Pagel, K.; Seeger, K.; Seiwert, B.; Villa, A.; Mark, A. E.; Berger, S.; Koksch, B., *Organic & Biomolecular Chemistry* **2005,** 3, (7), 1189-1194.
146. Yadav, M. K.; Redman, J. E.; Leman, L. J.; Alvarez-Gutárrez, J. M.; Zhang, Y.; Stout, C. D.; Ghadiri, M. R., *Biochemistry* **2005,** 44, (28), 9723-9732.
147. O'Shea, E. K.; Lumb, K. J.; Kim, P. S., *Current biology : CB* **1993,** 3, (10), 658-667.
148. O'Shea, E. K.; Rutkowski, R.; Kim, P. S., *Cell* **1992,** 68, (4), 699-708.
149. O'Shea, E. K.; Rutkowski, R.; Stafford, W. F.; Kim, P. S., *Science* **1989,** 245, (4918), 646-648.
150. O'Shea, E. K.; Klemm, J. D.; Kim, P. S.; Alber, T., *Science* **1991,** 254, (5031), 539-544.
151. Zhou, H. X.; Lyu, P. C.; Wemmer, D. E.; Kallenbach, N. R., *Journal of the American Chemical Society* **1994,** 116, (3), 1139-1140.
152. Lumb, K. J.; Kim, P. S., *Biochemistry* **1995,** 34, (27), 8642-8648.
153. Przezdziak, J.; Tremmel, S.; Kretzschmar, I.; Beyermann, M.; Bienert, M.; Volkmer-Engert, R., *ChemBioChem* **2006,** 7, (5), 780-788.
154. Portwich, M.; Keller, S.; Strauss, H. M.; Mahrenholz, C. C.; Kretzschmar, I.; Kramer, A.; Volkmer, R., *Angewandte Chemie International Edition* **2007,** 46, (10), 1654-1657.
155. Sakurai, Y.; Mizuno, T.; Hiroaki, H.; Oku, J. I.; Tanaka, T., *The Journal of Peptide Research* **2005,** 66, (6), 387-394.
156. Betz, S. F.; Bryson, J. W.; DeGrado, W. F., *Current Opinion in Structural Biology* **1995,** 5, 457-463.
157. Yadav, M. K.; Leman, L. J.; Price, D. J.; Brooks, C. L.; Stout, C. D.; Ghadiri, M. R., *Biochemistry* **2006,** 45, (14), 4463-4473.
158. Liu, J.; Deng, Y.; Zheng, Q.; Cheng, C.-S.; Kallenbach, N. R.; Lu, M., *Biochemistry* **2006,** 45, (51), 15224-15231.
159. Liu, J.; Zheng, Q.; Deng, Y.; Cheng, C.-S.; Kallenbach, N. R.; Lu, M., *Proceedings of the National Academy of Sciences* **2006,** 103, (42), 15457-15462.
160. Frank, B. S.; Vardar, D.; Buckley, D. A.; McKnight, C. J., *Protein Science* **2002,** 11, (3), 680-687.
161. Tripet, B.; Wagschal, K.; Lavigne, P.; Mant, C. T.; Hodges, R. S., *Journal of Molecular Biology* **2000,** 300, (2), 377-402.
162. Vagt, T.; Jäckel, C.; Samsonov, S.; Teresa Pisabarro, M.; Koksch, B., *Bioorganic & Medicinal Chemistry Letters* **2009,** 19, (14), 3924-3927.
163. Vagt, T.; Nyakatura, E.; Salwiczek, M.; Jackel, C.; Koksch, B., *Organic & Biomolecular Chemistry* 8, (6), 1382-1386.

164. Wieczorek, S., *M. Sc.Thesis, Freie Universität Berlin* **2010**.
165. Choulier, L.; Laune, D.; Orfanoudakis, G.; Wlad, H.; Janson, J.-C.; Granier, C.; Altschuh, D., *Journal of Immunological Methods* **2001,** 249, (1-2), 253-264.
166. Hari, S. B.; Byeon, C.; Lavinder, J. J.; Magliery, T. J., *Protein Science* 19, (4), 670-679.
167. Alben, J. O.; Bare, G. H.; Bromberg, P. A., *Nature* **1974,** 252, (5485), 736-738.
168. Johansson, J. S.; Gibney, B. R.; Rabanal, F.; Reddy, K. S.; Dutton, P. L., *Biochemistry* **1998,** 37, (5), 1421-1429.
169. Zhou, N. E.; Kay, C. M.; Hodges, R. S., *Biochemistry* **1993,** 32, (12), 3178-3187.
170. Smaldone, R. A.; Moore, J. S., *Chemistry – A European Journal* **2008,** 14, (9), 2650-2657.
171. Müller, M. M.; Windsor, M. A.; Pomerantz, W. C.; Gellman, S. H.; Hilvert, D., *Angewandte Chemie International Edition* **2009,** 48, (5), 922-925.
172. Maayan, G.; Ward, M. D.; Kirshenbaum, K., *Proceedings of the National Academy of Sciences* **2009,** 106, (33), 13679-13684.
173. Dawson, P. E.; Muir, T. W.; Clark-Lewis, I.; Kent, S. B., *Science* **1994,** 266, (5186), 776-779.
174. Lee, D. H.; Severin, K.; Yokobayashi, Y.; Ghadiri, M. R., *Nature* **1997,** 390, (6660), 591-594.
175. Yao, S.; Ghosh, I.; Zutshi, R.; Chmielewski, J., *Nature* **1998,** 396, (6710), 447-450.
176. Lee, D. H.; Granja, J. R.; Martinez, J. A.; Severin, K.; Ghadiri, M. R., *Nature* **1996,** 382, (6591), 525-528.
177. Severin, K.; Lee, D. H.; Martinez, J. A.; Ghadiri, M. R., *Chemistry – A European Journal* **1997,** 3, (7), 1017-1024.
178. Li, X.; Chmielewski, J., *Journal of the American Chemical Society* **2003,** 125, (39), 11820-11821.
179. Issac, R.; Chmielewski, J., *Journal of the American Chemical Society* **2002,** 124, (24), 6808-6809.
180. DeGrado, W. F.; Gratkowski, H.; Lear, J. D., *Protein Science* **2003,** 12, (4), 647-665.